MODELLING OF TRANSMISSION RANGE IN VEHICULAR AD HOC NETWORKS

by

Maen M. Artimy

Submitted in partial fulfillment of the
requirements for the degree of

DOCTOR OF PHILOSOPHY

Major Subject: Engineering Mathematics

at

DALHOUSIE UNIVERSITY

Halifax, Nova Scotia

February 27, 2006

Your file Votre référence
ISBN: 978-0-494-27637-2
Our file Notre référence
ISBN: 978-0-494-27637-2

DALHOUSIE UNIVERSITY

To comply with the Canadian Privacy Act the National Library of Canada has requested that the following pages be removed from this copy of the thesis:

Preliminary Pages
- Examiners Signature Page
- Dalhousie Library Copyright Agreement

Appendices
- Copyright Releases (if applicable)

To my family

Table of Contents

List of Tables x

List of Figures xi

List of Abbreviations and Symbols xiv

Glossary xxiv

Acknowledgements xxvii

Abstract xxviii

Chapter 1 Introduction 1

1.1 Motivation 1

1.2 Contributions 4

1.3 Thesis outline 7

Chapter 2 Overview of Vehicular Ad Hoc Networks 10

2.1 Introduction 10

2.2 VANET characteristics 12

2.3 Intelligent transportation systems 13

2.4 Research directions in VANETs 15

2.4.1 Enabling technologies 15

2.4.2 MAC layer issues 17

2.4.3 Network layer issues 20
2.4.4 Applications 22
2.5 Vehicle mobility 24
2.5.1 Vehicle mobility models and traffic simulations in VANETs research 25
2.5.2 Integrated communication and mobility simulators 28
2.6 Summary and conclusions 29

Chapter 3 Brief Introduction to Vehicle Traffic Theory 30
3.1 Introduction 30
3.2 Traffic flow characteristics 31
3.3 Fundamental relationship of traffic flow 33
3.4 Traffic flow models 35
3.4.1 Macroscopic (continuum) traffic models 36
3.4.2 Car-following models 38
3.4.3 Two-fluid model 40
3.4.4 Cellular automata models 41
3.5 Phase transition and order parameter 42
3.6 Traffic simulation 45
3.7 Summary and conclusions 47

Chapter 4 VANET Simulations using *RoadSim* 49
4.1 Introduction 50
4.2 The NaSch model 51
4.2.1 Properties 54
4.2.2 Extensions to randomization rules in the literature 55
4.2.3 Multi-lane extensions in the literature 56
4.3 The microsimulator (*RoadSim*) 58
4.3.1 Support for VANET research 59
4.3.2 Data structures 60
4.3.3 Bi-directional traffic 61

4.3.4 Multi-lane traffic 61
4.3.5 Intersections 61
4.3.6 Speed options 62
4.3.7 Initialization modes 62
4.4 Validation tests 63
4.4.1 Generating bivariate relationships 64
4.4.2 Free-flow speed 65
4.4.3 Estimation of the sensitivity factor (λ) 67
4.4.4 Estimation of the network resistance factor 68
4.4.5 Slow-to-start rule 69
4.4.6 Multi-lane traffic 71
4.4.7 Effect of various speed limits 72
4.5 Summary and conclusions 75

Chapter 5 Minimum Transmission Range in Uninterrupted Highways 77

5.1 Introduction 78
5.2 Homogenoues transmission range 79
5.3 Traffic jams and critical density 82
5.4 Distribution of vehicle locations in a highway 83
5.5 Estimation of lower-bound MTR in vehicular ad hoc networks 84
5.6 Evaluation 88
5.6.1 Vehicle distribution 89
5.6.2 Minimum transmission range 91
5.7 Summary and conclusions 95

Chapter 6 Minimum Transmission Range Across Intersections 97

6.1 Introduction 97
6.2 Connectivity across intersections 98
6.3 Signalized intersection 104
6.4 Simulation of signalized intersections 112

6.5 Unsignalized intersection 115
6.6 Summary and conclusions 120

Chapter 7 Estimation of Local Vehicle Density 122
7.1 Introduction 122
7.2 Estimation of local density 123
7.3 Unified framework for traffic models 126
7.4 Fraction of stopped vehicles as an order parameter 127
7.5 Simulated highway configurations 129
7.6 Simulation results 132
7.7 Summary and conclusions 133

Chapter 8 Dynamic Transmission Range Assignment Algorithm 134
8.1 Introduction 134
8.2 Non-homogenous range assignment 136
8.3 Communication model 137
8.4 Dynamic transmission range assignment 138
8.5 Performance evaluation 140
8.6 Modification of IEEE 802.11 using the DTRA algorithm 144
8.7 Practical considerations 149
8.8 Summary and conclusions 150

Chapter 9 Conclusions and Future Research 152
9.1 Summary 152
9.2 Future research 155

References 157

Appendix A ITS Related Projects 171
A.1 Projects in Germany 171
A.2 Projects in Europe (including Germany) 172
A.3 Projects in the United States 173

A.4 Projects in Japan 174

Appendix B *RoadSim* Class Diagrams **176**

Appendix C *RoadSim* Topologies and Generated ns-2 Scripts **177**

C.1 *RoadSim* racetrack topology 177

C.2 Motion script 179

C.3 Power assignment script 181

C.4 Connection script 183

C.5 Main ns-2 script 186

List of Tables

Table 6.1 Descriptive statistics. 115
Table 6.2 MTR values (meters) downstream of a stop-sign intersection in low interfering flow. 118
Table 7.1 Calculated values of λ, k_1 and k_c. 129
Table 8.1 Percentage of partitions during simulation time. 143

List of Figures

Figure 3.1 Spot and instantaneous traffic observations [72]. 32
Figure 3.2 The Fundamental Diagram of Road Traffic. 34
Figure 3.3 The speed-density relationship (Pipes Equation). 39
Figure 3.4 Phase Transition. 43
Figure 3.5 A reverse λ shape fundamental diagram showing free-flow, congested, and mixed state traffic conditions. 44

Figure 4.1 Cell grid and quantities relevant to the NaSch model (occupied cells are shown in grey). 53
Figure 4.2 Two-lane cell grid and quantities relevant to lane changing rules. 57
Figure 4.3 Examples of objects simulated in *RoadSim*. 60
Figure 4.4 Test configuration. 64
Figure 4.5 *RoadSim* generated a) flow–density, and b) speed–density relationships using the rules of the original NaSch model. 66
Figure 4.6 Estimation of the normalized sensitivity factor, λ'. 68
Figure 4.7 Estimation of network resistance factor. 69
Figure 4.8 *RoadSim* generated a) flow–density, and b) speed–density relationships using the NaSch-S2S model. 70
Figure 4.9 Lane utilization in a three-lane highway. 72
Figure 4.10 *RoadSim* generated a) flow–density, and b) speed–density relationships of traffic of dual maximum speed. 73
Figure 4.11 Lane utilization in three-lane highway. 74

Figure 5.1 The flow-density relationship in a) deterministic NaSch model, and b) stochastic NaSch-S2S model. 82
Figure 5.2 Congested traffic in a highway section 85
Figure 5.3 The lower bound of MTR in a highway of 1000-cell length and various values of maximum speed, U_{max}. 88
Figure 5.4 Racetrack configuration. 89
Figure 5.5 Vehicle density in 26 consecutive road sections of 5-cell length in a) free-flow traffic, b) congested traffic. 91
Figure 5.6 The value of Var(k_l) vs. system-wide traffic density in a) 1-lane road, and b) 3-lane road. 92
Figure 5.7 MTR in single-lane road. 93
Figure 5.8 MTR in three-lane road. 95

Figure 6.1 The MTR value, r_c in a) an uninterrupted road, and b) across an intersection. 99
Figure 6.2 An example of intersection that illustrates some of the used terminology. 100
Figure 6.3 Scatter plot of MTR values across intersections 103
Figure 6.4 Traffic light increases the headway in traffic of moderate density. 106
Figure 6.5 Headway between vehicles across intersection. 107
Figure 6.6 The pdf and cdf of the sum of Lognormal and Exponential distributions 110
Figure 6.7 A plot of $f_{r_L}(r)$ and $F_{r_L}(r)$. 111
Figure 6.8 Simulated highway configuration. 113
Figure 6.9 Histogram of MTR values collected in simulations of signalized intersection. 114
Figure 6.10 Vehicle trajectories upstream and downstream from a stop-sign intersection. 115
Figure 6.11 The MTR as a function of the interfering traffic flow. 118

Figure 6.12 Analytical and empirical estimates of the lower bound and mean MTR across an unsignalized intersection. 119

Figure 7.1 The order parameter ($f_s = N_s/N$) in a) 1-lane road, and b) 3-lane road. 128

Figure 7.2 The average speed of vehicles is compared to the fraction of stopped vehicles 128

Figure 7.3 Highway configurations used to evaluate the local density estimate and DTRA algorithm 131

Figure 7.4 Estimation of local vehicle density. 132

Figure 8.1 Vehicle density vs. the average transmission range and the number of partitions. 141

Figure 8.2 Change in vehicle density during network simulations of modified IEEE 802.11. 145

Figure 8.3 Performance comparison between IEEE 802.11 and DTRA protocols in the single-lane racetrack configuration. 147

Figure 8.4 Performance comparison between IEEE 802.11 and DTRA protocols in the signalized and stop-sign intersection configurations. 148

List of Abbreviations and Symbols

3G Third Generation

AODV Ad-hoc On-demand Distance Vector routing

BER Bit Error Rate

BJH Benjamin, Johnson and Hui

C2CCC Car-to-Car Communication Consortium

C2CC Car-to-Car Communication

CA Cellular Automata

CBR Constant-Bit-Rate

cdf cumulative distribution function

CSMA/CA Carrier Sense Multiple Access with Collision Avoidance

CTS Clear-To-Send

DSRC Dedicated Short Range Communication

DTRA Dynamic Transmission Range Assignment

GPS Global Positioning System

GSR Georaphic Source Routing

ID Node Identifier

ISM Industrial, Scientific, Medical

ITS Intelligent Transportation Systems

IVC Inter-Vehicle Communication

IVHS Intelligent Vehicles Highway Systems

LAN Local Area Network

MAC Medium Access Control

MANET Mobile Ad Hoc Network

MDDV Mobility-Centric Data Dissemination Algorithm for Vehicular Networks

MST Minimum Spanning Tree

MTR Minimum Transmission Range

NaSch-S2S Nagle and Schreckenberg with Slow-to-Start rule

NaSch Nagle and Schreckenberg

NOW Network on Wheels

ns-2 Network Simulator-2

OFDM Orthogonal Frequency Division Multiplex

PASTA Poisson Arrivals See Time Averages

pdf probability density function

PHY Physical

PRT Perception-Response Time

QoS Quality of Service

RA Range Assignment

RPGM Reference Point Group Mobility

RTS Ready-To-Send

RV Random Variable

RWP Random WayPoint

SAR Spatially Aware Packet Routing

STRAW STreet RAndom Waypoint

T^2 Takayasu and Takayasu

TC Topology Control

TPC Transmission Power Control

TRANSIMS TRansportation ANalysis SIMulation System

UDP User Datagram Protocol

UMB Urban Multi-hop Broadcast

UML Unified Modeling Language

UMTS Universal Mobile Telecommunications System

UTRA TDD UMTS Terrestrial Radio Access Time Division Duplex

V2R vehicle-to-roadside

V2V vehicle-to-vehicle

VANET Vehicular Ad Hoc Network

VDR Velocity-Dependant Randomization

WLAN Wireless Local Area Network

List of Symbols

α, β, γ = constants

$\bar{d}$ = average distance between vehicles

$\bar{h}$ = average headway

η = traffic quality of service factor

λ = sensitivity factor of a two-vehicle interaction in the car-following model

λ' = normalized sensitivity factor, $\lambda' = \lambda/(U_{max}k_{jam})$

λ_w = signal wavelength

$\mathbb{R}$ = set of real numbers

$\mu_{\ln(t)}$ = the mean of Lognormal distribution

μ_{R_L} = mean value of the transmission range across a signalized intersection

μ_{T_L}, μ_{T_r} = mean value of delay components

$\sigma^2_{T_r}$, $\sigma^2_{T_1}$, $\sigma^2_{T_2}$ = standard deviation delay components

$\sigma_{\ln(t)}$ = the standard deviation of Lognormal distribution

τ = driver's reaction time in the car-following model

τ_0 = period of red phase in traffic light

τ_1 = average time difference between the departure of last vehicle and the start of the red phase

τ_2 = average driver reaction time

τ_3 = average time required to accelerate to free-flow speed

τ_3 = delay due to acceleration

τ_d = deterministic delay component

τ_L = average total delay encountered at a signalized intersection

τ_U = that headway introduced between vehicles by an unsignalized intersection

$\mathrm{Var}(k_l)$ = variance of local densities

$\xi_j(t)$ = random variable that takes the value of 1 or 0

$\zeta_j(t)$ = random variable that takes a value in the range [0,1] at time t for the j^{th} vehicle

a = vehicle acceleration rate

c = cell index

c = wave speed

$C_j(t)$ = boolean variable representing a lane-change decision for the j^{th} vehicle at time t

d = dimension

d = distance between two vehicles

$D(\cdot)$ = dynamic transmission range assignment function

E = edge set in a network graph

$E[\cdot]$ = expected value of a random variable

$f(h)$ = probability density function of headway

f_r = fraction of running vehicles

f_s = fraction of stopped vehicles

f_s = fraction of stopped vehicles

F_{r_L} = cdf of transmission range across signalized intersection

F_{T_1} = cumulative distribution function of delay T_1

fR_L = probability density function of the transmission range across a signalized intersection

$g_j(t)$ = gap between the j^{th} and $(j+1)^{th}$ vehicle at time t

g_s = safety gap

$gb_j(t)$ = backward gap for the j^{th} vehicle in the target lane at time t

$gf_j(t)$ = forward gap for the j^{th} vehicle in the target lane at time t

H = mean headway

h = headway

$h_{\min}$ = minimum headway

h_r = height of the receiver antenna

h_t = height of the transmitter antenna

i = index variable

K = local estimate of vehicle density

k = vehicles density

k' = normalized vehicle density, $k' = k/k_{jam}$

k_1 = vehicle density separating free-flow traffic from co-existing traffic state

k_c = critical density

k_d = density of downstream traffic

k_F = vehicle density in a jam-free highway section

k_i = vehicle density of the i^{th} lane

k_L = system-wide vehicle density

k_l = local density within a short highway segment

$k_l(i)$ = local density of the i^{th} highway segment

k_u = density of upstream traffic

k_{det} = critical density in the deterministic NaSch model

k_{jam} = jam density

L = edge length of d-dimensional space

L = length of highway segment

l = lane index

l = length of a short highway segment

L_F = length of a jam-free highway section

L_J = length of a traffic jam

M = number of simulation time steps

m = number of short highway segments

N = number of vehicles on a highway segment

n = number of nodes

N_{s2s} = a random variable representing the number of time steps a vehicle may wait before it moves

n_{s2s} = number of time steps a vehicle may wait before it moves

N_J = number of vehicles in a traffic jam

n_l = number of traffic lanes

N_s = number of stopped vehicles

$N_{i,j}$ = number of vehicles in the highway segment i at time step j

$P[\cdot]$ = probability function

p_{noise} = probability of braking

p_{reject} = probability of accepting a lane change

p_{s2s} = probability of a slow start

P_r = received signal power

P_t = transmitted signal power

q = vehicles flow

q_d = flow of downstream traffic

q_F = vehicle flow in a jam-free highway section

q_n = flow of non-priority traffic

q_p = flow of priority traffic

q_u = flow of upstream traffic

$q_{det,max}$ = maximum flow in the deterministic NaSch model

q_{max} = maximum flow (capacity)

r = node's transmission range

r = transmission range of a vehicle

$r_c(k)$ = minimum transmission range as function of vehicle density

r_i, r_j = transmission range of the i^{th} and j^{th} vehicles

R_L = transmission range across a signalized intersection

r_L = transmission range across signalized intersection

r_{avg} = average transmission range as function of density

r_{c,L_F} = minimim transmission range in a jam-free highway section of length L_F

$r_{c,L}$ = minimim transmission range in a highway section of length L

r_{max} = maximum transmission range in a highway segment

s = inter-vehicle distance

$s(t)$ = inter-vehicle distance at time t

s_{max} = maximum inter-vehicle distance

SF = constant representing the safety factor

T = observation period for spot measurements

t = time

$T_j^{(1)}$–$T_j^{(5)}$ = boolean variables representing lane-change conditions for the j^{th} vehicle at time t

T_1 = random variable representing the time difference between the departure of last vehicle and the start of the red phase

t_c = safety time gap

t_f = follow-up time

T_L = random variable representing total delay

T_r = random delay component

T_s = vehicle's stopped time

T_t = vehicle's average trip time

T_{avg} = measurement period in instantaneous observation

u = vehicles speed

u' = normalized average vehicle speed, $u' = u/U_{max}$

$u(k)$ = vehicle speed as a function of vehicle density

u_0 = initial speed

u_f = the free-flow speed

u_I = speed of vehicle approaching on an interfering lane

u_i = i^{th} vehicle

$u_j(t)$ = speed of the j^{th} vehicle at time t

u_r = average speed of running vehicles

u_S = space-mean speed

u_T = time-mean speed

u_w = speed of a traffic wave

$U_{i,max}$ = the maximum speed of the i^{th} vehicle

U_{max} = the maximum speed (number of cells a vehicle may travel in one time step) in the NaSch/NaSch-S2S model

u_{max} = average maximum running speed of vehicles

V = node set in a network graph

v_0, v_1 = vehicle 0 and vehicle 1

v_i, v_j = ID of i^{th} and j^{th} vehicle

$X(\cdot), Y(\cdot)$ = mapping functions

x, y = vehicle position

x_i = position of the i^{th} vehicle

$x_j(t)$ = position of the j^{th} vehicle at time t

z_i = utilization of the i^{th} lane

Glossary

congested traffic a vehicle traffic condition in which drivers cannot maintain a desired vehicle speed due to the close presence of other neighbouring vehicles. The speed in this traffic is influenced by the surrounding vehicles. Vehicles in congested traffic may experience stop-go movement patterns due to traffic jams., p. 2.

critical density a vehicle density at which traffic exhibits a transition between free-flow and congested phases., p. 37.

free-flow speed the average speed of vehicles in free-flow traffic conditions., p. 35.

free-flow traffic a vehicle traffic condition in which drivers can maintain a virtually constant speed. The constant speed is determined by factors such as vehicle engine capability and traffic laws but it is not dependent on the speed of, or the distance to, other vehicles., p. 2.

gap the number of empty cells between two consecutive vehicles in the NaSch model., p. 52.

headway the gap, measured in time units, between two consecutive moving vehicles., p. 26.

highway a paved ground route that carries vehicle traffic within a city or between cities. Depending on the country, this type of road may be known also as freeway, arterial, motorway, or autobahn. A highway is used usually for

ground transportation among major urban centres or between rural areas and urban centres. Arterials are also found in major urban centres. The highway may have multiple lanes of traffic in one or two directions. Access to the highway is through connections that are more widely separated than connections on standard city streets., p. 4.

interfering lane a lane whose traffic direction intersects with the direction of a vehicle attempting to enter the intersection, which raises the possibility of a collision, p. 62.

interfering traffic vehicle traffic on an interfering lane., p. 5.

intersection an area where two highways join one another at, or approximately at, right angles and at the same elevation level., p. 2.

lane a path within a road that is defined by painted lines., p. 4.

non-priority traffic a vehicle traffic on the secondary highway that faces a Stop or Yield sign when approaching an unsignalized intersection., p. 116.

order parameter a physical property that changes abruptly when the underlying system experience a phase transition from one phase to another (such as between solid, liquid, and gas)., p. 6.

phase transition a transformation of a system from one state to another characterized by an abrupt change in one or more physical properties., p. 2.

priority traffic a vehicle traffic on the main highway that faces no traffic sign when approaching an unsignalized intersection., p. 116.

shockwave a traffic shockwave is an interface between two traffic phases where properties (density, flow, speed) change almost instantaneously., p. 37.

signalized intersection an intersection that depends on (electrical) traffic signals to indicate which vehicle traffic can enter the intersection at any particular time., p. 5.

slow lane a lane for slow moving vehicles., p. 58.

traffic control traffic signals and signs., p. 40.

traffic jam a number of vehicles blocking one another in a queue so that they cannot move., p. 2.

unsignalized intersection an intersection that employs traffic signs (Stop or Yield) to indicate which vehicle has the priority to enter the intersection, but leave the driver to decide when it is safe to enter the intersection., p. 5.

vehicle an automobile, a car, a truck, or a similar device that is used for ground transportation of passengers and property., p. 2.

Acknowledgements

During the writing of this thesis and the preceding years of study, I have enjoyed the personal and academic support of many individuals to whom I would like to express my sincere thanks.

I thank my wife, Muna, for her patience and understanding through the most trying of times. I also thank Muna for making me believe that I could finish this journey. I extend my gratitude to my parents, Sakeena and Mohamed, and my parents-in-law, Maream and Nuri, for their words of encouragement and their endless prayers for my success.

I am grateful to my supervisors, Dr. William (Bill) Robertson and Dr. William (Bill) Phillips, for allowing me to pursue my research interests and explore new ideas. This thesis could not have been completed without their valuable guidance and help. I also thank Dr. Robertson for offering me the position of a Research Assistant in the Master's of Engineering in Internetworking Program, which allowed me to gain the research experience and the financial support I needed to continue my study.

I thank the other members of my supervisory committee, Dr. Shyamala Sivakumar and Dr. Srinivas Sampalli, for their valuable comments on the organization and contents of this thesis. A special word of thanks goes to Dr. Guy Kember for suggesting the use of Cellular Automata models and for many stimulating discussions.

I would like to express my appreciation to Dr. Azzedine Boukerche for agreeing to act as the External Examiner and for his encouraging comments about this thesis.

I thank my friend and colleague Samer Mansour for his moral support and continued reinforcement of my self-confidence.

My research would not have been possible without the support of the Director and the staff of the Master's of Engineering in Internetworking Program who provided me with an unlimited access to the Program's laboratory and facilities.

Abstract

This thesis discusses the transmission range assignment problem in Vehicular Ad Hoc Networks (VANET) on highways. The unique mobility characteristics of vehicle traffic affect VANETs by creating a non-homogenous distribution of nodes on the network. Determining the Minimum Transmission Range (MTR) that guarantees the connectivity in various traffic conditions entails considering traffic situations that result in disturbing the homogenous distribution of vehicles. Such situations arise either from spontaneous traffic jams that occur at high vehicle densities or from road constraints. A variation of the Nagel and Schreckenberg (NaSch) model is used in this thesis to analyze vehicle traffic and develop a traffic simulator, *RoadSim*, to generate vehicle movements.

This thesis provides a number of contributions related to estimating the MTR in VANETs. A lower bound for the MTR is derived for VANETs on uninterrupted highways. This lower bound is the first analytical work that takes into account the non-homogeneous distribution of vehicles caused by traffic jams. Additional analytical and empirical relationships are derived to estimate the MTR in VANETs on a highway interrupted by an intersection. These relationships relate the MTR to the flow of vehicles approaching the intersection. This work indicates that a VANET that employs a homogenous transmission range must rely on a higher transmission range than a network of homogeneously distributed nodes to maintain connectivity.

To support non-homogenous transmission range, traffic flow models are used to derive an estimate of a vehicle's local density in congested traffic. The vehicle mobility pattern is employed to detect the phase transition from free-flow to congested conditions in the local area surrounding the vehicle. The vehicles' ability to estimate their local density and detect traffic conditions is used to develop the Dynamic Transmission Range Assignment (DTRA) algorithm. The DTRA algorithm sets the transmission range of a vehicle dynamically as the density of vehicles surrounding it changes. The proposed scheme does not require any global information such as vehicle locations, nor does it require any exchange of information among vehicles. The IEEE 802.11 protocol is modified so that each vehicle can determine its own transmission range based on the DTRA algorithm.

Chapter 1

Introduction

1.1 Motivation

Interest has increased in the past decade towards the use of computer and communication technologies to improve several aspects of transportation networks such as safety, efficiency, and productivity. This interest has led to the creation of a research field under the names of Telematics, Intelligent Vehicles Highway Systems (IVHS), and Intelligent Transportation Systems (ITS) [152]. Inter-Vehicle Communication (IVC) is usually viewed as a critical element of the ITS architecture. Many ITS projects employ short-to-medium range wireless technology to build vehicle-to-vehicle (V2V) and vehicle-to-roadside (V2R) communication networks. These networks provide the means to collect and disseminate time-critical information that helps improve the safety and increase the efficiency on the transportation infrastructure [39, 85, 144].

Given the current advances of Mobile Ad Hoc Network (MANET), it is apparent that such technology should be suitable for ITS applications. As a result, there is a growing interest among the research community in Vehicular Ad Hoc Network (VANET). VANETs include on-board active systems that facilitate V2V or V2R communication. These systems may assist drivers in avoiding collisions or dangerous road conditions. Non-safety applications include adaptive cruise control, real-time traffic congestion and routing information, high-speed tolling, mobile infotainment,

and many others [57, 116].

VANETs have many characteristics that distinguish them from other MANETs. For instance, vehicles' mobility is restricted to predetermined paths, and the speed of one vehicle may depend on the speed of the vehicles surrounding it. Moreover, density of vehicles varies greatly along the roads due to changes in speed, presence of intersections, road constructions, or other road conditions. Lessons from traffic flow theory indicate that speed and flow of vehicles become more dependent on vehicle density as the latter increases [42, 60]. The increase in vehicle density and fluctuations in speed cause vehicle mobility to shift from free-flow traffic, where vehicles can travel at any desired speed, to congested traffic due to traffic jams, where speed is a function of vehicles density. This phenomenon is well studied and compared to the phase transition phenomenon in physics [106]. In addition to spontaneous traffic jams, permanent or temporary constraints, such as intersections, access ramps, accidents or road constructions also create congestions and influence speed.

The direct result of the unique mobility characteristics of vehicle traffic in VANETs is two fold. First, congestions resulting from traffic jams and road constraints affect the homogenous distribution of nodes on the transportation network. Second, the nodes mobility, as determined by their speed, cannot be distinguished from the nodes density. Both results are in contradiction with most studies of MANETs that usually assume homogenous distribution of nodes and deal with speed and density as separate properties that can be controlled independently. For instance, common node mobility models, such as the Random WayPoint (RWP) model [41], do not have any provision for node density when setting a node's speed, and it is expected that the resultant distribution of mobile nodes remains homogenous [32, 35].

VANETs, and MANETs, face the difficult challenge of maintaining connectivity so that a vehicle (mobile node) may establish a single- or multi-hop communication link to any other vehicle in the network. The connectivity of the network is affected by factors that include transmitter power, environmental conditions, obstacles, and mobility. Increasing the transmission range of mobile transceivers may solve the connectivity problem. This solution results in more neighbours being reached and packets traveling fewer hops to their destination. However, more nodes have to share

the medium, causing more contentions, collisions, and delays that reduce capacity. Reducing the transmission range, on the other hand, may increase the capacity of the network by allowing simultaneous transmissions in different geographic locations (due to frequency reuse), at the expense of connectivity.

For these reasons, the connectivity problem is considered an optimization problem, where the objective function is the Minimum Transmission Range (MTR) that guarantees full connectivity in the network while minimizing the power needed by the transmitters. This problem is challenging in mobile networks since the network topology is constantly changing [76]. There are several approaches to solve the range assignment problem in the literature. Analytical solutions are possible in a one-dimensional network but only approximations are available in networks of higher dimensions [126]. These approaches rely on the assumption of homogenous distribution of nodes within the boundaries of the network.

The work in this thesis is unique in its focus on the discussion of the range assignment problem in VANETs within the entire range of vehicle densities (and mobility). Determining the MTR that guarantees connectivity in the entire range of densities is not possible without considering traffic situations that result in disturbing the homogenous distribution of vehicles. Such situations arise either from spontaneous traffic jams that occur at high vehicle densities or from road constraints even at low vehicle density. From a VANET perspective, nodes can be concentrated on one section of a road and scattered in another section. In such an environment, a homogenous (common for all nodes) and static (fixed) transmission range is inefficient in keeping the network connected in all traffic situations. A large transmission range wastes energy and reduces the network's capacity in traffic jams while a small transmission range partitions the network in free-flow traffic. In MANETs, a dynamic transmission range is found to be more efficient [62].

A VANET is defined in this thesis as a data communication network that is created using wireless links, without relying on a fixed infrastructure, among vehicles (automobiles, trucks, or similar devices) travelling on highways. The main topological model used throughout this thesis is defined as a continuous stretch of paved road that

consists of single or multiple lanes. This type of road may be known as highway, freeway, arterial, motorway, or autobahn, and it is used usually for ground transportation among major urban centres or between rural areas and urban centres. Moreover, vehicles are all assumed to be of the same type (say, passenger vehicles); thus, they have the same physical dimensions. Unless otherwise noted, it assumed that all vehicles are equipped with omni-directional wireless transceivers and are willing to participate in the VANET. Vehicle mobility is based on a Cellular Automata (CA) model that was introduced by Nagel and Schreckenberg in 1999 and commonly known as the Nagle and Schreckenberg (NaSch) model [104]. The NaSch model is widely used as an analytical tool to study the phase transition phenomenon in vehicle traffic. A variation of the NaSch model, which is known as the Nagle and Schreckenberg with Slow-to-Start rule (NaSch-S2S) model [46] is used in this thesis for analyzing and simulating vehicle traffic.

1.2 Contributions

Regarding the topics discussed in this thesis, a number of contributions are made which are summarized here and discussed in more details in the following chapters:

- A traffic simulator, *RoadSim*, is designed to carry all simulations of vehicle traffic in this thesis. *RoadSim* is an object-oriented traffic microsimulator based on the NaSch-S2S model. *RoadSim* extends the NaSch-S2S model by adding the several capabilities towards the support of VANET research, which distinguishes *RoadSim* from other traffic simulators. In addition to the many features of *RoadSim*, which are discussed in Chapter 4, *RoadSim* creates network graphs based on vehicle locations (vertices) and transmission ranges (edges). These network graphs are used in all computations of the MTR and measurements of connectivity provided in the other chapters. In addition, traces of vehicle movements can be translated into scripts that can be read by networks simulators, such as Network Simulator-2 (ns-2) [18]; thus, enabling the use of all features of the network simulators in the VANET research.

- A lower bound for the MTR is derived in Chapter 5 for VANETs on single-lane

highways. This lower bound is an improved version of the one developed by Santi and Blough [124] for one-dimensional networks of uniformly distributed nodes. The revised lower bound takes into account the non-homogeneous distribution of vehicles at high density due to traffic jams. Simulations show that the new lower bound estimate correctly predicts the rise in the MTR at densities beyond a critical value. The new formula provides a tighter estimate of the minimum MTR values than the original lower bound within the congested region of the vehicle density range. As densities approach a wide traffic jam, the MTR values determined from simulations are lower than the estimate as vehicles' distributions returns to the homogenous state. This work on the lower-bound estimate is the first that focuses on the non-homogeneous distribution of vehicles. The estimate indicates that VANETs must employ a higher (static) transmission range than what was estimated in [124] in order to maintain connectivity.

- Analytical and empirical relationships are derived in Chapter 6 to estimate the MTR in VANETs across a signalized intersection (controlled by traffic lights) and an unsignalized intersection controlled by a stop sign. A closed-form expression of the MTR distribution is proposed for signalized intersections. The distribution is based on the flow of traffic facing the traffic light and the duration of the red phase. Simulations of vehicle traffic are used to estimate the lower bound and the mean values of the MTR based on the flow of traffic facing the stop sign and the interfering traffic. No other known work studies the MTR requirements across intersections. The lesson learned from this work is that a VANET that employs a static transmission range must account for the non-homogenous distribution of vehicles at intersections by increasing the MTR dramatically.

- The fraction of time during which a vehicle remains stationary due to traffic jams, is used to estimate the vehicle's local density in congested traffic. The local density estimate derived in Chapter 7 is based on the speed-density relationships derived from a car-following model [111], the NaSch-S2S model [104], and the

two-fluid model [70]. Moreover, the time ratio is used as an order parameter to detect the phase change from free-flow to congested traffic conditions in the local area surrounding the vehicle. Simulations of vehicle traffic in different highway configurations show that vehicles are able to estimate the local density correctly. This contribution is significant since it differs from previous work in VANETs, which rely on message exchange among vehicles (and with fixed infrastructure) to estimate the local vehicle density. Moreover, the use of the order parameter provides the means for individual vehicles to detect local traffic conditions (free-flow and traffic jams). The ability to predict the local vehicle density and the traffic condition can be employed by VANET protocols to adapt their operations to traffic conditions by taking advantage of the favourable ones and avoiding the others.

- The vehicles' ability to estimate their local density is used to develop the Dynamic Transmission Range Assignment (DTRA) algorithm in Chapter 8. The DTRA sets the transmission range of a vehicle dynamically as the density of vehicles surrounding it changes. The proposed scheme does not require any global information such as vehicle locations, nor does it require any exchange of information among vehicles. Moreover, the algorithm inherently adapts to vehicle mobility. The use of the DTRA algorithm provides a trade-off between the choice of a homogenous transmission range, whose value remains constant regardless of connectivity requirements, and an optimal transmission range that must be computed frequently as the topology changes at the cost of additional communication overhead. Simulations show that employing the DTRA algorithm in VANETs maintains a high level of network connectivity regardless of the change in topology and in vehicle distribution due to traffic jams and intersections. The IEEE 802.11 protocol is modified so that each vehicle can determine its own transmission range based on the DTRA algorithm. The evaluation of the modified protocol shows an improved throughput at high offered load, reduced packet latency, and shorter routes in all simulated scenarios when compared the original IEEE 802.11 protocol.

1.3 Thesis outline

The remainder of this thesis is organized as follows:

Chapter 2: provides a survey of the main areas of research related to VANETs. It is noticeable that, currently, there is no published review of the literature that covers all aspects of research on this topic. This chapter provides a literature survey that covers the main research issues within VANETs with more focus on the topics related to connectivity, transmission range assignment, and vehicle mobility simulation.

Chapter 3: presents introductory material to the theory of traffic flow that provides a summary of the terminology and parameters used to describe traffic flows.The chapter's goal is to offer the reader a basic understanding of the behaviour of traffic flows, and an awareness of the methods available for vehicle traffic analysis.

Chapter 4: introduces the NaSch model and surveys many of its extensions in the literature. The NaSch model has been used extensively in the literature to study and describe the behaviour of congested vehicle traffic. This model is employed as the main analytical and simulation tool in this thesis. The chapter introduces also the traffic microsimulator, *RoadSim*, which is designed to support VANET research and is considered the first main contribution in this thesis. *RoadSim* implements the NaSch-S2S model and adds the following capabilities toward supporting VANET research: 1) generating network graphs based on vehicle positions and their transmission range, 2) translating vehicle movement into ns-2 simulator scripts, and 3) generating ns-2 scripts for initiating communication links among vehicles. In terms of implementation, *RoadSim* improves upon the NaSch-S2S model by handling additional components such as intersections and two-way roads.

Chapter 5: discusses the impact of the non-homogeneous distribution of vehicles on the connectivity problem in VANETs. The non-homogeneous distribution of vehicles is caused by the phase transition from free-flow traffic to congested

traffic. The discussion is applicable to a vehicular network in a long stretch of a highway with few lanes and without interruptions caused by intersections or entry and exit ramps. The main contribution of this chapter is to formulate a new relationship that provides a tighter estimate for the lower bound of the MTR in VANETs by considering the phase separation in vehicle traffic.

Chapter 6: formulates two relationships between vehicle flow and the MTR required to maintain connectivity in VANETs that span the two sides of an intersection. A probability density function (pdf) for the MTR is derived for a signalized intersection. The resultant MTR estimates are compared with *RoadSim* simulations. An empirical relationship between traffic flows and the MTR is obtained from traffic simulations for an unsignalized intersection.

Chapter 7: proposes a relationship that allows a vehicle to estimate the local traffic density. As a result, the vehicle will be able to estimate the density of the surrounding traffic and distinguish between free-flow and congested traffic conditions based on its own travel pattern and without any exchange of information with other vehicles or a fixed infrastructure.

Chapter 8: proposes the Dynamic Transmission Range Assignment (DTRA) algorithm. This algorithm employs the local density estimate derived in the previous chapter to set a vehicle's transmission range dynamically. The algorithm does not require any exchange of information with other vehicles or a fixed infrastructure. Therefore, there is no communication overhead involved since the algorithm uses only the vehicle's internal state to determine the transmission range. As a result, the algorithm produces a dynamic transmission range that is highly adaptable to the change in vehicle traffic conditions (density and speed). The algorithm is transparent to the data communications protocols. Therefore, it can be integrated with existing systems with little or no change to the latter.

Chapter 9: summarizes the main topics of the thesis and provides conclusions and insights into future research areas.

Appendix A: lists the main international projects related to ITS and IVC.

Appendix B: shows the Unified Modeling Language (UML) class diagrams for *RoadSim*.

Appendix C: lists examples of the *RoadSim*-generated scripts for ns-2 simulations that are used for the experiments in Chapter 8..

Chapter 2

Overview of Vehicular Ad Hoc Networks

This chapter provides a survey of the main areas of research related to VANETs. It is noticeable that, currently, there is no published review of the literature that covers all aspects of research on this topic. This chapter provides a literature survey that covers the main research directions within VANETs with more focus on the topics related to connectivity, transmission range assignment, and vehicle mobility simulation.

2.1 Introduction

Interest has increased in the past decade towards the use of computer and communication technologies to improve several aspects of transportation networks such as safety, efficiency, and productivity. This interest has led to the creation of a research field under the names of Telematics, IVHS, and ITS.

Inter-vehicle communication is usually viewed as a critical element of the ITS architecture. Many ITS projects (see Appendix A) employ short-to medium range wireless technology to build V2V and V2R communication networks. These networks collect and disseminate time-critical information that helps improve the safety and increase the efficiency on the transportation infrastructure.

With the current advances of MANETs, it is apparent that such technology should be suitable for ITS applications. VANET applications will include on-board active safety systems leveraging V2V or V2R networking. These systems may assist drivers in avoiding collisions or dangerous road conditions. Non-safety applications include adaptive cruise control, real-time traffic congestion and routing information, high-speed tolling, mobile infotainment, and many others.

Research on MANETs has covered vast ground in the past decade. The majority of this research has focused on networks where nodes assumed to be mobile devices carried by people or vehicles with a range of applications from controlling military units to e-commerce. Recently, a number of projects in Europe, Japan, and North America have initiated research that aim at investigating the use of ad hoc networks as a communication technology for vehicle-specific applications within the wider concept of ITS.

Establishing reliable, scalable, and secure VANETs poses an extraordinary engineering challenge [36]. Yet, VANETs have some advantages over general ad hoc networks that include the ability to assemble large computational resources, plentiful power sources, and constrained mobility patterns. As such, VANET can use significantly different approaches than other ad hoc networks.

This chapter provides a literature survey that covers the main research directions within VANETs. The chapter focuses on the topics related to connectivity, transmission range assignment, and vehicle mobility simulation, which are relevant to the contributions of this thesis.

This chapter is organized as follows: The characteristics that distinguish VANETs from traditional ad hoc networks are listed in Section 2.2, followed by an introduction to ITS in Section 2.3. Research directions in VANETs and IVC are summarized in Section 2.4. A closer look at research related to the scope of this thesis is provided in Section 2.4.2 that introduces the Range Assignment (RA) problem and Transmission Power Control (TPC). Vehicles mobility is discussed in Section 2.5. The chapter is concluded in Section 2.6.

2.2 VANET characteristics

VANETs are distinguished from the superclass of MANETs by the type of applications they support, their mobility patterns, and constraints. Among the special characteristics of VANETs are:

One-dimensional: While most research effort on MANETs assumes that networks consist of nodes moving freely in 2-dimensional space (e.g. walking people), vehicles mobility is restricted to the roads. In cellular networks where cells may cover several square kilometres, vehicle mobility in an urban network of streets may still be considered 2-dimensional. Current Ad Hoc standards have a limited coverage of a few hundred meters. From the perspective of these networks, vehicles on long highways move in one dimension. The work presented in this thesis is focused on the study of VANETs among vehicles traveling on highways, which can be modeled as one-dimensional networks.

Mobility Pattern: Factors such as road configuration, safety limits, traffic laws, and physical limits affect the mobility of vehicles. Drivers' behaviour and interaction with each other also contribute to the vehicle mobility pattern. As a result, vehicles do not move freely on the road, instead, they follow a complex set of rules that determine their direction, speed, and acceleration/deceleration patterns. Simulating vehicle traffic is a complex task that has been the focus of study for its applications in transportation engineering. Chapter 3 introduces some concepts from the theory of traffic flow, which form the basis for the vehicle mobility model and the traffic simulator described in Chapter 4 and used throughout the thesis.

Dynamic Topology: Vehicular Ad Hoc Networks may be created and re-configured spontaneously in a variety of traffic situations. In heavy traffic congestions vehicles may be within a couple of meters proximity of one another, whereas on a sparsely populated road the distance may be hundreds of meters. A vehicle approaching congested traffic at 135 km/hr will change in proximity from 1 kilometre to 5 meters in approximately 26.5 seconds, whilst two vehicles travelling in opposite directions at such a speed will be within a 1 kilometre range

for approximately 13 seconds. As result, communication protocols adopted by VANETs must be capable of operating in such a highly dynamic topology. Chapters 5 and 6 discuss the impact of traffic flow and highway constrains on the topology of VANET. Chapter 7 describes a mechanism to estimate the vehicle density while Chapter 8 proposes an algorithm to set the transmission range accordingly so that the network's connectivity can be maintained under various mobility conditions.

Connectivity: Research shows that the end-to-end connectivity is limited to short range communications in one-dimensional networks and in strip networks of finite width and infinite length. These networks remain almost surely divided into an infinite number of partitions, whereas end-to-end connectivity is often implicitly assumed in much of ad hoc networking research. Chapters 5 and 6 discuss the RA problem in VANETs and estimate the lower-bound transmission range needed to maintain the network's connectivity.

Resources: Mobile nodes in most MANETs are expected to be small devices such as laptops, Personal Digital Assistants (PDA), or cell phones. These devices have limited resource due to their small size and mobile nature. Therefore, MANET protocols have to incorporate power saving schemes and utilize less processing and memory resources that their counterparts in wired networks. Vehicles, on the other hand, can provide more resources; thus, they offer less restriction on the design of inter-vehicle communication protocols. Vehicles can carry large batteries, antennas and processing power. Therefore, conserving such resources is not discussed in this thesis.

2.3 Intelligent transportation systems

Intelligent Transportation Systems (ITS) include the application of computers, communications, sensor and control technologies and management strategies in an integrated manner to improve the functioning of the transportation system. These systems provide traveler information to increase the safety and efficiency of the ground

transportation system for passengers and freight in both urban and rural areas and inter-city and international corridors, including border crossings. ITS also provide valuable, real-time information to system operators such as transit systems, commercial vehicle fleets, and emergency and security vehicle fleet operators. These applications bring system users, vehicles and infrastructure together into one integrated system that enables the exchange of information for better management and use of available resources.

Interest in ITS began in the early 1990's. ITS beginnings originated in Europe where applications from the fields of information technology and transportation were developed under the notion of transport telematics. These applications take advantage of many exciting technologies such as cellular systems and position locating systems. In addition, there has been a steady increase in the role of electronics in vehicles for the past few decades, which inspired the creation of on-board data networks to organize and coordinate the activities of different electronic units used in a vehicle to serve many functions.

The major elements of ITS are categorized into seven groups [86]:

1. Travel and transportation management
2. Travel demand management
3. Public transportation operations
4. Electronic payment
5. Advanced vehicle control and safety systems
6. Emergency management
7. Commercial vehicle operations

In order to better understand the importance of ITS in the future of transportation, it is important to look at the potential functions of ITS within each of the four key components of the system: the vehicle, the user, the infrastructure, and the communication system [137]:

The Vehicle: ITS application include fleet management; in-vehicle navigation and routing advice; efficient enforcement of regulations; toll collection; tracking of freight or critical cargo movements; data collection; and automated control

functions.

The User: ITS offers in-vehicle navigation, route guidance dynamic route guidance in response to changing traffic conditions, and driver monitoring capabilities.

The Infrastructure: ITS provides services such as monitoring of weather, environmental and traffic conditions. ITS response capabilities include responding to emergencies and management of both planned and unexpected events. Other ITS services include control functions that are traditionally performed by traffic signals and similar devices, and administration functions such as toll collection.

The Communications System: ITS providers the ability to exchange information between the above three components in the system to allow for the gathering of data that can be processed into intelligence, which can then be used to determine and activate appropriate command and control actions.

ITS projects implemented in Canada, Europe, Japan, and the United States [137], showed that the potential benefits of ITS applications are considerable in all aspects of transportation systems. The key benefits of ITS technologies are improved safety of the transportation system, reduced congestion and improved mobility, enhanced economic productivity, reduced travel time and government, traveler and operator costs, improved energy efficiency and reduced impacts on the environment. A list of the main projects and activities in this field is found in Appendix A.

2.4 Research directions in VANETs

2.4.1 Enabling technologies

Two approaches exist in developing wireless technologies for VANETs. The first starts from existing Wireless Local Area Network (WLAN)technologies such as IEEE 802.11. The second approach depends on the modification of Third Generation (3G) cellular technologies to VANET environment.

IEEE 802.11

The IEEE 802.11 standard [74] specifies the Physical (PHY) and the Medium Access Control (MAC) layers of a WLAN and offers the same interface to higher layers as other IEEE 802.x Local Area Network (LAN) standards. The physical layer can be either infrared or spread spectrum radio transmission. Other features also include the support of power management, the handling of hidden nodes, licence-free operation in the 2.4 GHz Industrial, Scientific, Medical (ISM) band, and data rates of 1 or 2 Mbps. The standard does not support routing or exchange of topology information.

The IEEE 802.11 standard is the most commonly used PHY/MAC protocol in the research and demonstration of MANET and VANET due to the standard's support of infrastructure or ad hoc network. There are three basic access mechanisms defined for IEEE 802.11. The first is a version of Carrier Sense Multiple Access with Collision Avoidance (CSMA/CA). The second uses Ready-To-Send (RTS)/Clear-To-Send (CTS) handshake signals to avoid hidden terminal problem. The third mechanism uses polling to provide time-bounded service.

Dedicated Short Range Communication

This Dedicated Short Range Communication (DSRC) standard [27] describes a MAC and PHY specifications for wireless connectivity. This standard is based on IEEE Standard 802.11a [74, 75] in the 5GHz Band and meant to be used in the high-speed vehicle environment. In fact, the PHY layer of DSRC is adapted from IEEE 802.11a PHY based on Orthogonal Frequency Division Multiplex (OFDM) technology. Moreover, the MAC layer of DSRC is very similar to the IEEE 802.11 MAC based on the CSMA/CA protocol with some minor modifications.

The DSRC standard utilizes the 75MHz spectrum, which is allocated by the United States' Federal Communications Commission to provide wireless V2R or V2V communications over short distances. The standard specifies communications that occur over line-of-sight distances of less than 1000 meters between roadside units and mostly high speed, but occasionally stopped and slow moving, vehicles or between high-speed vehicles. It is expected, with the support of industry and government organizations, that the DSRC system will be the first wide-scale VANET in North America.

UMTS Terrestrial Radio Access Time Division Duplex

The FleetNet and CarTALK projects have selected UMTS Terrestrial Radio Access Time Division Duplex (UTRA TDD) as a potential candidate for the air interface that can be used for their VANET applications [95, 57, 121]. The UTRA TDD offers connectionless and connection-oriented services as well as control over Quality of Service (QoS) through flexible assignment of radio resources and asymmetric data flows. Other features include: availability of unlicensed frequency band at 2010–2020 MHz in Europe; large transmission range; support of high vehicle velocities; high data rates of up to 2Mbps .

To adapt UTRA TDD to ad hoc operation, decentralized schemes for synchronization, power control, and resource management are needed to replace the centralized schemes. Coarse time synchronization for time multiplexing is achieved using the Global Positioning System (GPS). For fine synchronization, an additional synchronization sequence is transmitted along every data burst. A combination of frequency, time slot, and code provides transmission capacity for one data connection, which can be a unicast, anycast, multicast, or broadcast connection. Only one station is allowed to transmit in one time slot. Up to 16 stations can be simultaneously reached by one station. This restriction eliminates the need for power control.

UTRA TDD reserves a number of time slots for high priority services. The remaining slots can be dynamically assigned and temporarily reserved by different stations for lower priority services using Reservation ALOHA (R-ALOHA) scheme. Potential collisions are reduced by reserving a small transmit capacity for a circuit-switched broadcast channel that is primarily used for signalling purposes but may also be used for transmitting small amounts of user data.

2.4.2 MAC layer issues

VANETs are considered a special case of MANETs with well defined applications and more severe operating constraints resulting from frequent partitioning of the network. While other research considers the sparseness of nodes as the major cause of network partitioning, this thesis is unique in its study of traffic jams as the cause of the

partitioning of the vehicular network.

Connectivity problem

VANETs, and MANETs, are faced with the nontrivial task of maintaining connectivity so that a vehicle (a mobile node) may establish a single- or multi-hop communication link to any other vehicle in the network. The connectivity of the network is affected by factors including transmitter power, environmental conditions, obstacles, and mobility. Increasing the transmission range of mobile transceivers may solve the connectivity problem. This solution results in more neighbours being reached and fewer hops being traveled by packets. However, more nodes have to share the medium, causing more contentions, collisions, and delays that reduce capacity. A short transmission range, on the other hand, increases the capacity of the network by allowing simultaneous transmissions in different geographic locations (due to frequency reuse), at the expense of connectivity. This problem is complicated by the fact that the network topology is constantly changing [76].

The problem of determining the MTR that guarantees full connectivity among a given number of nodes while minimizing the power needed by the transmitters is known as the homogenous RA problem [48, 125, 127]. The RA problem can be expressed by the question [127]: "suppose n nodes are placed in d-dimensional space, $\mathbb{R} = [0, L]^d$; what is the minimum value of the transmission range, r, such that the resultant graph among nodes is connected?" Research found that the exact solution to the RA problem in one-dimensional networks is achievable, but the problem is NP-Hard in 2- and 3-dimensional networks where only approximations are available [125, 127]. The MTR is defined in this thesis as,

Definition 2.1 *The Minimum Transmission Range (MTR) is the minimum (also called critical) value of a homogeneous transmission range that guarantees connectivity in an ad hoc network.*

Chapter 5 of this thesis summarizes some of the main results of the RA problem in the literature then continues to formulate the lower bound MTR in VANETs of non-homogenous distribution of vehicles. Chapter 6 studies the MTR in VANETs

across an intersection. In general, the MTR is studied because, in many situations a dynamically-adjusting node transmission range is not feasible. Thus, it becomes necessary for the system designer to determine the static MTR required to maintain connectivity. In this thesis, there is as additional motivation for studying the MTR, which is to show the effect of non-homogeneous distribution of vehicles on connectivity. These topics have not been discussed previously in the literature.

Transmission power control

Unlike wired networks, the network topology in wireless networks, including VANETs, is not fixed and can be changed by varying the nodes' transmission range. This problem gave rise to the research in TPC and Topology Control (TC), whose goal is to dynamically change the nodes transmission range in order to maintain the connectivity (or some other global property) of the communication graph. The main benefits of these techniques include reducing the energy consumed by node transceivers, which is directly related to the transmission range, reducing contention when accessing the wireless channel, and increasing capacity as a result of spatial reuse.

Santi [126], classifies approaches to TC according to the resultant transmission range into homogeneous and non-homogeneous. In the homogeneous case, all nodes are assumed to use the same transmission range, and the TC problem reduces to the one of determining the minimum value of r_c, as discussed in the previous section. Non-homogeneous TC allows nodes to have different transmitting ranges. This type of TC is classified into three categories based on the type of information that is used to compute the topology, the exact positions for the neighbouring nodes, their relative direction, or their identifiers [126]. The non-homogeneous TC approaches can also be classified into TPC and hierarchical topology organization approaches [29].

The DTRA algorithm proposed in Section 8.4 can be classified as a TPC mechanism. Unlike other approaches, in this algorithm no information about neighbouring nodes is collected and no central authority is required. A vehicle can determine its transmission range based on its own mobility pattern, which provides hints about the local traffic density.

2.4.3 Network layer issues

VANETs are intended to support many of the potential ITS applications that include safety alerts, warning message, and traffic information. These applications usually rely on multicast delivery services provided by the network, where the membership of the multicast groups depends on the location of vehicles and the proximity to the events of interest (e.g. all vehicles approaching a traffic accident). By the nature of these applications, multicast routing and delivery (geocast) is the most suitable "delivery strategy" for such applications. Moreover, data produced by some VANET applications (e.g. road condition warning) has a useful lifetime beyond which it may become obsolete or even harmful. Therefore, there is much interest in developing timely data dissemination mechanisms in VANETs.

Data dissemination

The work in this field is concerned about delivering vital information such as accident warnings in a timely manner to drivers to whom the information is relevant. The packet delivery mechanism needed to support such applications is multicast in nature. However, the membership of the multicast group is defined implicitly by location, speed, driving direction, and time, instead of explicit identification (e.g. all vehicles that are upstream of a traffic accident and within one kilometre range) [38].

In [144], a system is proposed where a road is divided into short segments. Mobile or stationary nodes aggregate the information relevant to the segment from sensors or received packets. The summary information is sent via one-hop broadcast to other nodes. The application layer is responsible for forwarding the per-segment information further to other nodes, after processing the relevant information. The nodes can relate the information to the corresponding segments with the help of digital maps.

For urban environments, an IEEE 802.11 based Urban Multi-hop Broadcast (UMB) protocol is proposed in [84]. This protocol assigns the duty of forwarding and acknowledging broadcast packets to only one vehicle by dividing the road segment inside the transmission range into smaller sections and choosing the vehicle in the furthest non-empty section without any priori topology information, such as the

ID or position of its neighbours. If an intersection lies in the path of the message dissemination, the authors propose the use of repeaters to initiate new directional broadcasts in all directions.

The effect of vehicle mobility was discussed in [43], which finds that when messages are stored while waiting for an opportunity to forward them, the end-to-end delay was reduced. Bi-directional and multilane highways provide additional freedom of movement, which also reduces the delay. In [129], four physical models are evaluated to measure the rate of information propagation. The study determines that the increase in operation rate, mobility rate, and vehicle density have a positive influence on the rapid propagation of information. In an urban environment, a hybrid physical model, which combines V2V and V2R communication models, achieves the best performance.

Geocast routing

In most cases, the classical schemes of routing packets cannot be applied in VANETs because the identities of the prospective receivers are not known. Therefore, many proposals rely on using geographic constraints to specify the destination of a packet. A survey of many approaches in position-based routing protocols for MANETs is provided in [132].

Some of the MANET routing protocols were modified to work in a VANET environment. The Ad-hoc On-demand Distance Vector routing (AODV) protocol is modified in [85] by adding new messages and including location (from the GPS), direction, and speed information in the route request and reply messages. The modified protocol forwards a message to a region if the interest rate (in the message) within the region is higher than a certain threshold. Depending on the size of the message and anticipated overhead, the interest rate is determined prior to sending the message or when the message reaches the boundaries of the forwarding area.

VANETs in urban environment faces the challenges of a two-dimensional system area and radio obstacles due to buildings. The authors in [94] respond to these challenges by proposing the Georaphic Source Routing (GSR) protocol, which combines position-based routing with topological knowledge obtained from digital maps. The

authors of [136] propose a Spatially Aware Packet Routing (SAR) approach to predict permanent topology holes caused by spatial constraints and avoid them beforehand. Relevant spatial information, like the road network topology is extracted from existing geographic databases, to generate a simple graph-based spatial model.

The Mobility-Centric Data Dissemination Algorithm for Vehicular Networks (MDDV) [147] is designed to exploit vehicle mobility for data dissemination. In a partitioned and highly mobile vehicular network, messages are forwarded along a predefined trajectory geographically. Moreover, since connectivity is not guaranteed, intermediate vehicles must buffer and forward messages opportunistically.

2.4.4 Applications

Many applications were proposed within the ITS projects and initiatives listed in Appendix A. Due to the current advances in wireless technology and the extensive research in mobile ad hoc, VANETs are advocated as a supporting technology for many of these applications. Among the applications intended for VANETs [54] are safety applications, traffic monitoring, and entertainment applications.

Safety Applications

In these applications, a vehicle that recognizes a dangerous situation, can report it instantly to neighbouring vehicles. The dangerous situation can be recognized by sensors that detect events such as the deployment of airbags (as a result of an accident), loss of tire traction, or sudden application of brakes. The critical requirements in these applications are latency and area of coverage [136].

Briesemeister et al [39] introduce the concept of zone-of-relevance. Inside this zone, a warning message is delivered to drivers to help them avoid dangerous situations. Vehicles outside the-zone-of-relevance may route the message but drivers are not alerted. This ensures that only relevant messages are delivered to drivers and unnecessary reactions are avoided.

Traffic monitoring

By utilizing existing capabilities of vehicles, such as Car Area Network (CAN) and GPS, VANET acts as an intelligent sensor and forms a powerful traffic information system. Vehicles take part in a signal and information processing system, allowing global information to be reconstructed from locally observed data. The advantages of using VANETs over other infrastructure-based systems include rapid deployment, self-organization, and lower-cost.

In the system proposed in [134], the vehicular ad hoc network is composed of fixed and mobile nodes (vehicles). Vehicles are organized into clusters where they exchange beacons to maintain a neighbouring relationship. Task requests are generated by nodes or from an external network and transmitted to immediate neighbours in order to monitor some condition (e.g. ice on the road). Forwarding of task requests may also occur to propagate the requests through the network. Upon receiving the request, a vehicle samples the data from the relevant sensor. The data is summarized and forwarded back to the originating node as a task response.

In another system [145, 144], each vehicle monitors the locally observed traffic situation by recurrently receiving data packets with detailed information from other vehicles. A traffic situation analysis is performed in each individual vehicle and the result is transmitted via wireless data-link to all vehicles in the local neighbourhood.

Automated highways and cooperative driving

This type of application is concerned with the automation of some driving functions in order to increase driving safety and improve the capacity of highways. Among the functions considered are platoon formation and lane merge [69, 73, 139, 79], obstacle avoidance and blind intersection assistance [Kato2003].

Entertainment

This type of application is concerned with delivering multimedia content for vehicle passengers. Among the challenges in this area is providing QoS guarantees and locating the media content. In [61] a Car-to-car peer-to-peer (C2P2) system for delivering media content using cellular and vehicular ad hoc networks.

2.5 Vehicle mobility

There is a general tendency among researchers to study sparse vehicular networks. This direction reflects the assumption that inter-vehicle communication in sparse networks is more challenging due to the difficulty in maintaining connectivity. Another reason for this choice is the reality of VANET at early stages of the market introduction when only a small fraction of vehicles support communication capabilities. Moreover, low density conditions offer more flexibility in setting the traffic parameters (flow, speed, and density) for analytical or simulation studies. As shown in Chapter 3, the assumption of independent parameters is valid only in free-flow traffic. Therefore, the results of these studies cannot be applied directly to dense traffic. It is argued in this thesis that research should focus more on dense traffic and traffic jams due to their significant influence on VANETs:

1. Vehicle density can contribute to rapid message dissemination [39, 97].

2. Higher node density aggravates the contention and collision problem in the communication protocols based on shared media.

3. It is shown in Chapter 5 of this thesis that traffic jams contribute to the non-homogenous distribution of vehicles; thus increasing the transmission range needed to maintain connectivity.

4. Vehicle traffic may change rapidly between free-flow to congested traffic due to traffic controls, road constraints, or accidents. The effect of intersections and traffic controls on connectivity is discussed in Chapter 6.

A review of research directions related to the use of vehicle mobility models and traffic simulators is provided in the next subsection. Chapter 4 will show the crucial role of a vehicular mobility model in creating traffic phenomena such as traffic jams.

2.5.1 Vehicle mobility models and traffic simulations in VANETs research

Vehicular mobility models (see Chapter 3) and traffic simulators have been in development and use since 1935 [63]. The primary focus of these simulators is on traffic analysis and forecasting in addition to the planning of transportation networks. Moreover, the ITS initiative generated an enormous number of vehicular traffic simulators since its introduction in the United States in 1991 [37]. These simulators are intended to support ITS applications, but not necessarily VANETs due to their recent introduction.

In several research papers in VANETs, simulation of vehicle movement is often considered a special type of a general mobility model such as the RWP model, perhaps with some extensions [135, 97, 136]. Such mobility models cannot produce complex vehicle manoeuvres such as car-following, accelerating, decelerating, or passing, nor can they produce global phenomena such as traffic jams. For this reason, many studies of VANETs rely on vehicular mobility models or traffic simulators to generate vehicle movement traces.

Mobility models

Studies of ad hoc networks often require keeping track of node positions at any given time, and vehicular networks are no exception. Currently, realistic vehicle movement patterns can be obtained from traffic micro-simulators, which can track many characteristics of individual vehicles, including position, speed, and direction. Earlier research in inter-vehicle communication relied on micro-simulators that were designed originally for the purpose of studying vehicle traffic in transportation networks. When adapted to VANETs research, simulators are used to generate traces of vehicle positions at regular time intervals so they can be fed later to network simulators such as ns-2 [18] to carry out the simulation of communication protocols. There is a growing interest in building traffic simulators for the purpose of VANET research [24, 45, 66, 97]. Generally, these simulators have a dual focus on the communication and mobility sides of VANETs. The microsimulator, *RoadSim*, which is developed

as a part for this thesis aims at creating realistic vehicle movement in various highway configurations, but leaves most of the simulation of communication protocols to specialized simulators. A brief review of other VANET simulators is provided in Section 2.5.2.

Traffic flow mode

Traffic simulations are used extensively in evaluating vehicular ad hoc networks. As in the analytical approaches, free-flow traffic conditions are usually preferred. The reason for this choice is the control it provides over, at least, two of the three traffic parameters in the fundamental relationship of traffic flow, as discussed in Chapter 3. Under free-flow conditions, Rudack et al [122, 121] assume that traffic flow and vehicle velocity are independent. The fundamental relationship of traffic flow (see Chapter 3) is used to derive the pdf of the communication duration between two vehicles and the pdf of the time between consecutive topology changes. Similar assumptions are made in [52] to derive the pdf for the distance at which it is possible to establish a multi-hop connection between two vehicles.

Selecting a headway (the time gap between consecutive vehicles) as an input parameter can control both the rate by which vehicles are injected to the simulation environment and the density of vehicles. In [1], the headway values are generated randomly from a Poisson distribution with an average value that ensures free-flow traffic. A uniform distribution with a minimum value that specifies the initial separation between vehicles is used in [1]. Both these examples assume that these initial traffic conditions persist throughout the simulations.

Vehicle speed

In most cases, the desired speed is provided as input to the simulations. The vehicle speed can be a constant value for each type of vehicles (e.g. cars and trucks) or sampled from a random distribution. In [59], the speed distribution is chosen to correspond to real measurements from German highways, while in [84] the speed is assigned from a Normal distribution.

One possible choice of random vehicle speed is based on the theory of "85^{th} percentile speed" that is usually used as a guide to set the speed limit on highways [131]. The 85^{th} percentile speed is defined as the speed 85% of drivers are moving at or below. About 70% of the drivers maintain a speed within a certain range around the average speed. Another 15% are slow drivers while the remaining 15% are driving at higher speeds. In [43, 121], vehicle speed is sampled from a Normal distribution using the standard deviation to mark the boundaries between slow, average, and high speeds. Although speed and headway change in real traffic, they are kept constant in [38, 39, 84].

The choice of the average speed varies according the choice of environment. In highway simulations, the average speed is set to 100–130 km/hr [59, 121]. Simulation of a city street grid sets the average speed to 40–80 km/hr either randomly [84] or according to the street type [97]. The choice of speed may reflect also the posted speed limit, road conditions and common driving habits.

Collisions

It is commonly assumed in the literature that vehicles move freely and collisions are not allowed. In contrast, vehicle density in [1] is specified to create congested traffic situations and vehicles may collide if drivers fail to react in time. This setup is necessary to evaluate the influence of V2V and V2R communication on safety [1].

Road Topology

A common choice of highway geometry is a straight highway segment of two or more lanes in each direction. The traffic flow in both directions may be asymmetric [121]. Divided highways may be used to limit the geographic area affected by message broadcast to one traffic direction [38, 39]. In [52] the effect of traffic passing through an intersection is also considered. More complex geometry is used in [45, 94, 97] to evaluate routing strategies and protocols in a city environment.

Traffic simulator

When it comes to the choice of traffic simulators, there is no apparent favourite. Among the simulators used are DYNAMO, SHIFT in [148], CORSIM in [36, 43], FARSI in [59], and Videlio in [94], in addition to proprietary traffic simulation models developed for the purpose of evaluating vehicular ad hoc networks. Traffic simulators based on CA models are easy to implement and can provide sufficient accuracy for low computational cost. These models are selected as candidates for FleetNet simulations [68, 145].

Most of the work presented in this section relies on free-flow traffic on the study of VANETs or IVC systems. The exceptions are in [1, 38, 39] where the aim is to create conditions for accidents and broadcast related safety message. Otherwise, the effect of the traffic density on the connectivity or the mobility of VANETs is not considered.

2.5.2 Integrated communication and mobility simulators

There are several new simulators and mobility models that have been developed for IVC and VANET research. These simulators integrate both communication and mobility components to a certain extent.

Lizee and Fapojuwo propose two mobility models based on velocity fields for cellular networks research [93]. Both models assume vehicles as particles instead of fluids, which provides a better estimate for the number of vehicles than other macroscopic models. The second model provides more realistic representation of traffic jams caused by accidents. The models are limited to representing traffic of single lane and single direction. Also, the models assume that vehicles follow the local traffic laws regarding the recommended headway distance.

Among the recently proposed simulators is GrooveSim [97]. In simulation using GrooveSim, vehicles can travel on real city street maps using one of four mobility models. The communication components of the simulator include routing and transport protocols. GrooveSim, however, does not support the car-following model or multi-lane traffic (i.e. it is possible for faster vehicles to go over the slower ones). Dense traffic can only be created by manipulating the input parameters of one of

the mobility models, and not by interactions between the vehicles. Moreover, the simulator does not account for buildings and other obstacles.

The simulator described in [45] also uses real street maps, but vehicles move according to the STreet RAndom Waypoint (STRAW) model. STRAW combines a car-following model, which sets the vehicle speed in relation to the speed of the preceding vehicle, with additional rules to deal with intersections and traffic controls (stop sign and traffic lights). The simulator does not support lane-change and it does not include the notion of buildings and obstacles.

The simulator, *RoadSim*, which is developed in this thesis, is based on a CA model where complex vehicles movement patterns can be created by specifying a few simple rules. The rules used in the NaSch-S2S model create behaviour similar to car-following models with a constant headway. In *RoadSim*, more rules are added for intersections, traffic controls, and lane-change. These manoeuvres cannot be created easily with car-following models. Moreover, it is possible, using *RoadSim*, to create any grid of intersections and roads (with multiple lanes and two directions). *RoadSim* includes some extensions for VANET research. Among these extensions are the components responsible for creating communication graphs among nodes based on their transmission range, and construction of a Minimum Spanning Tree (MST) to determine the MTR. *RoadSim* can translate node movements and transmission range into ns-2 scripts and generate connection scenarios for ns-2 simulations.

2.6 Summary and conclusions

The chapter provides an overview of the characteristics that distinguish VANETs from traditional ad hoc networks. Most of these characteristics are addressed in different parts of this thesis. International interest in ITS applications provides the main driving force in VANET research. An introduction to ITS and summaries of the main IVC projects are provided. Research directions in VANETs and IVC are summarized and listed according to their classification in the communication layers. The topics of vehicle mobility, connectivity, and TPC are covered in separate sections.

Chapter 3

Brief Introduction to Vehicle Traffic Theory

This chapter presents introductory material to the theory of traffic flow that provides: 1) a summary of the terminology and parameters used to describe traffic flows, 2) a basic understanding of the behaviour of traffic flows, and 3) an awareness of the methods available for vehicle traffic analysis.

3.1 Introduction

Problems of road traffic are complex; they involve human nature on one hand and physical laws of time, space, and movement on the other. At least five approaches to study traffic problems are possible [26]: Empirical and intuitive studies collects traffic statistics (e.g. accidents) and use standard data analysis techniques to determine the connections between various relevant quantities. Several deterministic theories are proposed to describe traffic dynamics at the macroscopic level. Probabilistic flow models and queuing theory may represent intersections or lengths of roads and help determine quantities of interest such as the delay, the capacity, or the average speed. Finally, traffic simulations are resorted to when analytical methods are deemed inadequate to solve traffic problems.

Theories of vehicle traffic flow are developed to define the relationships among quantities such as vehicle density, speed, and flow. In general, the mathematical bivariate relationships among the three quantities have discontinuities that predict an abrupt change of the relationship. These changes manifest themselves as the familiar congestion waves experienced by drivers.

Research in traffic flow theory has been advanced with the introduction of CA models in the past decade. Simulation of vehicle traffic using the CA models has shown that vehicle traffic exhibits characteristics similar to the well-known phase transition phenomenon in physics. As a result, it is proposed that vehicle traffic may be in a state that resembles the gas or liquid states in substances, which are homogenous states. Traffic can also be in a non-homogeneous state where both gas and liquid exist.

The chapter starts by defining the main characteristics that are used to describe traffic flow in Section 3.2, and the fundamental relationship of traffic flow that relates these characteristics to each other in Section 3.3. This relationship will be used extensively throughout the thesis. Section 3.4 introduces four of the main models that have been used in the literature to study vehicle traffic. These models form the basis for the MTR estimates in Chapters 5 and 6, and density estimates in Chapter 7. This thesis makes an extensive use of the concepts of phase transition and order parameter; both are introduced in Section 3.5. Later in this chapter, a brief summary of various approaches to traffic simulations is provided in Section 3.6.

3.2 Traffic flow characteristics

In studying road traffic as a stream, the interest is focused primarily on three characteristics of the stream. The flow, q, measures the number of vehicles that pass an observer per unit time. The density, k, measures the number of vehicles per unit distance. The speed, u, measures the distance a vehicle travels per unit time.

In general, traffic streams are not uniform, but vary over both space and time. Because of that, the quantities q, k, and u are meaningful only as averages or as samples of a random variable. In reality, the traffic characteristics that are labelled

as flow, speed, and density are parameters of statistical distributions, not absolute numbers [26, 67].

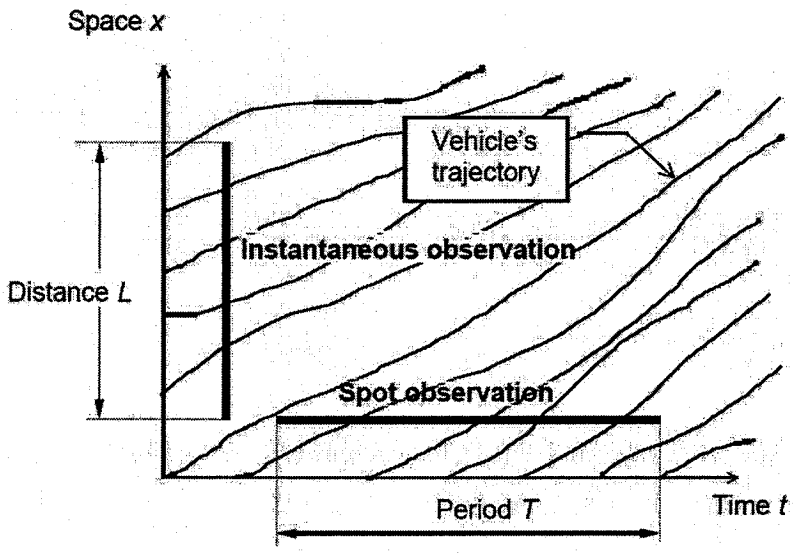

Figure 3.1: Spot and instantaneous traffic observations [72].

Vehicles can be counted and their speeds measured as they pass a specific location during an observation period. This type of observation is called spot observation. There is a second type of observation, instantaneous observation, in which vehicles on a designated highway segment are counted and their speeds measured instantly, see Figure 3.1. Traffic density and space-mean speed are directly estimated with instantaneous observations. Traffic volume and time-mean speed are directly estimated with spot observations [133].

Instantaneous observations render the number of vehicles, N, on some highway segment at a given time of measurement. This count can be converted to traffic density, k:

$$k = \frac{N}{L \times n_l}, \tag{3.1}$$

where k is measured in vehicles per kilometre per lane (veh/km/lane), L is the length of the segment expressed in kilometres, and n_l is the number of traffic lanes. Typically, density is measured in each direction separately. The speeds of vehicles, u_i, at the moment of measurement can be averaged to calculate the so-called space-mean speed,

u_S:

$$u_S = \frac{1}{N}\sum_{i=1}^{N} u_i \ . \tag{3.2}$$

Spot observations render the number of vehicles passing a spot during an observation period, T. This count can be converted to traffic flow, q:

$$q = \frac{N}{T} \ . \tag{3.3}$$

The speeds of vehicles can be also measured in spot observations. The resultant average speed, called time-mean speed, is calculated as follows:

$$u_T = \frac{1}{N}\sum_{i=1}^{N} u_i \ , \tag{3.4}$$

where u_T is the time-mean speed calculated based on N spot measurements, and u_i is the speed of the i^{th} vehicle included in the observation. The time-mean and space-mean speeds measured for the same traffic are typically not equal since the former does not account for stopped vehicles [26]. All measurements of density and speed in this thesis are based on instantaneous observation as given in (3.1) and (3.2). As a result, the average (mean) speed refers to the space-mean speed, i.e. $u = u_S$.

3.3 Fundamental relationship of traffic flow

Traffic flow is related to the headway between vehicles. The headway is defined here as the difference in arrival time between two consecutive vehicles as measured by a person standing at a fixed point on the road. Assuming that all vehicles move at the same speed of u, then the headway between two consecutive vehicles, h, is obtained by dividing the distance, d, between these two vehicles by speed, u, ($h = d/u$). If someone measures the headways and the distances between consecutive vehicles and calculates the average values, $\bar{h}$ and $\bar{d}$, the relationship between the average values will be preserved, i.e. $\bar{h} = \bar{d}/u$. Notice also that $q = 1/\bar{h}$ and $k = 1/\bar{d}$ [42]. Thus,

$$q = u \times k \ . \tag{3.5}$$

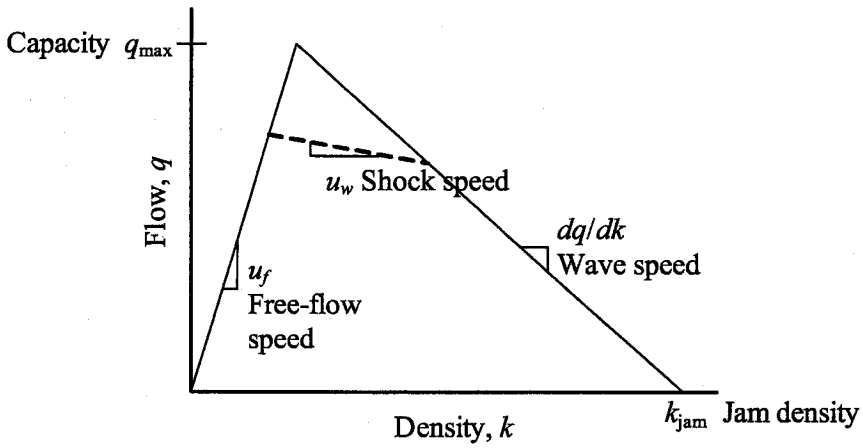

Figure 3.2: The Fundamental Diagram of Road Traffic.

Equation (3.5) is called the Fundamental Traffic Flow Relationship. For comprehensive derivation of this relationship, see [65]. All bivariate relationships among the variables of (3.5) are studied in the literature. Some of the efforts begin with mathematical models while others are primarily empirical (see the discussion in [67]). The bivariate relationship between traffic flow and density is so useful it is called The Fundamental Diagram of Road Traffic. The q–k relationship can be deduced intuitively [26] as follows. The flow must be zero when density is zero. Flow also falls to zero when density is at maximum (vehicles are stationary in a traffic jam). For values of density between these limits flow must rise to at least one maximum. Experimental data seem to confirm this argument, but there is some conflicting evidence regarding the exact shape of the curve. Earlier studies assumed the curve to take a parabolic shape [26, 65]. Recent studies predict the triangle shape shown in Figure 3.2 (see the references in [42, 67]). Furthermore, empirical data such as those reported in [106, 100, 81], and simulations using CA models [106], including the simulations produced in Chapter 4, show that the fundamental diagram may take the so-called reverse λ shape. The latter shape is an extension of Figure 3.2 and will be described in more detail in Section 3.5.

Figure 3.2 shows that vehicle density has a maximum value denoted k_{jam}, the density of a traffic jam. The traffic jam density is regarded as the reciprocal of the

average length a vehicle occupies in a traffic jam. The maximum value of flow is denoted q_{max}. The maximum flow is also known as the 'capacity' of the road.

The left branch of the fundamental diagram describes free-flow traffic. Vehicles in this traffic condition move free from interference from other vehicles. The average free-flow speed of vehicles, u_f, is the ratio of flow to density. Figure 3.2 suggests that the free-flow speed remains constant as density increases up to a point where the increase in vehicle density starts to influence drivers and force them to reduce speed. Beyond this point, vehicle speed is dependent on the density.

The right branch of the fundamental diagram describes a congested traffic condition whereby q decreases with increasing k. The slope of this branch represents the speed of the traffic jam wave propagating backward relative to the direction of traffic, dq/dk [42, 65]. Given the previous discussion, it is possible to define the following terms to be used in the remainder of the thesis:

Definition 3.1 *free-flow traffic is a vehicle traffic condition in which drivers can maintain a virtually constant speed. The constant speed is determined by factors such as vehicle engine capability and traffic laws but it is not dependent on the speed of, or the distance to, other vehicles.*

Definition 3.2 *congested traffic is a vehicle traffic condition in which drivers cannot maintain a desired vehicle speed due to the close presence of other neighbouring vehicles. The speed in this traffic is influenced by the surrounding vehicles. Vehicles in congested traffic may experience stop-go movement patterns due to traffic jams.*

Definition 3.3 *traffic jam is a number of vehicles blocking one another in a queue so that they cannot move.*

3.4 Traffic flow models

Traffic flow characteristics – volume, density, and speed – do not vary independently from one another. The fundamental relation of traffic flow (3.5) ties these three characteristics together and allows for calculating the quantity of one of them when

the other two are known. An additional equation is needed in order to calculate two unknown flow characteristics from one known.

There is no single theory that can explain all the complexities of traffic. Instead there are several models that try to explain the relationships between traffic parameters. The oldest among these is a macroscopic model based on the fluid-dynamic theory, a gas-kinetic model based on the Boltzmann equation, and a microscopic, optimal velocity model (car-following model) based on the assumption of a delayed adaptation of velocity. Recently, many publications in physics journals [150, 80, 46, 53, 107, 30] model traffic as a system of interacting vehicles. These traffic models are more successful in describing physical phenomena such as the phase transition. One CA model, the NaSch model will be used extensively in this thesis as an analytical tool to derive various relationships in Chapters 5 through 7. The CA models will be introduced briefly in Section 3.5 and in more detail in Chapter 4.

Like other traffic models, the NaSch model does not describe all aspects of vehicle traffic. The following sub-sections include an overview of three main traffic models. Each one of these models describes some aspect of vehicle traffic that will be employed in later chapters. These models are related in many ways. In Chapter 5 a relationship between the car-following model, the two-fluid model, and the NaSch will be proved. This relationship will be employed in Chapter 7 to allow vehicles to estimate their local density without relying on any infrastructure or on exchange of information with other cars.

3.4.1 Macroscopic (continuum) traffic models

Highway traffic can be visualized as a stream or a continuum fluid. Because of this analogy, traffic is often associated with fluid flow and treated similarly as a one-dimensional compressible fluid. Applications of continuum models include describing traffic-waves and shock waves at traffic signals (see Chapter 6). The theory can also describe traffic flow along a multi-lane highway. This section will introduce the basics of this theory; a comprehensive review is found in [87].

The continuum theory of traffic flow is based on two relations. One is the law of conservation of vehicles. The other is an assumed relation between the flow and

density [26, 87]. In one-dimensional flow, consider that measurements of the flow, q, are taken at two points, $x = a$ and $x = b$, a short distance apart, assuming there are neither entrances nor exits between these points. Then the change in the number of cars results from car crossings at $x = a$ and $x = b$ only. The conservation of cars is expressed as follows [65]:

$$\frac{\partial k}{\partial t} + \frac{\partial q}{\partial x} = 0 \,. \tag{3.6}$$

This equation states that if, at a specific location, the flow coming in from the left is less than the flow going out to the right, then density has to decrease at that location over some time, t. On the other hand, the density must increase if the incoming flow is greater than the outgoing flow. An additional equation or assumption is needed to solve (3.6). One possible option is to state that speed is a function of density, $u = u(k)$, which is a very reasonable assumption, but it is only valid in dense traffic. It follows from this assumption that drivers adjust their speed according to the density (i.e., as density increases the speed has to decrease to maintain safe headway). Then q is assumed to be a function of density only, $q = ku(k)$. It should be noted that $u(k)$ can be any function (see Section 3.4.2). Then, (3.6) can be written as

$$\frac{\partial k}{\partial t} + \frac{dq}{dk}\frac{\partial k}{\partial x} = 0 \,, \tag{3.7}$$

where $dq/dk = u(k) + ku'(k) = c$.

The solution of (3.7) suggests that the density k is constant along a family of curves called characteristics or waves; a wave represents a change in flow and density along the roadway. The speed of the wave is c, a constant representing the slope of the flow as a function of density evaluated at a constant density . It is shown in [26, 65] that the value of c is negative when the road is used beyond a critical density and it represents the traffic wave velocity propagating backwards (see Figure 3.2).

A shockwave is created when two characteristic lines intersect. A shock then represents a mathematical discontinuity in q–k, or u–k relations. Physically, a shockwave is an interface between congested and free-flow traffic; it is created where vehicles slow down or accelerate rapidly. The shock wave can travel forward or backward (the end of a growing queue moves backward while the end of a dense column of vehicles

behind a truck can move forward). The speed of the shock wave, u_w, is [133, 87]:

$$u_w = \frac{q_d - q_u}{k_d - k_u} . \tag{3.8}$$

where k_d, q_d and k_u, q_u represent downstream and upstream traffic parameters, respectively. In Figure 3.2, the shockwave speed is represented by the slope of the dotted line connecting the two traffic conditions (free-flow and congested traffic).

3.4.2 Car-following models

The car-following models apply to single-lane dense traffic with no overtaking. The models are based on the assumption that each driver reacts in some specific fashion to a stimulus from the vehicles ahead or behind. In general, road conditions do not affect interactions between vehicles. A different approach is necessary for low densities where interactions between vehicles disappear. The basic equation of the car-following model is [26], *Response* = *Sensitivity* × *Stimulus*. The response is taken as the acceleration of the following vehicle. It has been established also that the stimulus is the relative speed between the following vehicle and the lead vehicle. One example of the stimulus-response equation of the car-following model is [26, 65, 119]:

$$\frac{d^2 x_i(t+\tau)}{dt^2} = \lambda \left(\frac{dx_i(t)}{dt} - \frac{dx_{i-1}(t)}{dt} \right) , \tag{3.9}$$

where x_i is the position of the i_{th} vehicle, τ is the driver's reaction time, and λ is the sensitivity of the interaction, which is considered proportional to the headway between the two consecutive vehicles. The sensitivity may take the value of one of several functions (see [26] pp.24, and [119] pp.20).

Equation (3.9) and similar equations [119] are used in the literature to derive the speed-density and the flow-density relationships for single-lane steady-state traffic flow. In the linear case, λ is assumed to be constant and the equation (3.9) is integrated to derive the velocity-density relationship [111]:

$$u = \lambda \left(\frac{1}{k} - \frac{1}{k_{jam}} \right) . \tag{3.10}$$

The linear car following model specifies an acceleration response which is completely independent of the inter-vehicle distance (i.e., for a given relative velocity,

response is the same whether the vehicle following distance is small or large). In order to take the following distance into account, the linear model can be modified by assuming that λ is inversely proportional to the following distance [119].

Equation (3.10), which was proposed by Pipes in 1953 [111], has an undesirable feature; the speed tends to be unrealistically high near low densities. Recent observations of freeway traffic and simplifications in traffic modeling have led to the modification of the equation (3.10) [133].

$$u = \min \left[u_{max},\ q_{max} \left(\frac{1}{k} - \frac{1}{k_{jam}} \right) \right] . \tag{3.11}$$

where the speed cannot exceed a maximum value of u_{max}.

Figure 3.3 shows the speed-density relationship of (3.11). The flow can be obtained by substituting (3.11) into the fundamental relationship (3.5),

$$q = \min \left[u_{max} k,\ q_{max} \left(1 - \frac{k}{k_{jam}} \right) \right] . \tag{3.12}$$

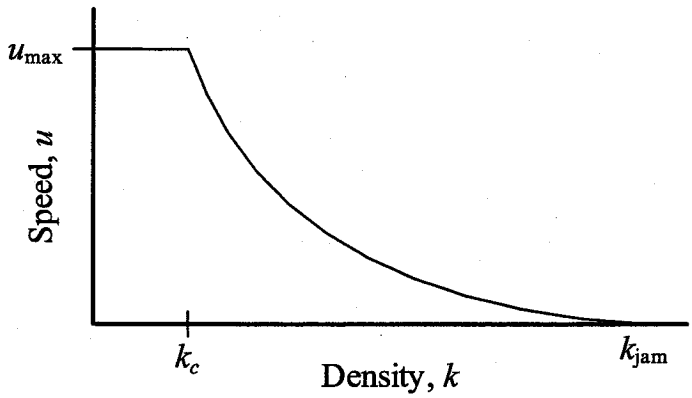

Figure 3.3: The speed-density relationship (Pipes Equation).

Equation (3.12) is represented by the q–k relationship of Figure 3.2. These equations are quite useful in understanding the effect of driver behaviour on traffic conditions. One plausible result is that drivers tend to slow down when density increases; another is that capacity is reached at a particular density value. If density grows beyond some critical value, k_c, the loss in flow caused by the speed decrease exceeds the gain caused by the density increase, and the flow drops. Capacity is determined

by the headway drivers maintain between vehicles. Drivers select spacing perceived as safe for the speed that persists in the capacity conditions.

Throughout this thesis, the relationships speed-density and flow-density are assumed to follow equations (3.11) and (3.12), respectively. The traffic simulations produced by *RoadSim* in Chapter 4 results in relationships that are similar to those shown in Figure 3.2 and Figure 3.3 (with some differences that will be clarified in Chapter 4). The reason for this similarity is that the NaSch model belongs to the same class of the car-following models as the Pipes model, which assumes a linear relationship between speed and the distance between vehicles. Moreover, in Section 4.4.3 the value of the sensitivity factor, λ, will be estimated using simulations. Later, in Section 7.3, the value of λ will be derived analytically by exploring the link between the Pipes equation and the NaSch model. Both results will be used in Chapter 7 to estimate the local vehicle density.

3.4.3 Two-fluid model

The two-fluid theory of traffic was proposed by Herman and Prigogine [70] to measure the quality of traffic service in an urban street network. The model applies to congested traffic - traffic in the right branch of the q–k relationship. Vehicles in the traffic stream are divided into two classes (hence, two fluids): running and stopped vehicles. Those in the latter class include vehicles stopped in the traffic stream due to traffic control signals and signs, blocking vehicles, normal congestion, but exclude those that are outside the traffic stream (e.g., parked cars). The model is based on two assumptions [21, 70]:

1. The average running speed in a street network is proportional to the fraction of vehicles that are moving, and

2. The fractional stop time of a test vehicle circulating in a network is equal to the average fraction of the vehicles stopped during the same period.

The first assumption of the two-fluid theory relates the average speed of the moving (running) vehicles, u_r , to the fraction of moving vehicles, f_r , in the following manner:

$$u_r = u_{max}\, {f_r}^{\eta} , \tag{3.13}$$

where u_{max} is the average maximum running speed, and η is an indicator of the quality of traffic service in the network.

The average vehicle speed can be defined as $u = u_r f_r$, and $f_r + f_s = 1$, where f_s is the fraction of stopped vehicles. Therefore, (3.13) can be rewritten as,

$$u = u_{max} (1 - f_s)^{\eta+1} . \tag{3.14}$$

The second assumption of the two-fluid model relates the fraction of time a test vehicle circulating a network is stopped during a trip time to the average fraction of vehicles stopped during the same time, or

$$f_s = \frac{T_s}{T_t} . \tag{3.15}$$

where T_s is the stopping time, and T_t is the trip time.

This relation has been proven analytically [21], and represents the ergodic principle embedded in the model, i.e., that the network conditions can be represented by a single vehicle appropriately sampling the network.

The parameter, η, is a measure of the resistance of the network to degraded operation with increased demand. Higher values of η indicate networks that degrade faster as demand increases. Field studies and simulations show that values of two-fluid parameters are influenced by drivers' behaviour and network features [143]. Simulations in Section 4.4.4 show that $\eta = 0$ when vehicles are moving according to the NaSch model.

The two-fluid theory is significant to this thesis because it shows that a single vehicle may predict the surrounding traffic condition, more specifically the fraction of vehicles stopped in the transportation network, based on the vehicle's own movement (and stopping) pattern. This result will be used in Chapter 7 in combination with results from other traffic models to derive a relationship that allows a vehicle to estimate the local density.

3.4.4 Cellular automata models

Recently, there has been much interest in studying traffic flow problems within the context of CA models. Cellular automata are dynamic models in which space, time,

and state are discrete. Discrete space consists of a grid of cells where each one can be in one of a finite number of possible states. The states of the cells in the grid are updated according to a local rule. That is, the state of a cell at the next time step depends only on its own current state, and the current states of its nearby neighbours. All cells in the grid are updated in parallel, so that the state of the entire grid advances in discrete time steps. Details of the system, including lane changing, complex turns and intersection configurations, are fully represented and each driver is given a destination and a preferred path.

Compared with the other traffic flow models, the CA models are conceptually simpler, and can be readily implemented on computers. These models capture the complexity of the nonlinear character of the problem and provide clear physical pictures. For example, CA models show the existence of a transition between a free-flow phase and a congested phase in the vehicle traffic as the car density is varied. A well-known CA model, the NaSch model [104], will be discussed in detail in Chapter 4.

3.5 Phase transition and order parameter

The behaviour of vehicles in a traffic jam can be described by this example [106]. Consider a situation when a constraint causing a traffic jam has just been cleared. Assume there is a queue of five vehicles of zero speed creating a small traffic jam. In the first time step, only the lead vehicle can move. In the second time step, the second vehicle can start, and so on. In the meantime, it can happen that other vehicles join the queue at the upstream end. Given the right conditions (no less vehicles joining at the upstream end than leaving at the downstream end), this results in a cluster of vehicles of zero speed moving against the traffic direction. The vehicle composition of this cluster is constantly changing–from the perspective of an observer. This represents the wave phenomenon that is described by the theory of kinematic waves equation (3.6).

It is believed that the scenario described above may occur without the presence of obvious constraints but mainly due to fluctuation (noise) in driving speed. These fluctuations may be caused by bumps, curves, lapses of attention, and different engine

capabilities. The amount and type of congestion induced by erratic drivers depend on how much the leading car's speed fluctuates. Moderate fluctuations of an erratically driven car can trigger a train of density waves, which moves upstream like shock waves. As the average speed decreases, isolated moving clusters may grow quickly into a nearly continuous jam [109]. This type of traffic jam has been studied extensively using traffic simulation models [78, 99, 100, 103, 118]. The phase transition phenomenon occurs in composite systems and is being described as emergent feature because it is observable at the macroscopic level but not the microscopic level [102].

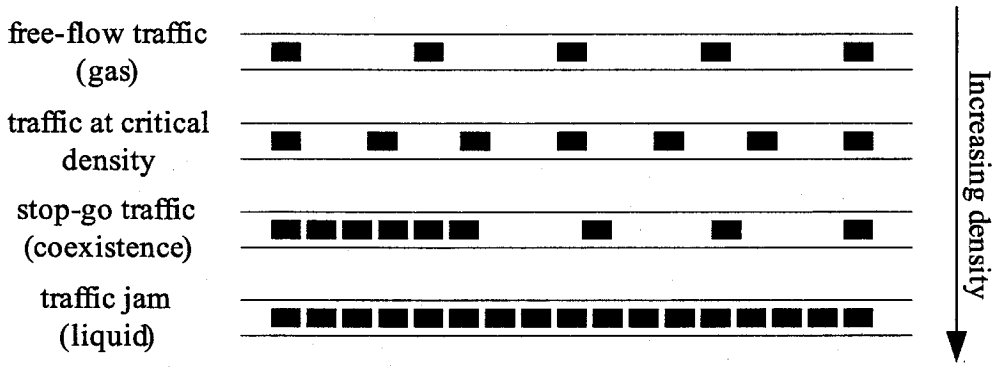

Figure 3.4: Phase Transition.

The breaking down of vehicle traffic into traffic jams has properties similar to phase transition in physical matter. Given the gas-liquid analogy of Figure 3.4, traffic has two phases and can be in one of three states. Free-flow traffic would correspond to the gas phase, jammed traffic would correspond to the liquid phase, and traffic characterized by stop–go waves would correspond to the coexistence of liquid and gas. A transition between the two phases occurs at a critical point [77]. An alternative point of view divides traffic into three phases where free-flow and jammed phases are separated by a synchronized flow phase, and there are two critical points that separates the three phases [80].

Figure 3.5 reflects the speed-density relationship that results from traffic conditions similar to ones shown in Figure 3.4 [102]. The left branch (OA) of the relationship represents free-flow traffic at densities below k_1. At densities above k_2, traffic

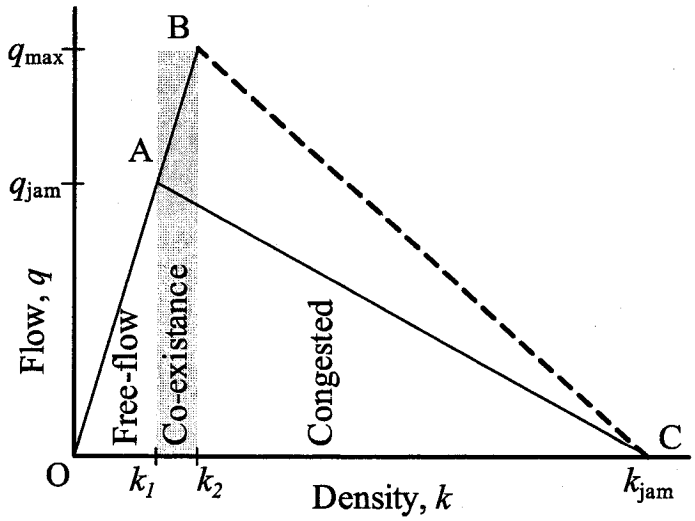

Figure 3.5: A reverse λ shape fundamental diagram showing free-flow, congested, and mixed state traffic conditions.

become congested and hindered by traffic jams. The q–k relationship of the congested traffic is represented by the right branch (AC). Empirical evidence [102] and traffic simulations suggest that traffic may also be in a coexistence phase. In densities between k_1 and k_2, drivers may accept shorter headways between vehicles; thus, achieving the maximum flow q_m, at the critical density, k_2. High fluctuations of speed in this traffic phase may cause a break down in the flow and drive the traffic into the congested phase. The dashed line (BC) shows the relationship between the reverse λ shape and the triangular shape of the fundamental diagram shown in Figure 3.2.

Although the traffic models described in Section 3.4 predict the occurrence of traffic jams and shock waves, they do not show the break down of traffic into three states. The speed-density relationship of Figure 3.5 can be generated by the NaSch-S2S model by the choice of appropriate parameters [77], which will be discussed in detail in Chapter 4.

Phase transitions are classified, in physics, into first and second order. The first order transitions are discontinuous. The system changes its state from one phase to the other in a spontaneous way such that there is an obvious interface between phases at a critical point. The second order transitions are continuous. There is a gradual change from one phase to the other such that there is no distinct phase at a critical

point.

Phase transitions describe systems going between a disordered state and an ordered state. Order is a macro feature that is characterized by an order parameter, which is a macroscopic variable that describes variations between macro states. The order parameter takes a finite value in the ordered state and zero in the disordered state.

As the previous example of the road scenario indicates, vehicles in a traffic jam are not permanently stopped. Instead drivers experience a repeated stop–go sequence. An external observer monitoring the traffic (say from a helicopter) will notice that there is a fraction of vehicles whose speed is zero at any given moment. This fraction can be considered an order parameter characterizing the traffic flow [96, 118, 140]. In the free-flow state of traffic, all vehicles are moving and the order parameter is zero (the system is disordered). In traffic jams, the order parameter is nonzero (the system is in ordered state).

The order parameter concept described here is not different from the fraction of stopped vehicles that was used in (3.14) to determine the average speed. The same concept will be used in the DTRA algorithm described in Chapter 8 to distinguish between free-flow and congested conditions.

3.6 Traffic simulation

Traffic simulation models are effective tools for analyzing complex problems that cannot be described easily in analytical terms because of the complex, simultaneous interactions of many system components. Traffic simulation models can be used for a wide range of applications [91]. Almost all traffic simulation models describe dynamical systems where time is always the basic independent variable. Continuous simulation models describe how the elements of a system change state continuously over time in response to continuous stimuli. Discrete simulation models represent real-world systems (that are either continuous or discrete) by updating their states abruptly at points in time.

There are generally two types of discrete models: discrete time models, and discrete event models. Discrete time models segment time into a sequence of time intervals. Within each interval, the simulation model computes the activities which change the states of selected system elements. Discrete event models are effective and economical when the system states change infrequently. However, for systems that experience a continuous change in state, such as vehicle traffic environment, and where the model objectives require very detailed descriptions, the discrete time model is the better choice due to the frequent change of the system states.

Simulation models may also be classified according to the level of detail with which they represent the system to be studied [91]:

A microscopic model describes both the system entities and their interactions at a high level of detail. For instance, a decision to change lanes is determined for each individual vehicle by considering the distance to its current leader, then its presumed leader and follower in the target lane. The duration of the lane-change manoeuvre can also be calculated.

A mesoscopic model generally represents most entities at a high level of detail but describes their activities and interactions at a much lower level of detail than would a microscopic model. In this model, the lane-change decision could be based, say, on relative lane densities, rather than detailed vehicle interactions.

A macroscopic model describes entities and their activities and interactions at a low level of detail. For instance, a traffic stream may be represented by scalar values of flow, density, and speed. Lane changes in this model may not be represented at all; instead, the model ensures that the traffic stream is properly allocated to lanes.

Microscopic models are known to be costly to develop, execute and to maintain, relative to the other models, but they possess the potential to be more accurate. Macroscopic models may be less accurate in their representation of the read-world system, but they are appropriate when the intended results are not sensitive to details, when the scale of application is too big to be accommodated by microscopic models, or when resources are limited.

Another classification addresses the processes represented by the model as either deterministic or stochastic. Deterministic models define all entity interactions by exact relationships (mathematical, statistical or logical). Stochastic models have processes that include probability functions. A car-following model, for example, can be formulated either as a deterministic or stochastic relationship by defining the driver's reaction time as a constant value or as a random variable, respectively.

RoadSim, which is discussed in Chapter 4, is a discrete-time, stochastic traffic simulator. Since it is based on a CA model, *RoadSim* is capable of creating interactions among vehicles at a high level of detail; thus it is considered a microscopic simulator. *RoadSim* has been developed to simulate vehicle traffic for VANETs research. This type of simulator is discussed earlier in Section 2.5.1.

3.7 Summary and conclusions

Vehicle traffic is characterized by three parameters: flow, density, and speed. Although there is a simple, 'fundamental relationship' that relates the three parameters, the bivariate relationships among them have been the subject of intensive research for the past five decades. The flow-density relationship is called the Fundamental Diagram of Road Traffic and it shows that traffic flow increases as density increases until it reaches a maximum value, called road capacity, then the flow starts to decline until it reaches zero at maximum density, called jam density. The density at which flow reaches capacity separates free-flow traffic from congested traffic where vehicle speed is influenced by vehicle density. Several theories are proposed to define the relationships among traffic parameters and explain field observations.

Similarities between traffic flow and fluids gave rise to continuum models, which discuss the relationship between traffic flow and density. The models determine the speed of traffic waves caused by congestions at bottlenecks. The models also explain discontinuities in flow-density relationship as a result of shock waves which occur due to abrupt changes in speed. Car-following models provide a relationship between vehicles' speed and density based on a stimulus-response model. These models apply to single-lane, congested traffic, but not to light traffic where vehicles tend to move

freely unaffected by other vehicles. Two-fluid theory predicts the relationship between the trip time of a test vehicle and the average speed of vehicles on the road.The previous models predict that vehicle traffic remains in free-flow state until density reaches a certain point beyond which sufficiently large fluctuations will cause traffic jams. This phenomenon is analogous to phase-transition in physics and is useful to explain discontinuities in bivariate relationships among traffic parameters. The CA models are dynamic systems in which space, time, and the states of the system are discrete. These models are particularly useful in studying the phase transition phenomenon.

All the above models predict that there is a direct relationship between vehicle speed and density in dense traffic. As a result, it is unreasonable to assume that these quantities are independent in VANETs as they are usually assumed in MANET research, except in free-flow traffic, where the traffic models do not provide any information about the speed–density relationship.

Complexities of vehicle traffic prevent the use of mathematical models in solving all but simple problems. Studies that involve complex traffic scenarios must resort to traffic simulations. Traffic simulators are classified according to the details in mimicking real-world traffic into microscopic, mesoscopic, and macroscopic. Microscopic traffic simulators, microsimulators, are highly accurate because they reproduce detailed interactions between vehicles. The CA models are used to build microsimulators due to their easy adaptation by computer systems.

In MANETs, analytical studies of connectivity in one-dimension usually assume that nodes are dispersed according to a uniform (or Poisson) distribution in order to derive a relationship between connectivity and node density. On several occasions, the assumption of uniform distribution is extended to vehicular networks due to their one-dimensional nature. While this assumption may be valid for traffic in homogenous states such as in free-flow traffic, it cannot be used to describe non-homogeneous traffic in the congested traffic that exhibit stop–go traffic wave and traffic jams. The latter case is important considering that phase transition may occur anywhere there is a constraint or bottleneck in traffic, or even because of high fluctuations in driving behaviour.

Chapter 4

VANET Simulations using *RoadSim*

This chapter introduces the Nagle and Schreckenberg (NaSch) model and surveys many of its extensions in the literature. The NaSch model has been used extensively in the literature to study and describe the behaviour of congested vehicle traffic. Among the attractive features of this model is that it is easy to understand and implement in computer programs while providing realistic and accurate representation of vehicle traffic. Therefore, this model is employed as the main analytical and simulation tool in this thesis.

This chapter introduces also a traffic microsimulator, *RoadSim*, which is designed to support Vehicular Ad Hoc Network (VANET) research and is considered the first main contribution in this thesis. *RoadSim* implements the Nagle and Schreckenberg with Slow-to-Start rule (NaSch-S2S) model and adds the following capabilities toward supporting VANET research: 1) generating network graphs based on vehicle positions and their transmission range, 2) translating vehicle movement into ns-2 simulator scripts, and 3) generating ns-2 scripts for initiating communication links among vehicles. In terms of implementation, *RoadSim* improves upon the NaSch-S2S model by handling additional components such as intersections and two-way roads.

4.1 Introduction

The movement pattern of mobile nodes plays an important role in the design and analysis of algorithms and protocols used in mobile wireless networks [2]. Due to the difficulty and high cost of obtaining real-world mobility traces, many mobility models were proposed to generate synthetic mobility patterns. The literature shows that the results of Mobile Ad Hoc Network (MANET) studies depend heavily on making the appropriate choice of the mobility model [28, 31, 33, 41]. Depending on the model used, mobile nodes direction and speed are expressed in a number of ways from deterministic to random.

Among the most commonly used mobility model is the Random WayPoint (RWP) model [41]. In this model, nodes' movements are completely independent from each other. Some cooperative characteristics of mobile nodes can be represented by group mobility models. In these models, node mobility is influenced by neighbouring nodes, such as when a group of people work together to accomplish a task (e.g. a rescue team, or a group of soldiers). The Reference Point Group Mobility (RPGM) model is used to create many of these models [72]. In RPGM, the group motion is set in two-dimensional space where nodes remain within some (random) distance from a reference point. Other models include the graph-based mobility model [135], and Manhattan mobility model [28].

It is noticeable that common MANET mobility models lack a relationship between nodes' densities and speed. As a result, a node's speed can be set independently of the nodes density. While this feature allows for a full control of both properties independently, it does not result in a realistic mobility patterns in dense networks, since it shows the nodes to be moving faster than they would be in a realistic situation. In some cases, the RWP model is used to generate vehicle movements by introducing acceleration and deceleration near the waypoints [33] or limiting nodes paths and speeds [97].

In reality, vehicles typically follow the road, which restricts their mobility to one dimension. Vehicles also interact with each other on the road by accelerating, decelerating, changing lanes, and obeying traffic controls (traffic signs and signals).

Moreover, modeling interactions between vehicles in dense traffic is necessary to create traffic jams. Therefore, representing vehicles as particles that move randomly does not result in realistic traffic patterns. As a result, a mobility model such as RWP is of limited use in studying vehicle traffic.

The VANET research community is increasingly aware of the limitations of the RWP model. There are several recent attempts to develop realistic vehicle mobility models based on car-following models [28, 45] or use proprietary traffic simulators to generate vehicle movement. The studies in [43, 59, 121], for example, show that realistic representation of vehicle traffic is necessary to evaluate inter-vehicle ad hoc networks in highway environments.

This chapter includes the following topics: The NaSch model [104] is discussed in Section 4.2. The discussion of the model includes a description of its properties and some of the proposed extensions in the literature. Among the relevant extensions to the scope of this thesis are the so-called the slow-to-start rule and the multi-lane rules. The traffic microsimulator, *RoadSim*, is introduced in Section 4.3. The section describes some implementation aspects and the additional components added to the NaSch model. Many experiments were performed to test the simulator. The results of the validation tests are reported in Section 4.4. The results show that *RoadSim* is capable of generating flow–density and speed–density relationship that match those described in Chapter 3. Some of the reported results will also be used in the following chapters. The summary and conclusions of this chapter are provided in Section 4.5.

4.2 The NaSch model

This section describes the original Cellular Automata (CA) model, which was introduced by Nagel and Schreckenberg in 1992 [104]. This model was studied extensively throughout the following years and many extensions and enhancements were suggested. Some of the most relevant extensions are reviewed in this section.

CA are simple discrete models of computation that can exhibit complex behaviour starting from simple rules of spatial interactions between cells in an infinite grid of one or more dimensions. CA models can be easily implemented by computer programs

and are used for many applications in several fields of study including mathematics, physics, biology, or computing [128].

An early proposed one-dimensional CA model for highway traffic flow is the so-called "CA rule 184" [146]. This model describes single-lane traffic on a road of length L with periodic boundary condition (closed-loop). Each of the L sites can either be empty or occupied by one vehicle. Let N be the total number of cars, then the average vehicle density on the road is $k = N/L$. The cars move from the left to the right according to the following rules: All the cars attempt a move of one step to the right simultaneously at each time step. If the site in front of a car is not occupied at that time step, the car moves one site ahead. Otherwise, the car cannot move.

Nagel and Schreckenberg proposed a variation on the "CA rule 184" in [104]. The new model has received considerable attention due to its ability to reproduce basic phenomena encountered in real traffic, particularly the phase transition phenomenon. In addition to the model's value as a theoretical tool, it has been applied successfully to simulate traffic flow in a large metropolitan area such as the North Rhine-Westphalia, in Germany [66]. The NaSch model also forms the basis for TRansportation ANalysis SIMulation System (TRANSIMS), which is a simulator developed by the Los Alamos National Laboratory to simulate people and vehicle traffic through the transportation network of a large metropolitan area [14].

In the basic NaSch model, the vehicle may travel in one direction from one cell to another at integer velocities in the range $[0, U_{max}]$, which correspond to the number of cells a vehicle can advance in one time-step. The movement of vehicles through the cells is simulated by updating the state (speed) of all cells in parallel according to a set of rules. The CA update rules are summarized as follows [104]:

Acceleration Rule: a vehicle increases its current speed by one each time step if there is enough gap (empty cells) to the vehicle ahead so that no collision occurs. The vehicle accelerates until it reaches the maximum speed, U_{max}.

Braking Rule: a vehicle reduces its speed if the gap ahead is too small to maintain the current speed. The new speed must match the gap so that no collision occurs.

Randomization Rule: the new speed resulting from the previous rules may be decreased by one with a probability of p_{noise}, except in the case of zero speed.

Motion Rule: a vehicle is moved a number of cells corresponding to its new speed.

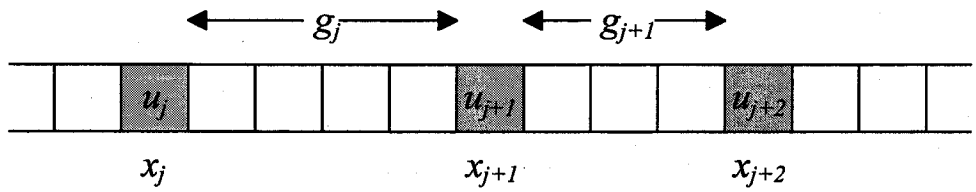

Figure 4.1: Cell grid and quantities relevant to the NaSch model (occupied cells are shown in grey).

These rules are stated formally using the following notation (see Figure 4.1):

$x_j(t)$:	position of the j^{th} vehicle at time t
$u_j(t)$:	speed of the j^{th} vehicle at time t, $u_j(t) = x_j(t) - x_j(t-1)$
$g_j(t)$:	gap between the j^{th} and $(j+1)^{th}$ vehicle (the vehicle immediately ahead) at time t, $g_j(t) = x_{j+1}(t) - x_j(t) - 1$
$\xi_j(t)$:	random variable that takes the value of '1' with probability p_{noise}, or '0' with probability $1 - p_{\text{noise}}$

The NaSch model dynamics can be formulated as [100]:

$$x_j(t+1) = x_j(t) + \max\left[0, \min\left[U_{max}, x_{j+1}(t) - x_j(t) - 1, x_j(t) - x_j(t-1) + 1\right] - \xi_j(t)\right] \tag{4.1}$$

In [104], the authors argue that, in a complete traffic jam, the average (front-bumper to front-bumper) distance between cars is about 7.5 meters. Thus, this value is set to be the length of one cell. The time for a single simulation step is determined so that a free traffic speed of 4.5 cells per time step should correspond to 120km/hr. Therefore,

$$\frac{7.5(m/cell) \times 4.5(cell/s)}{120(km/hr) \times 3.6} \approx 1\ second$$

The randomization noise combines three different behavioural patterns of the individual drivers into one: 1) fluctuations at maximum speed, 2) delayed acceleration,

and 3) overreactions at braking [101]. The non-deterministic acceleration as well as overreaction in the slowing-down process is crucially important for the spontaneous formation of traffic jams [150]. For $p_{\text{noise}} \rightarrow 0.5$, the system does not show spontaneous phase separation. Therefore, the value of p_{noise} determines whether the model exhibits spontaneous phase separation between laminar and jammed traffic [77]. The choice of value of p_{noise} has other effects on the dynamics of the traffic model. For instance, increasing p_{noise} decreases the free-flow speed (the average speed of vehicles in free-flow traffic conditions) by the same amount [105],

$$u_f = U_{max} - p_{\text{noise}}\,(cell/s)\ . \tag{4.2}$$

As a result, increasing the noise (speed fluctuations) decreases the maximum flow and shifts it towards smaller densities [53].

4.2.1 Properties

The NaSch model has several interesting properties, which are summarized here:

- The NaSch model is minimal in the sense that any simplification of the rules can no longer produce realistic traffic behaviour [30].

- The NaSch model belongs to the class of constant-gap car-following models [105], where the vehicle's new speed is a time-delayed reaction to the gap to the vehicle ahead. This becomes apparent when equation (4.1) is rewritten as,

$$u_j(t+1) = \max\left[0,\ \min\left[U_{max},\ g_j(t),\ u_j(t)+1\right] - \xi_j(t)\right]\ . \tag{4.3}$$

- The motion of a single car might exhibit unrealistic features, such as linear acceleration, rather than proportional to $1/u$; or stopping within one time step instead of a more realistic alternative that considers the speed of the vehicle ahead [105]. It is not known whether these features has any effect on VANET simulations.

- At the macroscopic level, the original NaSch model ($p_{\text{noise}} = 0.5$) underestimates the capacity. The maximum flow is much lower than the 2500 vehicles/hr/lane

given by measurements in highway traffic [104, 150]. The simulations in this thesis use a smaller value of p_{noise}, which yields more realistic flow (see later).

- The NaSch model is recognized for its ability to reproduce the so called spontaneous traffic jams, which occur for no obvious reason (such as bottlenecks), when density exceeds critical value [30]. The model does not show critical behaviour in the strict sense because the order parameter does not vanish below the critical point [53]. The model, also, does not show the existence of metastable states that appear in real traffic [30]. Section 4.2.2 describes some proposed extensions in the literature that overcome these limitations.

The original NaSch model has inspired many researchers to use it to study vehicle traffic. The model is flexible enough to be modified to fine-tune its properties by adding new rules or modifying the existing ones. Section 4.2.2 and Section 4.2.3 review some of modified models that build on the basic rules.

4.2.2 Extensions to randomization rules in the literature

Slow-to-start models such Takayasu and Takayasu (T^2), Benjamin, Johnson and Hui (BJH), and Velocity-Dependant Randomization (VDR), modify the randomization rule to model the delayed acceleration of a vehicle after stopping (due to inertia and driver reaction time) [30]. A slow-to-start rule assigns a higher probability, p_{s2s}, for rejecting the acceleration from speed 0 to 1(cell/s) than p_{noise}. With the slow-to-start rule, the NaSch model exhibits a phase separation and coexistence states [30, 77]. The *RoadSim* simulator is based on the NaSch model with slow-to-start rule, which will be referred to as the NaSch-S2S model.

Changing the order of the rules changes the resultant fundamental diagram. The order of braking and randomization rules can be exchanged so that randomization applies to acceleration only while keeping deceleration deterministic. This change increases the maximum capacity to the level of realistic traffic. Another change to the randomization rule also creates synchronized traffic [150]. Deterministic deceleration can also be made proportional to the speed of the vehicle ahead by an anticipation factor. By varying the anticipation parameter, three different traffic regimes can

be observed. Free-flow traffic, congested traffic, and an additional regime called v-platoon where platoons of cars move with the same speed [88]. Fukui and Ishibashi [58] introduced another variation on the basic model in which the increase in speed may not be gradual and stochastic delay only applies to the high speed cars.

Another model [82] combines some aspects of the above models. It incorporates anticipation by adding the state of the brake light to determine the speed of the following vehicle. The randomization parameter may take one of three values depending on the speed and the status of the brake light. In addition, the cell size is reduced to 1.5 metres for more realistic acceleration [82]. These modifications and others are the basis for a microsimulator that is being developed in Germany [66].

4.2.3 Multi-lane extensions in the literature

The NaSch model applies to single-lane traffic which does not allow passing. As a result, vehicles that have multiple maximum speeds will eventually form platoons where vehicles of low velocities are being followed by faster ones and the average speed is reduced to the free-flow speed of the slowest vehicles [98].

The basic NaSch model can be extended by adding rules for changing lanes. Vehicle states are updated in parallel according to the lane-changing rules. If a vehicle is to change lanes, it does so by moving sideways to another lane without advancing. Later, the speed update rules are executed to advance the vehicle.

There are several proposals for the lane-changing rules, which all agree that the criterion for lane change is the vehicle's desire to avoid slowing down due to a small headway. In addition, a vehicle may not move to an adjacent lane unless there is enough gap on the target lane so that the lane change manoeuvre does not disturb traffic on the target lane. A randomization is included so that a vehicle may abandon the lane change with a probability of p_{reject}, even if all conditions for safe lane change are met [66, 105, 107, 117].

The lane-change rule used in the implementation of *RoadSim* is summarized using additional notation, see Figure 4.2:

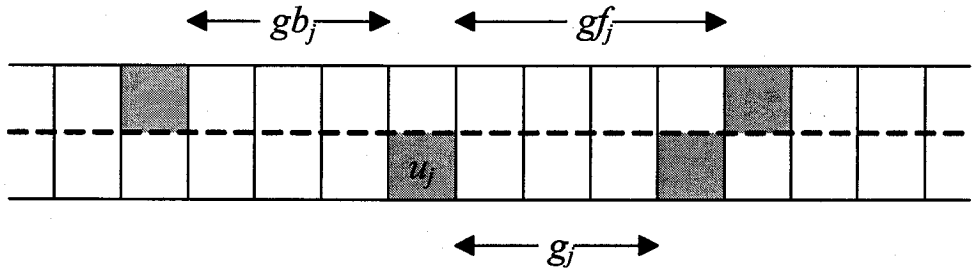

Figure 4.2: Two-lane cell grid and quantities relevant to lane changing rules.

$gf_j(t)$	: forward gap for the j^{th} vehicle in the target lane at time t
$gb_j(t)$	: backward gap for the j^{th} vehicle in the target lane at time t
$\zeta_j(t)$	: random variable that takes a value in the range [0,1] for the j^{th} vehicle at time t
U_{max}	: maximum speed in the CA model

The lane change is executed if all conditions, $T^(1)$–$T^(5)$, are met:
$T_j^{(1)}(t) = u_j(t) + 1 > g_j(t)$,
$T_j^{(2)}(t) = gf_j(t) > g_j(t)$,
$T_j^{(3)}(t) = gf_j(t) \geq U_{max}$,
$T_j^{(4)}(t) = gb_j(t) \geq U_{max}$, and
$T_j^{(5)}(t) = \zeta_j(t) > p_{\text{reject}}$.
Then, the lane-change decision $C_j(t)$, for the j^{th} vehicle at time t, is determined by,

$$C_j(t) = T_j^{(1)}(t) \cap T_j^{(2)}(t) \cap T_j^{(3)}(t) \cap T_j^{(4)}(t) \cap T_j^{(5)}(t) \,, \tag{4.4}$$

where p_{reject} is used to add a stochastic behaviour to the lane change move and prevent synchronized lane change. Therefore,

Lane-Change Rule: a vehicle, j moves to the target lane if all conditions in (4.4) are met, i.e. $C_j(t) = true$.

In roads of three or more lanes, the parallel implementation of the lane-change decision can lead to accidents. Consider, for example, that two vehicles on the left and right lane decide to move to the same position in the middle lane. Therefore,

the lane-change is allowed in alternate direction (left-right, or right-left) in each time step [105].

The lane-change rules have some properties that depend on the chosen set of conditions [117]. Symmetric traffic occurs when all lanes are utilized equally. In more realistic traffic, the slow lane may be preferred over the others, which creates asymmetric traffic. The latter scenario can be created by dropping the condition $T^{(1)}$ for vehicles attempting to move to the right (slow) lane.

A stochastic behaviour is introduced in the condition $T^{(5)}$ to eliminate a situation where vehicles move frequently back and forth between two lanes (ping-pong effect) [117]. Unlike the single-lane model, the backward gap is incorporated in the rules in $T^{(4)}$, so that the lane-change does not disturb the traffic on the target lane. The current implementation of *RoadSim* relies on symmetric traffic distribution among lanes.

Finally, the above lane change conditions apply to vehicles that have no planned route to follow. In more realistic scenarios, a driver's decision to change lanes may be influenced by the desire to follow a specific route. Thus, lane change rules are modified to favour some lanes over others [105]. All traffic simulations used in this thesis are based on highway configurations where only one or two highway segments are used; thus, no route planning is needed.

4.3 The microsimulator (*RoadSim*)

All simulations of vehicle traffic in this thesis are carried out using a traffic microsimulator, *RoadSim*[1]. *RoadSim* is an object-oriented implementation of a traffic microscopic simulator based on the NaSch-S2S model that was described in Section 4.2. The following sections describe the main extensions and improvements to the NaSch-S2S model that are included in *RoadSim*.

[1]A quick search in Internet reveals that the name 'RoadSim' is being used to label many computer programs or programming libraries that are being used for vehicle traffic simulations. The program, *RoadSim*, described in this chapter is an original and independent creation of the author. The similarity in name is coincidental.

4.3.1 Support for VANET research

RoadSim provides useful extensions to the NaSch model to support VANET research. Some of these extensions are described briefly as follows:

Network Graphs: *RoadSim* creates network graphs based on vehicle locations (vertices) and transmission ranges (edges). These graphs are used for all Minimum Transmission Range (MTR) estimates in Chapters 5 through 7.

Road Geometry: Tracking the spatial coordinates of mobile hosts has a significant importance in the operation of a VANET simulator. The simulation uses this information to determine, for example, if a mobile host can establish a link with another host within its transmission range. The coordinates are also important for the operation of some protocols such as geocast routing protocols. *RoadSim* maps each cell in the CA grid into a point (x, y) in a 2-D plane. The distances in the x- and y-axis are calculated using mapping functions,

$$(x, y) = (X(c, l)\ , Y(c, l)) \qquad c = 0, 1, \ldots\ ,\ l = 0, 1, \ldots \tag{4.5}$$

where c and l are the cell and lane index, respectively. The mapping functions, $X(\cdot)$ and $Y(\cdot)$, determine the geometric shape of the highway.

Node Identifiers: Vehicles in the NaSch model are anonymous entities since only their travel pattern is significant. *RoadSim*, on the other hand, assigns a unique identity for each vehicle to track its movement. The Node Identifier (ID)s are used for building network graphs, and generating scripts for Network Simulator-2 (ns-2) simulator [18].

Network Simulator Script: *RoadSim* does not implement any communication protocol; instead, it can generate three types of command scripts to be used by ns-2. The mobility script sets the trajectories and speeds of vehicles in ns-2 simulations. The power assignment script sets the transmission power for each vehicle according to the Dynamic Transmission Range Assignment (DTRA) algorithm proposed in Chapter 8. The communication script creates pairs of data transmitters and receivers according to some communication scenario. An example of each of these scripts is provided in Appendix C.

4.3.2 Data structures

Some public implementations of the NaSch model (e.g. [130]) are based on an array data structure where the array items represent vehicle locations (cells) on the road. The values of each item represent the state of the cell. Albeit simple, this data structure is not useful for applications beyond traffic simulations of single road segments. *RoadSim* is an object-oriented program that consists of many classes. Real-world entities such as a vehicle, an intersection, a highway, and a parking facility are represented as classes in *RoadSim*, see Figure 4.3. Appendix B shows a UML class diagram of the main classes in *RoadSim*.

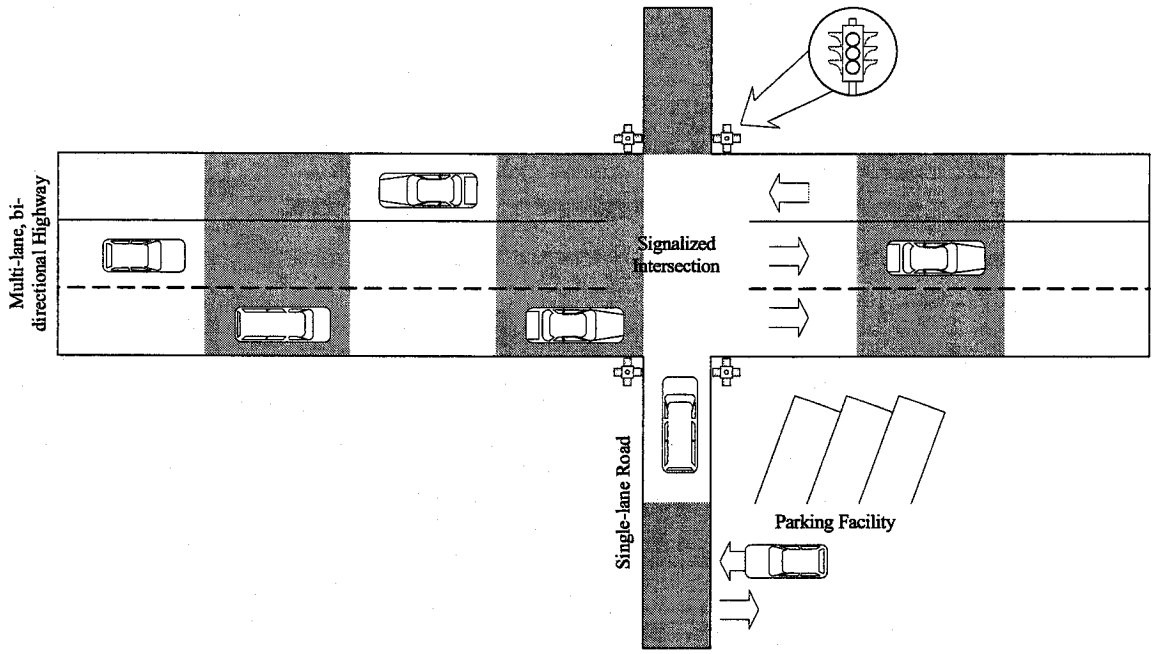

Figure 4.3: Examples of objects simulated in *RoadSim*.

The performance of the CA model based on array data structure is slow since the state of each cell has to be updated every time step. The original NaSch model and some proprietary simulators that are based on it use parallel computing to simulate different parts of the CA grid on different computers [104, 101, 14]. *RoadSim* achieves a higher performance than array based simulators without the complexity of parallel computing by using a linked-list data structure to represent road segments. Only occupied cells in the CA grid are tracked by the simulator; thus the time complexity

is reduced from $O(m)$ to $O(n)$, $n \leq m$, where m and n are the number of cells and number of cars, respectively.

4.3.3 Bi-directional traffic

The recent implementation of *RoadSim* supports bi-directional roads. This is an improvement over the previous implementation of *RoadSim* [24] where highway simulations have to be executed once for each direction of traffic before combining the data from both simulations. Bi-directional traffic is used in simulations conducted in [22] to study connectivity in VANETs using static transmission range, which provides the ground work for the discussion in Chapter 6.

4.3.4 Multi-lane traffic

Multi-lane roads are supported in *RoadSim* by including the lane-change rule described in Section 4.2.3. Experiments that are based on multi-lane traffic are used in Chapters 5 and 7.

4.3.5 Intersections

RoadSim implementation of intersections is inspired by the description provided in [105]. Similar work is also found in [66]. *RoadSim* implements two intersection types. Signalized intersections control traffic approaching the intersection using traffic lights. Traffic lights have red and green phases only but the period of each phase can be determined independently. In unsignalized intersections, vehicles approaching the intersection from a secondary road face either a Stop sign or Yield sign. Traffic on the main highway does not face any traffic sign.

Vehicles that face a traffic light can proceed immediately if the light is green and there is enough space to move in on the destination lane. Otherwise, the vehicle must wait until the light turns green and a space becomes available.

A vehicle approaching a Stop sign must stop for a minimum of one second before crossing the intersection. In order to move to the destination lane, there must be a safety gap, g_s, that satisfies $g_s \geq g_I$, where g_I is gap between the vehicle and the

traffic on all interfering lanes (the lanes whose traffic direction may intersect with the direction of the vehicle attempting to cross the intersection, which raises the possibility of a collision),

$$g_s = SF \times u_I \ (cells) \ , \tag{4.6}$$

where SF is a safety factor and u_I is the speed of the closest vehicle on the interfering lane. *RoadSim* sets a default value for the global variable SAFETY_FACTOR=3, and this is the value used for the simulations in Chapter 6.

Vehicles may proceed immediately at a Yield sign if equation (4.6) is satisfied. A vehicle may turn in any direction at the intersection given that there is at least one lane available in that direction. The probabilities of turning are specified by the user for each intersection. Intersections are used in the simulations of Chapter 6. A dummy intersection, an intersection without any traffic control, is used to link two ends of a highway segment to form a closed-loop highway. This configuration is used in many simulations throughout this thesis.

4.3.6 Speed options

RoadSim sets the maximum speed to Global.V_MAX=5. This value is used as the default speed value for all vehicles in the simulations. However, each vehicle object has its own value of maximum speed, which allows vehicles to have different maximum speed values if desired. The value of maximum speed is determined before a vehicle is loaded into the simulations. Simulations of vehicles with various values of maximum speed are used in Chapters 5 and 7.

4.3.7 Initialization modes

RoadSim allows the user to introduce vehicles into the simulations using two methods. In the first method, vehicles are generated at random time intervals representing the initial time headway, h, between vehicles. The headway is determined by a displaced Exponential distribution that specifies the traffic flow while guaranteeing a minimum headway [91],

$$f(h) = \frac{exp\left(-(h - h_{min})/(H - h_{min})\right)}{H - h_{min}} \tag{4.7}$$

where $h_{\min}$ is the minimum headway in seconds, $H = 3600/q_{in}$ is the mean headway in seconds, q_{in} is the desired input flow in vehicle/hour. Notice the equation (4.7) is reduced to the Exponential probability density function (pdf) when $h_{min} = 0$.

Once a new vehicle is generated, it is inserted into a parking facility where it tries immediately to exit into the highway. The vehicle must wait for $g_s \geq g_I$ (see Section 4.3.5) before entering the intersection. In light traffic densities, the condition is easily satisfied and the vehicle usually succeeds in entering the highway and the specified headway is maintained. In other traffic conditions, the vehicle may wait for a while before it can enter the highway. This does not influence the generation of new vehicles which will continue to occupy the parking facility. This initialization method results in realistic traffic behaviour on the highway; thus, it is the most common method in the simulations performed in this thesis.

In the second method, all vehicles are created and placed in the highway at the start-up of the simulation. The initial location of vehicles is determined using a uniform distribution. This method is useful when a specific vehicle density of a specific number of vehicles is needed in the simulation. This method was used in [23] for a preliminary study of connectivity in VANETs.

4.4 Validation tests

This section describes several simulation experiments performed using *RoadSim* to 1) validate its correctness by comparing the simulation results with the relationships produced by the traffic models described in Chapter 3, and 2) illustrate its capabilities and obtain some results that will be used in the next chapters.

A similar test network to the one recommended in [105] is adopted for the experiments performed to validate the simulator. The simple highway configuration shown in Figure 4.4 is used to generate the three bivariate relationships of traffic flow (flow–density, speed–density, and flow-speed).

The test configuration consists of a highway of 1000 cells (7.5km) of one or more lanes in a single direction. The highway is made into a closed-loop by joining both ends using an unsignalized intersection where vehicles do not face any traffic signs.

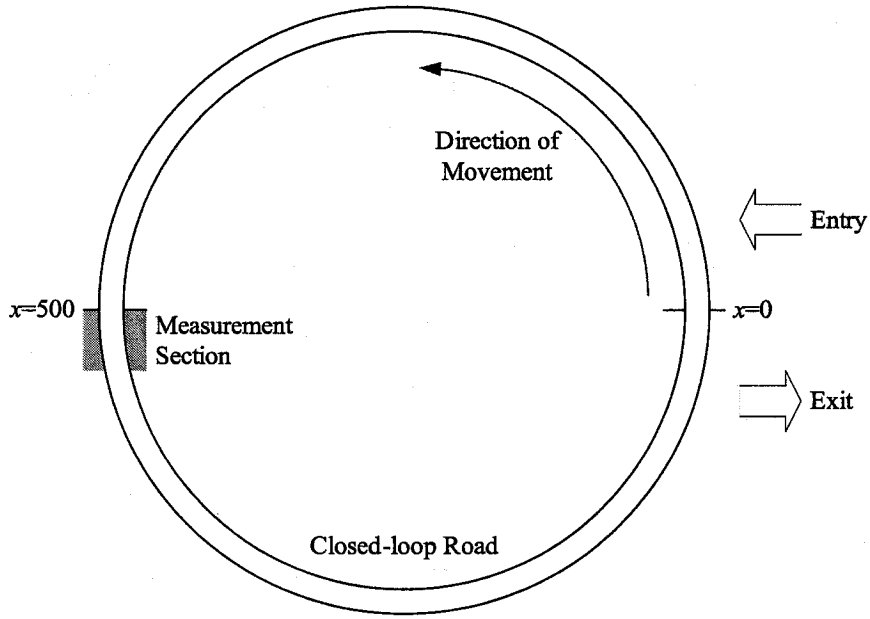

Figure 4.4: Test configuration.

This configuration resembles a racetrack where vehicles travel in circles. The vehicles enter from a parking facility located at $x = 20$. Optionally, vehicles may exit the highway to a parking facility located at $x = 980$.

The traffic characteristics are measured using instantaneous observations, as will be described in Section 4.4.1. The measurement section starts at $x = 500$ and spans a length of $L = 5$ cells (37.5m). This distance is chosen to be equal to the maximum speed allowed in the simulation, Global.V_MAX=5, so that a vehicle cannot pass the measurement section without being counted during a simulation time step [105].

Unless otherwise noted, all vehicles are assumed to be of the same size that occupies one cell and have a maximum speed of Global.V_MAX=5 (cell/s), and a single-lane highway is used.

4.4.1 Generating bivariate relationships

In order to generate a complete flow–density relationship in one simulation run, vehicle density must be increased gradually, in one lane, from zero to a wide traffic jam where all cells in the highway are occupied. The following quantities are measured every

simulated second using instantaneous observations, as described in Section 3.2. The resultant measurements of density, k, and speed, u, are averaged over a period of time, $T_{avg} = 180$ seconds, following the technique used in [105]. Therefore,

$$k = \frac{N}{L \times n_l \times T_{avg}} \tag{4.8}$$

and

$$u = \frac{1}{N \times T_{avg}} \sum_{i=1}^{N} u_i \ , \tag{4.9}$$

where N is the number of vehicles located within a measurement section of length L, n_l is the number of lanes, and u_i is the speed of i^{th} vehicle. The flow, q, can be obtained directly from the fundamental relationship (3.5). The resultant quantities are in units of (veh/cell/lane), (cell/s), and (veh/s/lane), respectively. If necessary, all quantities above may be converted to the units of (veh/km/lane), (km/hr), and (veh/hr/lane), respectively.

At a constant rate of 1 veh/s (3600 veh/hr), a highway of the test network can be filled in just 1000 seconds. However, the collected measurements in this case are too few to be useful. Instead, vehicles enter slowly at flow rate of $\frac{1}{60}$ veh/s (60 veh/hr). A simulation time of 60,000 seconds generates 333 measurements of each of the three quantities, which provides a complete plot for all bivariate relationships.

Figure 4.5 shows the result of generating the flow–density and speed–density relationships using the test network described above and the same parameter setting as the original NaSch model described in [104, 150], i.e. $p_{\text{s2s}} = p_{\text{noise}} = 0.5$. The resultant flow–density relationship in Figure 4.5(a) is similar to the one shown in Figure 3.2. The flow increases linearly until reaches its maximum density at some critical density before it declines. The slope of the straight line is the free-flow speed $u_f = q/k$. Figure 4.5(b) also matches the speed–density relationship of Figure 3.3. Both figures indicate that vehicles maintain their free-flow speed as long as vehicle density is low enough to prevent any interactions among them.

4.4.2 Free-flow speed

Vehicles in the NaSch model have a maximum speed of U_{max}, which is the maximum number of cells a vehicle may travel in one time step. In a simulation setup, each

vehicle may have its own maximum speed, $U_{i,max} \leq U_{max}$. The free-flow speed is the average speed of vehicles traveling in free-flow conditions. In this case, the number of empty cells ahead of the vehicle is always greater than or equal to U_{max}. The free-flow speed, u_f is related to maximum speed, U_{max} by equation (4.2) [104].

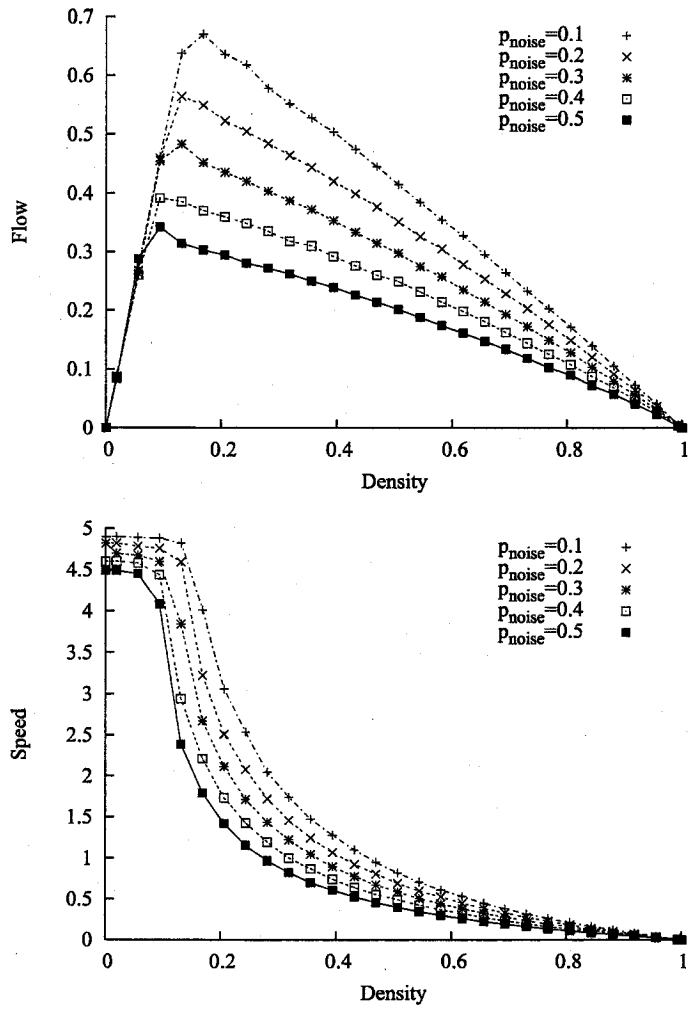

a)

b)

Figure 4.5: *RoadSim* generated a) flow–density, and b) speed–density relationships using the rules of the original NaSch model.

The plots of Figure 4.5(a) and Figure 4.5(b) show the flow-density and the speed-density relationships for various values of p_{noise}, respectively. The plots are generated by averaging the flow and speed values at equidistance density intervals. The figures show also that increasing the value of p_{noise} results in a reduction of the critical density

where the maximum flow occurs.

Figure 4.5(a) indicates that the choice of p_{noise} affects the resultant maximum flow, q_{max}. It is shown in [104] that the value of $p_{\text{noise}} = 0.5$ results in a maximum flow that is a half of what is expected in real traffic. Moreover, setting $p_{\text{noise}} = 0$ eliminates the stochastic behaviour in the model and maximizes the flow. *RoadSim* uses the default value $p_{\text{noise}} = 0.01$, which yields a realistic maximum flow [78].

4.4.3 Estimation of the sensitivity factor (λ)

It was mentioned in Section 3.4.2, that the relationships of speed-density and flow-density produced by *RoadSim* follow equations (3.11) and (3.12), respectively. The reason for this similarity is that the NaSch model belongs to the same class of car-following models as the Pipes model (see Section 4.2.1). In this section, the Pipes' equation (3.10) will be fitted into the flow-density data shown in Figure 4.5(b). This can be achieved by determining the value of the sensitivity factor, λ.

Recall that Pipes' equation (3.10) relates vehicle speed and density,

$$u = \lambda \left(\frac{1}{k} - \frac{1}{k_{jam}} \right) . \tag{4.10}$$

The value of the sensitivity factor, λ, in (4.10) may be determined experimentally from the simulation data using curve fitting techniques. Measurements of density and speed were collected from 20 simulation runs of the test network. Since equation (4.10) applies to dense traffic only, data points that correspond to free-flow densities were removed. Then, the collected values of u and k were normalized using the values of maximum speed and maximum density, $u' = u/U_{max}$, $k' = k/k_{jam}$, and $\lambda' = \lambda/(U_{max}k_{jam})$. After normalization, equation (4.10) can be written as

$$u' = \lambda' \left(\frac{1}{k'} - 1 \right) , \tag{4.11}$$

which is similar in form to a straight line equation. Therefore, a linear fit can be used to find the slope, λ', of the straight line shown in Figure 4.6 where the speed values, u' , are plotted against the corresponding values of $1/k' - 1$. The process was repeated for each simulation run. The resultant slope has a mean of $\mu_{\lambda'} = 0.1072$ and

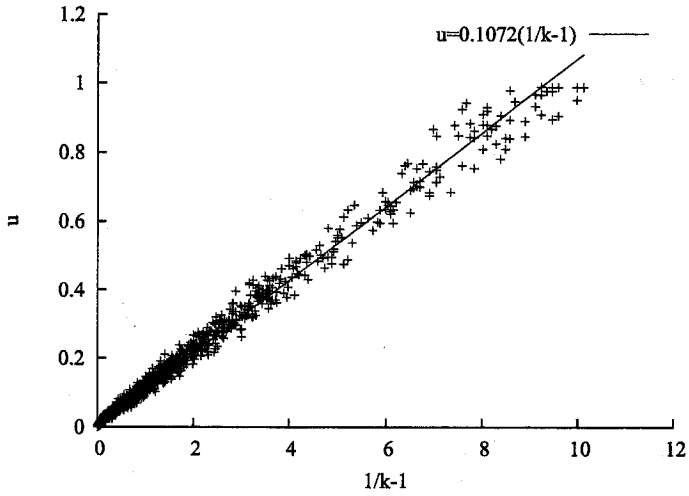

Figure 4.6: Estimation of the normalized sensitivity factor, λ'.

a standard deviation of $\sigma_{\lambda'} = 0.0034$ (0.95% confidence interval of [0.1056, 0.1088]).

Using λ, the maximum flow (capacity) of the highway, q_{max}, can be obtained from (4.11) and the fundamental relation (3.5) at the critical density, k_c,

$$q_{max} = u(k_c)k_c = \lambda\left(1 - \frac{k_c}{k_{jam}}\right) . \tag{4.12}$$

The resultant capacity is slightly lower than the value of λ when $k_c \ll k_{jam}$. This justifies replacing λ (which has the same units as the flow) with q_{max} in (3.12) to approximate the u–k relationship [133].

4.4.4 Estimation of the network resistance factor

Recall from Section 3.4.3 that the two-fluid model assumes the fraction of stopped vehicles is related to vehicle speed,

$$u = u_{max}\,(1 - f_s)^{\eta+1} . \tag{4.13}$$

where η was described as the network resistance factor (also called traffic quality of service factor).

RoadSim simulations were used to find the value of the resistance factor, η, in equation (4.13). In a manner similar to the previous section, 20 simulations were used to collect speed measurements in a small section of the test network.

Figure 4.7 shows a scatter plot of normalized speed against the value of $1 - f_s$. The straight line that fits this data has a mean slope of 0.9255 and standard deviation of 0.0144 (0.95% confidence interval of [0.9187, 0.9322]). Therefore, it is reasonable to assume that the traffic generated by *RoadSim* has a network resistance factor of $\eta = 0$ This result will be used in the derivations based on the two-fluid model in Chapters 5 and 7

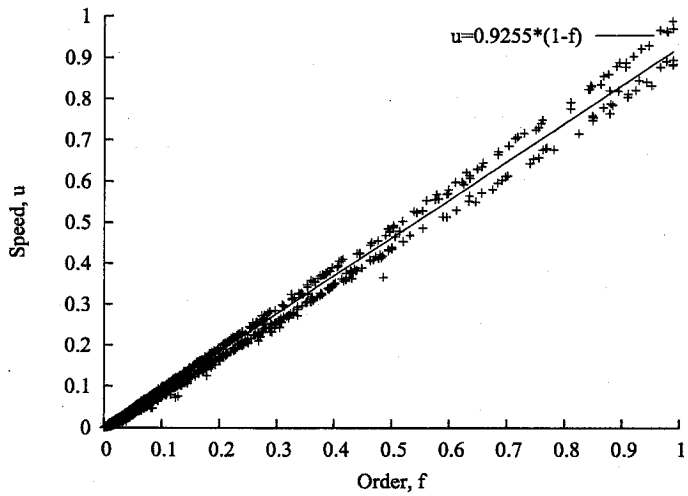

Figure 4.7: Estimation of network resistance factor.

4.4.5 Slow-to-start rule

One important extension to the NaSch model involves adding speed-dependant randomization (see Section 4.2.2). The so called slow-to-start rule determines that once a vehicle is stopped, its probability of acceleration in the next time step is much lower than a moving vehicle. Reference [78] shows the significance of the slow-to-start rule in creating the phase transition phenomenon in vehicle traffic.

Figure 4.8(a) shows the affect of changing the slow-to-start probability, p_{s2s} on the

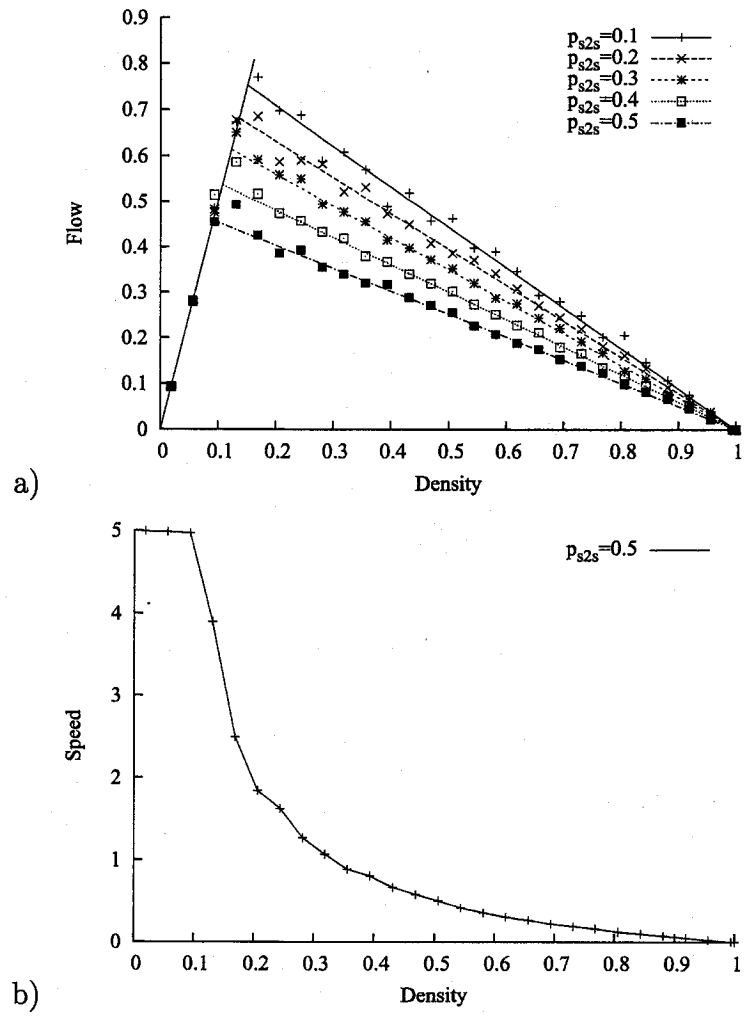

Figure 4.8: *RoadSim* generated a) flow–density, and b) speed–density relationships using the NaSch-S2S model.

flow–density relationship. Figure 4.8(b) shows the effect on speed–density relationship. The data in both figures are obtained using the same conditions for those in Figure 4.5 with $p_{\text{noise}} = 0.01$ and $U_{max} = 5$ (the default values in *RoadSim*). When straight lines are fitted to the data points obtained from simulations, the resultant plots match Figure 3.5. Notice that the area of mixed-state traffic diminishes as $p_{\text{s2s}} \rightarrow p_{\text{noise}}$, which is the case in the NaSch model (without the slow-to-start rule).

4.4.6 Multi-lane traffic

In multi-lane roads, vehicles change lanes according to a set of rules that considers the gap to the vehicle ahead and the available gap in the target lanes. The rules are either symmetric, i.e. no lane is preferred over the other, or asymmetric, where vehicles always try to return to the slow lane after passing. Some rules also incorporate the planned travel route into the lane-change decision. Moreover, randomization is added to prevent synchronized lane change.

RoadSim implements the symmetric lane-change rules described in Section 4.2.3. These rules are chosen because they allow all lanes to be utilized equally rather then concentrating traffic in some lanes; thus, reducing unnecessary complexities when studying VANETs. However, as will be shown later, vehicles of multiple speed capabilities will arrange themselves so that vehicles of higher speeds will travel in different lanes than those of lower speed. This occurs naturally without any special rules.

Figure 4.9 depicts the lane utilization in a three-lane highway. To obtain the plots in the figure, the test configuration described in the introduction of Section 4.4 is modified by adding two additional lanes and increasing the input follow of vehicles to $\frac{1}{20}$ veh/s (180 veh/hr). The utilization, z_i, of lane i is calculated from the vehicle density on that lane, k_i:

$$z_i = \frac{k_i}{\sum_i k_i} . \tag{4.14}$$

Figure 4.9 indicates that the utilization of the three lanes tends to be equal as the simulation time progresses. Since vehicles are placed in the first lane when they enter the highway, utilization of this lane starts at 1.0. The lane-change rules allow

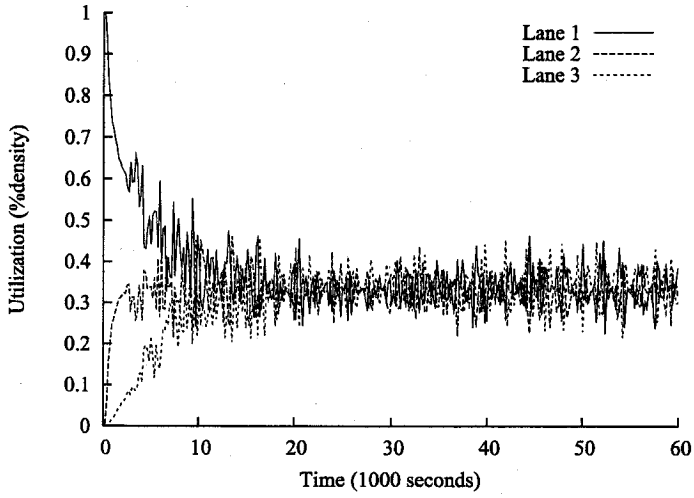

Figure 4.9: Lane utilization in a three-lane highway.

vehicles to move to the immediate neighbouring lane only; thus, the utilization of the second lane is the next to increase, then the third lane, and so on.

4.4.7 Effect of various speed limits

All previous experiments were intended to show the traffic characteristics when all vehicles are of homogenous type (e.g. passenger cars) with the same maximum speed. In a more realistic scenario, vehicles may be of different types (e.g. cars and trucks) and different maximum speed. In a single-lane highway, where overtaking is prohibited, fast vehicles will be held behind slow ones. Effectively, the slowest maximum speed will be the speed limit of all vehicles. Therefore, the effective free-flow speed is given by,

$$u_f = \min\left\{U_{i,max}\right\} - p_{\text{noise}} \ , \tag{4.15}$$

where $u_{i,max}$ is the maximum speed of the i^{th} vehicle.

Depending on the distribution of slow vehicles on the highway, vehicles may travel in platoon-like formations. Each platoon is led by a slow-vehicle. This situation is often encountered on highways when several cars are held behind a slow moving truck. The plots in Figure 4.10(a) show the flow-density and speed-density relationships in two situations, in one of which all vehicles have a maximum speed of $U_{max} = 5$, and

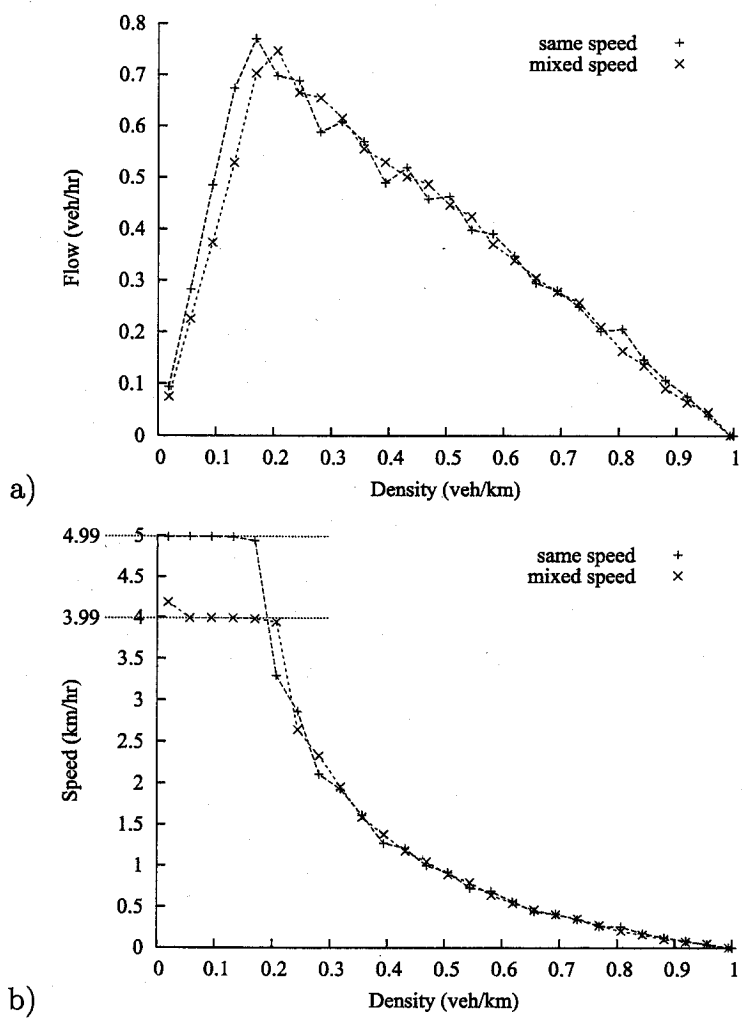

Figure 4.10: *RoadSim* generated a) flow–density, and b) speed–density relationships of traffic of dual maximum speed.

in the other, 50% of the vehicles have a maximum speed of $U_{max} - 1 = 4$. The figure does not show a major difference from the previous figures except the change in the free-flow speed, which confirms (4.2). The flow-density plot shows that the capacity of the highway is reached at higher density when the free-flow speed is lowered.

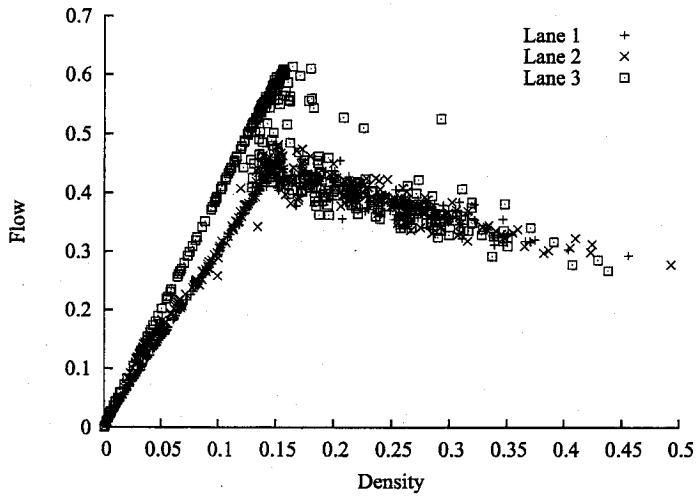

Figure 4.11: Lane utilization in three-lane highway.

In a different experiment, the vehicles were divided into three groups that represent 15%, 70%, and 15% of the total number of vehicles. The maximum speed of each group is set to 3 (81), 4 (108), and 5 (135) cell/s (km/hr). The choice of this speed allocation corresponds, roughly, to the 85 percentile rule that is used as a guide to set the speed limit so that 85% of vehicles travel below the speed limit [131]. The resultant flow-density curve in each lane is shown in Figure 4.11. The figure shows that there are two distinctive free-flow speeds of 2.99 cell/s and 3.99 cell/s. Most slow vehicles are concentrated in the slow lane (lane 1), while the fast vehicles tend to move to the higher lanes. This indicates that realistic traffic behaviour may result regarding lane choice even without special rules. However, this particular result is a side effect of the vehicle loading mechanism which puts the vehicles in the first lane initially. Once fast vehicles are obstructed by slow ones, they move to higher lanes. Eventually, only slow vehicles remain in the first lane.

Eventually, the increase in density causes the average speed of all vehicles to decrease. Therefore, there is no distinction between the lanes in the right branch of

the flow-density relations (whose slope represent the speed of density waves).

4.5 Summary and conclusions

The main tool for traffic analysis in this work is NaSch-S2S that the literature shows has value in creating three traffic states, free-flow traffic, congested traffic, and a mixed state where both conditions co-exist. The NaSch-S2S model is used in this thesis to study congested traffic conditions. These conditions deserve special consideration in the design and analysis of IVC and VANETs. Some of the answers sought are the effect a traffic jam has on the connectivity of the network or on the propagation of broadcast messages. Intersections and traffic lights also affect the normal flow of traffic and disturb vehicle distribution, even when vehicle density is low. Analyzing the performance of vehicular networks under these conditions may lead to protocols that are operational under more realistic conditions.

This chapter introduced a traffic microsimulator, *RoadSim*, as the first main contribution in this thesis. *RoadSim* implements the NaSch-S2S model and provides many improvements that include 1) handling of additional components such as multi-lane traffic and intersections, 2) enhancing the performance by using linked-lists, instead of arrays, to represent roads, and 3) adding several capabilities toward supporting VANET research such as building network graphs, and generating ns-2 scripts to port vehicle movement traces into simulations of communication networks.

RoadSim can create more elaborate road configurations than the closed-loop highway of the NaSch model. Simulated road configurations may include multi-lane, bi-directional roads connected via a grid of intersections. The intersections are either signalized or unsignalized. Other components of *RoadSim* include vehicle generators. The vehicle generators provide control on how the vehicles are loaded to the simulation. The vehicles may be positioned randomly on a road at the beginning of the simulation or enter gradually through a parking facility. The generators control the vehicle arrival rate as well as the initial and maximum speeds, so that it is possible to simulate traffic of various speed capabilities. Vehicles may also exit the simulation through parking facilities.

The validation simulation experiments show that *RoadSim* produce flow-density and speed-density relationships that are virtually identical to those provided in the related papers. Since the NaSch model belongs to the class of the car-following models, the produced speed-density relationship is similar to Pipes' equation. Because of this similarity, it is possible to estimate the sensitivity constant in the Pipes' equation from the simulation data. In Chapter 5, the value of the constant will be determined analytically and compared to the simulation results. Also, a similar experiment is used to verify that *RoadSim* exhibit a relationship between average speed and fraction of stopped vehicles predicted by the two-fluid model.

The use of the slow-to-start rule produces a slightly different form of flow-density relationship similar to the one described in Chapter 3, where the free-flow and congested regions of traffic are separated by a region of mixed state. This behaviour distinguishes the NaSch-S2S model from other traffic models.

The remaining experiments show the effect of multilane traffic and traffic of various maximum speeds. All lanes tend to be utilized equally when vehicles have the same maximum speed. In traffic of various speed capabilities, the number of lanes has a significant impact. In a single-lane highway, the average free-flow speed will be determined by the smallest maximum speed among all vehicles. In multi-lane traffic, fast vehicles tend to choose different lanes than the lanes chosen by slow vehicles, which results in a different free-flow speed for each lane. It is important to note that the general shape of the flow-density and speed-density relationships are not affected regardless of the choice of number of lanes or speed distribution. As a result of these experiments, simulations of vehicles of various speed capabilities in the remainder of this thesis will be limited to multi-lane highway configurations.

Chapter 5

Minimum Transmission Range in Uninterrupted Highways

This chapter discusses the impact of the non-homogeneous distribution of vehicles on the connectivity problem in VANETs. The non-homogeneous distribution of vehicles is caused by the phase transition from free-flow traffic to congested traffic. The discussion is applicable to a vehicular network in a long stretch of a highway with few lanes and without interruptions caused by intersections or entry and exit ramps. Moreover, the effect of the traffic of the opposite direction is not considered. These conditions are chosen in order to allow a direct comparison of the thesis results with similar one-dimensional networks considered in the literature.

The main contribution of this chapter is to formulate a new relationship that provides a tighter estimate for the lower bound of the MTR in VANETs by considering the phase separation in vehicle traffic. This relationship is an improvement to the estimate of the MTR given in [124] for one-dimensional networks of homogenous node distribution.

5.1 Introduction

The most fundamental property in any communication network is the connectivity among its nodes since the network can not exist without it. MANETs face the difficult challenge of maintaining connectivity so that a node may establish a communication link to any other node in the network. The connectivity of the network is affected by several factors including transmitter power, environmental conditions, obstacles, and mobility, among others.

Extensive research is dedicated to determine the transmission range that guarantees the network's connectivity, also known as the RA problem [48, 125, 127]. The RA problem is NP-hard in networks of two or three dimensions [47]; thus only approximate solutions can be obtained. In MANETs, there is an additional level of complexity because of the frequent topology changes.

A vehicular ad hoc network (VANET) constructed among vehicles in a highway may be viewed as an example of one-dimensional MANETs. The MTR in such networks is determined in the literature using several approaches. However, all these approaches are based on the assumption that the network nodes are distributed in a homogeneous manner along a line. In other words, the distribution of the nodes in any segment of the line is representative of the distribution in the other segments.

Traffic jams are a common phenomenon in the modern networks of streets and highways. As described in Chapter 3, traffic jams are not only caused by constraints in the transportation network, but also by fluctuations in vehicles' speeds whose effect intensifies as the vehicle density increases. The effect of these traffic jams on VANETs is manifested in disturbing the free flow of vehicles and the homogenous distribution of vehicles. As a result, analytical estimates of MTR that assume a homogenous distribution cannot be directly applicable to VANETs except under free-flow conditions.

The NaSch-S2S model, which was discussed in Chapter 4, is used throughout the chapter to derive the relationship for the lower bound MTR. In addition, the NaSch-S2S model is employed to identify the critical density that separates free-flow traffic from congested traffic.

Simulations of vehicle traffic are employed to verify the change of vehicle distribution from homogenous to non-homogeneous as density changes. Simulations demonstrate the veracity of the analytical estimates of the fraction of stopped vehicles (order parameter), which is used to distinguish between phases of traffic flow. Lastly, simulations are employed to verify the estimates for the lower bound of MTR and provide an empirical estimate for the upper bound of the MTR. All simulations are carried out in 1- and 3-lane highway configurations.

The chapter is organized as follows. A summary of the related literature is provided in Section 5.2. The separation of traffic phases in the NaSch model is illustrated in Section 5.3. The distribution of vehicles in VANETs is discussed in Section 5.4. The lower-bound MTR is derived in Section 5.5. Simulation experiments and their results are described in Section 5.6. The conclusion to this chapter is given in Section 5.7

5.2 Homogenoues transmission range

If all node positions in a network are known, the MTR is determined by the length of the longest edge of the Euclidean MST in a geometric graph composed of all nodes [108]. In the most realistic scenarios, node positions are unknown but it can be assumed that the nodes are distributed according to some probability distribution in the network. In the latter case, it is necessary to estimate the MTR that provides connectivity with a probability that converges to 1 as the number of nodes or the network size increases.

In the probabilistic approaches to determine the MTR, authors have relied on the theory of geometric random graphs (GRG) to represent wireless ad hoc networks [50]. A network can be modeled by a graph $G(V, r_c)$ in which two nodes are connected if the Euclidean distance between them is no more than r_c. Most studies consider how the transmission range is related to the number of nodes n, dispersed according to a uniform or Poisson distribution in a fixed area (or line). The continuum percolation theory and the occupancy theory have also been used in the probabilistic analysis of ad hoc networks.

In the case of one-dimensional models, Piret [112] discussed the coverage problem

to find that the lower bound of the transmission range, r_{cover}, for nodes located according to the Poisson distribution in a line of length L, with density k, is $r_{\text{cover}} = \ln(Lk)/(2k)$. The author shows that, if $r_c = m\, r_{\text{cover}}$, then connectivity among nodes approaches $\lim_{L\to\infty} Q(r_c, L) = 1$ when $m > 2$.

In two dimensional networks, Gupta and Kumar [64] used percolation theory to study connectivity among nodes distributed uniformly in a unit disc. They determine that if $r_c = \sqrt{(\ln n + c(n))/\pi n}$, then the resulting network is asymptotically connected with probability of 1 iff $c(n) \to \infty$.

Santi and Blough [124] provide tighter bounds on MTR using occupancy theory. Their primary result shows that when nodes are distributed uniformly over a line of length L, the network is connected if

$$r_c n \in \Theta(L \ln(L)) \qquad r_c \gg 1\,. \tag{5.1}$$

Equation (5.1) is the primary result that will be used in Section 5.5 to develop the MTR estimate for 1-dimensional VANET.

Dousse, Thiran and Hasler [51] approach the connectivity problem in both pure ad-hoc and hybrid networks. They conclude that connectivity is limited to short range communications in one-dimensional and strip networks (two-dimensional networks of finite width and infinite length), because the network remains divided (with high probability) into an infinite number of bounded clusters. Since VANETs in highway environment can be represented as 1-dimensional or strip network, it can be concluded that it is not practical to maintain connectivity in the entire network that may stretch for tens of kilometres. Instead a VANET should tolerate a certain level of partitioning.

The work summarized above considers Euclidean distance only in the discussion of connectivity. Bettstetter and Hartmann [34] discuss connectivity in a shadow-fading environment where a link between two nodes may not exist even though they are located within the transmission range. Cheng and Robertazzi [44] use packet broadcast to derive a relationship between the transmission range, the node density, and the expected number of broadcasts needed before a gap is encountered in the network. The authors assume nodes are distributed according to a Poisson distribution along a line. Another approach to solve the connectivity problem involves finding how many

neighbours a node should be connected to in order that the overall network is connected. The work of Feng Xue and Kumar in [149] and the paper [110] are examples of such an approach.

To invistigate the effect of mobility, Sánchez, Manzoni and Haas [123] present an algorithm to calculate the MTR required to achieve (with high probability) full network connectivity. The main empirical results show that the MTR decreases as $\sqrt{\ln(n)/n}$ and, when considering mobility, the range has little dependence on the mobility model. The results were obtained through simulation of using RWP, random direction, and Brownian-like mobility models.

Santi and Blough [124, 125] also used simulations to investigate the relationship between the MTR in stationary and mobile networks. They consider RWP and Brownian-like mobility models to analyze different MTR values in various connectivity requirements. The simulation results show that, due to mobility, the MTR has to be increased relative to the stationary case to ensure the network connectivity during 100% of the simulation time. Furthermore, the simulation results show that the transmitting range can be reduced considerably if the connectivity is maintained during 90% of the simulation time.

The paper by Füßler et al [59] focuses on vehicular networks. In the context of comparing various routing strategies, simulations are used to find the effect of the transmission range on the number of network partitions and provide an estimate of the transmission range that minimizes the partitions. It should be noted that the simulations in [59] are limited to free-flow traffic of low density.

Most of the work presented above assumes that nodes are distributed homogeneously according to uniform or Poisson distributions within the network space. Moreover, mobility is usually modeled in two-dimensional space. This chapter discusses the affect of the non-homogeneous distribution on connectivity and derives an estimate for the lower bound of transmission range for VANET on a highway of no constraints or bottlenecks.

5.3 Traffic jams and critical density

This section revisits the subject of traffic jams in order to define some terms and introduce some background information, which will be needed for the derivation of relationships in the following sections. The fundamental diagram of road traffic of Figure 5.1 shows a discontinuity in the flow-density relationship that marks the transition point between two distinct modes of traffic flow, the free-flow traffic and the congested traffic.

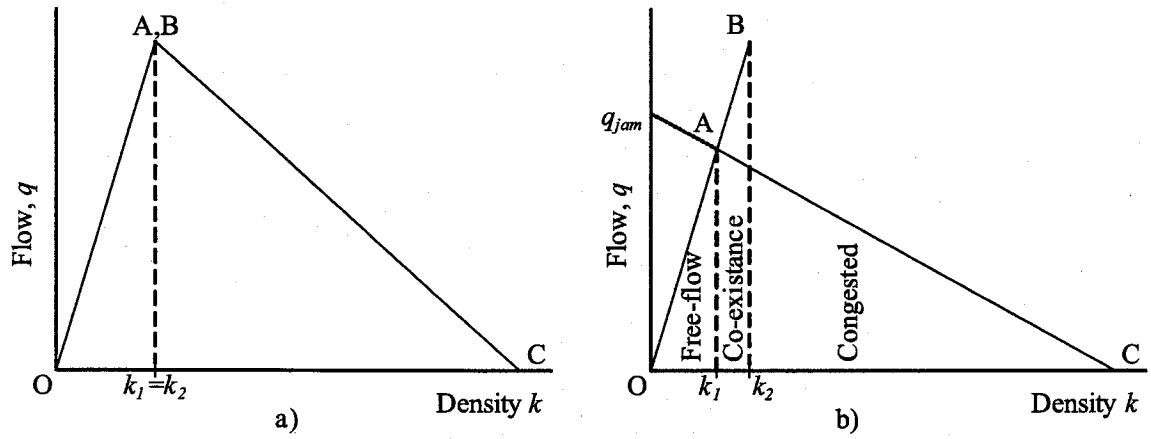

Figure 5.1: The flow-density relationship in a) deterministic NaSch model, and b) stochastic NaSch-S2S model.

In the deterministic case of the NaSch model (which is created when the randomization rule is dropped or, equivalently, when $p_{\text{noise}} = 0$), the traffic exhibits free-flow characteristics when all gaps between vehicles are equal to or greater than U_{max} so that vehicles are never forced to slow down. This situation arises when the system-wide density, k_L, of a closed system of size L, is smaller than the critical density, k_{det}. In the deterministic NaSch model (in which $p_{\text{noise}} = 0$), the critical density is [103],

$$k_{det} = \frac{1}{U_{max} + 1} . \tag{5.2}$$

Substituting (5.2) in the fundamental relationship (3.5) provides the maximum flow, which occurs at the density k_2 (point B in Figure 5.1),

$$q_{det,max} = \frac{U_{max}}{U_{max} + 1} . \tag{5.3}$$

In the NaSch-S2S model, gaps of size U_{max} are not enough to guarantee free-flow since fluctuations of the lead vehicle's speed may force the following vehicles to slow down and create traffic waves. Figure 5.1(b) shows three regions in the q–k relationship; only large disturbances create traffic jams; thus, forcing the free-flow traffic in the co-existence region to enter the congested region. Small disturbances force the traffic in the congested region to break into traffic jams [100].

In the NaSch-S2S model, small fluctuations are represented by the parameter p_{noise}. The slow-to-start probability, p_{s2s}, is the source for the large disturbances. In such a system, the flow in the free-flow and congested regions are given by [30, 103]. Notice that in the original NaSch model, the randomization value p_{noise} applies to all speed values, while in the NaSch-S2S the value of p_{s2s} applies to stopped cars ($u = 0$ cell/s). Therefore, the corresponding equations are to be modified accordingly,

$$\begin{aligned} q &= u_f \times k \\ &= (1 - p_{\text{s2s}})\,(1 - k/k_{jam}) \ , \end{aligned} \tag{5.4}$$

where $u_f = U_{max} - p_{\text{noise}}$, and k is the vehicles' density. The lines representing the two modes of traffic meet at,

$$k_1 = \left(\frac{u_f}{1 - p_{\text{s2s}}} + \frac{1}{k_{jam}} \right)^{-1} . \tag{5.5}$$

In equation (5.5) the density k_1 (of Figure 5.1(b)) is the density value that separates the free-flow traffic from the co-existing traffic. Beyond this density value, the traffic is characterized by start-stop waves. When compared to the deterministic model, the critical density of the NaSch-S2S model is lower, $k_c < k_{det}$. However, the choice of randomization parameters ($p_{\text{noise}} = 0.01$) makes the critical density very close to that of the deterministic case since $u_f \approx U_{max}$.

5.4 Distribution of vehicle locations in a highway

Information about the distribution of vehicles in transportation networks is valuable in any research concerning some aspect of these networks. Typically, analytical research

in inter-vehicle communication relies on Exponential distribution to model either the inter-vehicle spacing in highways [121] or the inter-arrival rate [145]. This assumption is also used to estimate the delay encountered by vehicles waiting to cross a highway [142, 71], or merge with highway traffic [55], and to estimate the delay pedestrians face before they cross crowded streets. Other work has used the platoon phenomenon to describe the inter-vehicle distance [49].

Traffic models such as the car-following models and CA models predict that drivers try to maintain a minimum safe distance between vehicles. This distance is highly correlated with the vehicle speed as described in the speed-density relationship (3.10). Therefore, the assumption of Exponential distribution of inter-vehicle spacing is valid only in free-flow traffic in which vehicle speed is uncorrelated with density.

Moreover, studies of traffic jams predict that vehicle traffic has homogenous density when in the free-flow phase or near total traffic jam. In congested traffic, density is non-homogeneous due to traffic jams that results in grouping of vehicles in long queues. Jost and Nagel [78] measured the homogeneity by dividing the road length into equal-length sections and computing the variance of the sections' density. Similar experiments are used in Section 5.6.1 to verify their results and extend the experiments to 3-lane highways.

5.5 Estimation of lower-bound MTR in vehicular ad hoc networks

Jost and Nagel's analysis and simulations [78] show that vehicles in free-flow conditions are distributed along the road according to uniform distribution. It is concluded from the summary of the related work in Section 5.2, that the work of Santi and Blough in [124] applies to an environment similar to free-flow vehicle traffic in a single-lane road.

In this section, an estimate for the lower-bound of the MTR is derived for VANETs in highways by considering the non-homogenous distribution of vehicles along the highway in congested traffic. The derived lower-bound is based on the assumption that all vehicles are equipped with wireless transceivers so that they can be active

nodes in the communication network. It is also assumed that vehicle mobility is described by the NaSch-S2S model.

The lower-bound proposed in [124] defines the minimum (critical) range, r_c in (5.1). For convenience, (5.1) is rewritten as an inequality,

$$r_c(k) \geq \frac{\ln(L)}{k}, \tag{5.6}$$

where k is the density of vehicles.

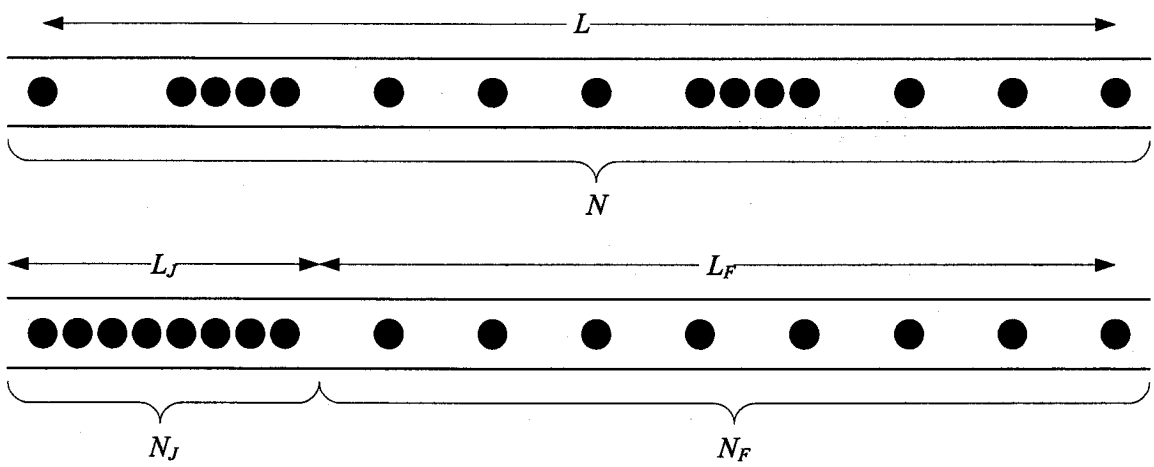

Figure 5.2: Congested traffic in a highway section: a) Original distribution; b) Consolidation of the free-flow and congested sections of the road.

A congested traffic system can be characterized as patches of traffic jams separated by jam-free regions [103], as shown in Figure 5.2(a). In a network such as the one shown in Figure 5.2(a), the worst case MTR value depends only on the traffic of the free-flow region since the MTR in the jam region is easily estimated as $1/k_{jam}$. To continue the derivation of the lower-bound, suppose that all free-flow regions can be consolidated in one side of the road and all congested regions are consolidated in the other side, as illustrated in Figure 5.2(b). Since equation (5.6) applies to the free-flow section, the critical range within the section, r_{c,L_F}, is given as,

$$r_{c,L_F} \geq \frac{\ln L_F}{k_F}, \tag{5.7}$$

where L_F is the length of the jam-free section of the road and k_F, is the density of the free flow traffic in the same section.

In a road such as the one shown in Figure 5.2, the flow of vehicles escaping the traffic jam, q_F, is a free-flow traffic that is virtually independent of the vehicle density. The value of q_F is determined by the average waiting time for the first vehicle in the traffic jam to move, $1/(1-p_{\text{s2s}})$ [30]. This outflow is the maximum flow achievable in the road [103]. Therefore, given that the speed in free-flow traffic is u_f, and from the fundamental relation (3.5), the maximum density in the free-flow section of the road is,

$$k_F = \frac{q_F}{u_f} = \frac{1-p_{\text{s2s}}}{U_{max}-p_{\text{noise}}} \,. \tag{5.8}$$

Let the traffic jam region in Figure 5.2(b) be occupied by N_J vehicles spanning a length of L_J. Also, let the free-flow region have N_F vehicles in a distance of L_F. Then, the total length and number of vehicles are:

$$L = L_F + L_J \,, \tag{5.9}$$

$$N = N_F + N_J \,. \tag{5.10}$$

Using $k = N/L$, $k_F = N_F/L_F$, $k_{jam} = N_J/L_J$, equation (5.9) can be rewritten:

$$\frac{N}{k} = \frac{N_F}{k_F} + \frac{N_J}{k_{jam}} \,. \tag{5.11}$$

Substituting (5.10) into (5.11) yields,

$$\frac{N_F}{k_F} - \frac{N_F}{k_{jam}} = \frac{N}{k} - \frac{N}{N_J} \,. \tag{5.12}$$

Therefore, the fraction of vehicles in free-flow traffic is,

$$\frac{N_F}{N} = \frac{k_{jam}k^{-1}-1}{k_{jam}k_F^{-1}-1} \,. \tag{5.13}$$

Continuing from (5.9),

$$\begin{aligned} L_F &= L - \frac{N-N_F}{k_{jam}} \\ &= L - \frac{N}{k_{jam}}\left[1-\frac{N_F}{N}\right] \,. \end{aligned} \tag{5.14}$$

Substituting (5.13) in (5.14) yields,

$$L_F = L - \frac{N}{k_{jam}} \left[1 - \frac{k_{jam} k^{-1} - 1}{k_{jam} k_F^{-1} - 1} \right] . \tag{5.15}$$

Hence, the fraction of the free-flow region is:

$$\frac{L_F}{L} = \frac{k_{jam} - k}{k_{jam} - k_F} . \tag{5.16}$$

Knowing that the MTR in the road must be equal to or higher than that of the free-flow region, then,

$$r_{c,L} \geq r_{c,L_F} . \tag{5.17}$$

Substituting (5.16) to (5.6), and using (5.17), the critical range for the entire road length, $r_{c,L}$, is given,

$$\begin{aligned} r_{c,L} &\geq \frac{\ln(L_F)}{k_F} \\ &= \frac{1}{k_F} \ln \left[\frac{L(k_{jam} - k)}{k_{jam} - k_F} \right] \\ &= \frac{1}{k_F} \left[\ln(L) + \ln \left(\frac{k_{jam} - k}{k_{jam} - k_F} \right) \right] \qquad k > k_c . \end{aligned} \tag{5.18}$$

The critical range, r_c, in (5.18) depends only on the length, L, of the road section and the vehicle density within the section, k, since both densities k_F and k_J are constants. The value of k_F is obtained from (5.8) using the values $U_{max} = 5$ cell/s, $p_{\text{noise}} = 0.01$, and $p_{\text{s2s}} = 0.5$,

$$k_F = \frac{1 - p_{\text{s2s}}}{U_{max} - p_{\text{noise}}} = \frac{0.5}{5 - 0.01} \approx 0.1 . \tag{5.19}$$

Finally, from equations (5.6) and (5.18), the lower-bound of the MTR in a highway of length L and density k is given by

$$r_c(k) = \begin{cases} \dfrac{\ln(L)}{k} & k \leq k_c \\ \dfrac{\ln(L)}{k_F} + \dfrac{1}{k_F} \ln \left(\dfrac{k_{jam} - k}{k_{jam} - k_F} \right) & k > k_c \end{cases} \tag{5.20}$$

Figure 5.3 shows the plot of equation (5.20). The values of k_c and k_F are determined for different values of U_{max} using (5.2) (assuming $k_c \approx k_{det}$) and (5.8), respectively.

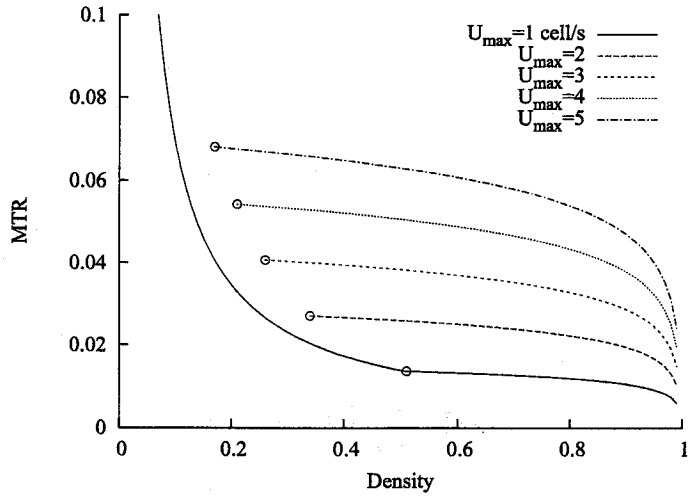

Figure 5.3: The lower bound of MTR in a highway of 1000-cell length and various values of maximum speed, U_{max}.

5.6 Evaluation

The analytical relationships that were derived in previous sections are verified through simulations of vehicle traffic. A closed-loop highway, with single or three lane(s), is used for all the simulations described in this section. The highway configuration is similar to the test network described in Section 4.4. The racetrack is 1000-cell (7.5 km) long; vehicles enter from a parking facility located at cell 20 with an input flow of $\frac{1}{60}$ veh/s (60 veh/hr) and continue to travel around the track indefinitely, which causes vehicle density to increase until the jam density is reached and no more vehicles can enter.

In single-lane roads with no overtaking, vehicles will travel at the speed of the slowest vehicle regardless of their maximum speed capabilities. Therefore, all vehicles have the same maximum speed in simulations of the single-lane highway while the three-lane highway configuration includes vehicles of various maximum speeds. Note that the maximum speeds are meaningful only in free-flow traffic. At higher densities, vehicles travel at a lower speed, which is unrelated to their maximum speed.

Simulation data was collected in a section of 134 cells (1005 meters) length in the middle of highway. This section is located at the furthest point from the vehicle entry

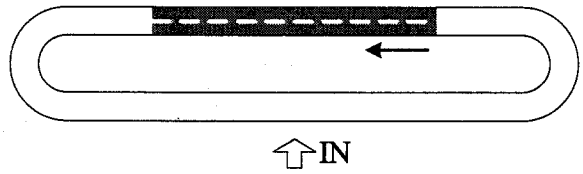

Figure 5.4: Racetrack configuration.

point in order to avoid the effect of the latter on the traffic. Each of the simulation experiments was executed 20 times.

The VANET within the measurement area is represented as a graph $G(V, E)$, where a set of vertices V represents vehicles, and a set of edges E represents direct communication links. In the simple communication model that is used here, a communication link, $e_{i,j} = (v_i, v_j)$ exists if and only if the Euclidean distance between vehicles v_i and v_j is less than or equal to the shortest transmission range between them, i.e,

$$E = \{(v_i, v_j) \in V^2 \mid |x_i - x_j| \leq \min(r_i, r_j)\} \tag{5.21}$$

where x_i, r_i are the position and transmission range of the node v_i, respectively. Equation (5.21) results in an undirected graph.

5.6.1 Vehicle distribution

Jost and Nagel [78] used the variance of local density as a metric to measure the homogeneity of vehicle distribution in the different phases of traffic using the NaSch-S2S model. In this scheme, a road is divided into m segments of equal-length, then the local density of each segment k_l, is determined. The variance of the local density is calculated as follows [78]:

$$\mathrm{Var}(k_l) = \frac{1}{m} \sum_{i=1}^{m} (k_l(i) - k_L)^2 \,, \tag{5.22}$$

where k_L is the system-wide density, and i is the segment index. The value of $\mathrm{Var}(k_l)$ indicates how much the density of each individual segment deviates from the average density value. The value of $\mathrm{Var}(k_l)$ will be at its lowest level when the density in all segments are equal, indicating a homogenous distribution of vehicles on the road. On

the other hand, if there is a traffic jam in one segment and free-flow traffic in another, densities in both segments will show a significant deviation from the system-wide density.

Unlike the measurements in [78], which are limited to a single-lane racetrack and a maximum speed of $U_{max} = 5$. The simulations in this section include 1- and 3-lane racetrack highways with multiple speed options. To be able to identify the effect of the maximum speed U_{max} on determining the transition point between free-flow and congested (or coexistence) phases, two sets of simulations were run using $U_{max} = 5$ and $U_{max} = 3$ cell/s in single-lane roads. Multi-lane road experiments were run using a single maximum speed of $U_{max} = 5$ in one scenario and a combination of three maximum speeds of $U_{max} = \{3, 4, 5\}$ cell/s (in %15, %70, and %15 of vehicles, respectively) in another.

Density is measured in $m = 26$ small sections of $l = 5 - cell$ length (in the middle of the highway configuration described in Section 5.6). In each section i, the number of vehicles in the section $N_{i,j}$, is counted once every time step, j; then, counts of $M = 120$ time steps are averaged. The density in each section, $k_l(i)$, is obtained by,

$$k_l(i) = \frac{1}{M \times l} \sum_{j}^{M} N_{i,j} \; . \tag{5.23}$$

This scheme resulted in 500 measurements of $\mathrm{Var}(k_l)$ in each simulation run of the 1-lane road and 208 measurements per lane in the 3-lane road.

A sample of the results is provided in Figure 5.5 to illustrate the difference in vehicles distribution at various traffic conditions. The two sets of bars in the figure show the value of the $k_l(i)$ in each of the sections where local density is measured. The dark bars in the figure show that the density is virtually identical in all road sections when density is low (≈ 0.1). The light bars show that density varies significantly from one part of the road to another due to traffic jams. This difference is measured quantitatively using $\mathrm{Var}(k_l)$ as shown in Figure 5.6.

Figure 5.6 indicates that at low densities of $k < k_c$, the value of $\mathrm{Var}(k_l)$ is close to zero, indicating a homogenous distribution of vehicles associated with the free-flow traffic phase. For higher densities, the variance grows significantly larger than zero indicating nonhomogeneous distribution of vehicles in the congested traffic phase. Note

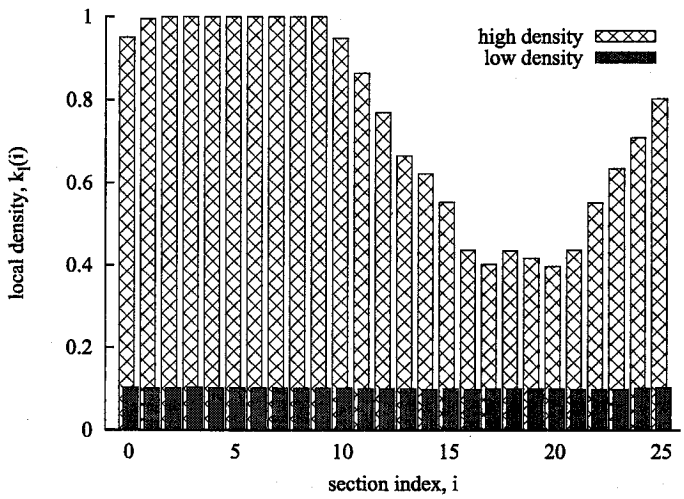

Figure 5.5: Vehicle density in 26 consecutive road sections of 5-cell length in a) free-flow traffic, b) congested traffic.

that the variance value declines as density approaches k_{jam} (=1 veh/cell) indicating another homogenous state when all vehicles are in wide traffic jams.

It can also be noted that multi-lane traffic (Figure 5.6(b)) exhibits less variance in density than single-lane traffic (Figure 5.6(a)) at densities higher than 0.4 veh/-cell. However, traffic enters the congested phase at the same critical density as in a single-lane road, indicating that the flow-density relationship of Figure 5.1(b) applies regardless of the number of lanes.

Figure 5.6 does not show a clear distinction between the coexistence state and the congested state as in Figure 5.1(b). In contrast, the point at which free-flow traffic ends is clear. This point is given by equation (5.5). In the single-lane road, the value of the transition densities are $k_1 \approx \frac{1}{11}$ veh/cell and $k_1 \approx \frac{1}{7}$ veh/cell for traffic of maximum speed $U_{max} = 5$ cell/s and $U_{max} = 3$ cell/s, respectively. In multi-lane highways of various maximum speeds, the transition occurs at a density that corresponds to the average maximum speed ($U_{max} = 4$ cell/s), at $k_1 \approx \frac{1}{9}$ veh/cell.

5.6.2 Minimum transmission range

This section illustrates the effect of vehicle traffic characteristics on the MTR when density is changed from free-flow to a total traffic jam. It should be emphasized that

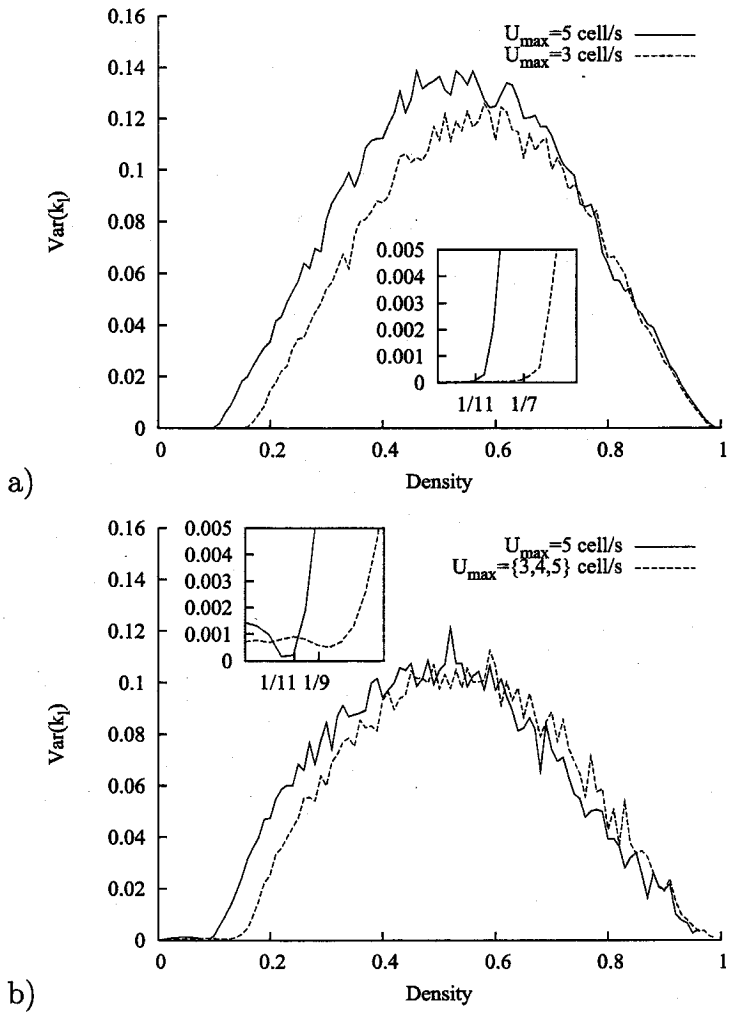

Figure 5.6: The value of $\mathrm{Var}(k_l)$ vs. system-wide traffic density in a) 1-lane road, and b) 3-lane road.

increasing the density not only increases the number of vehicles on the road but also creates traffic jams and lowers the average speed of vehicles when the vehicle density is higher than some critical density.

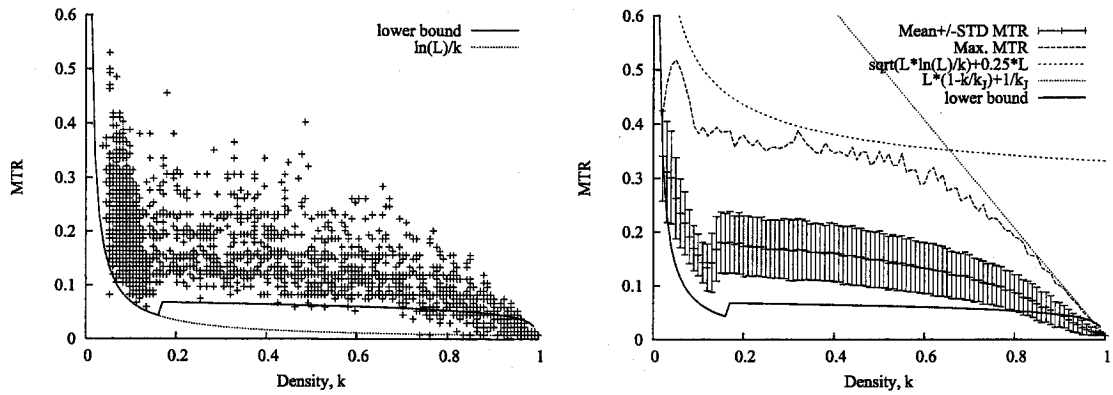

Figure 5.7: MTR in single-lane road.

In general, the MTR is determined by constructing a MST in the graph $G(V, E)$ among the vehicles using Prim's algorithm. The MTR is the longest edge in the MST [108]. In a single-lane VANET, the MTR is the widest gap between any two consecutive vehicles.

Simulations were used to determine the MTR needed to connect the wireless network among vehicles in the road configurations described at the begining of Section 5.6. The MTR was determined in every simulation time-step and stored along with the vehicle density. Figure 5.7(a) shows a scatter plot of MTR values vs. density in a 1-lane VANET. The plot shows clearly that the MTR values are concentrated above the modified lower bound of MTR of equation (5.20) in densities higher than the critical density. However, MTR values drop below this bound to that of equation (5.6) at much higher densities indicating the return to the homogenous distribution of vehicles as traffic jams increase in size and merge to become a wide traffic jam (as illustrated in Figure 5.6).

The data collected from the simulations is classified into 100 density intervals that cover the entire density range. The mean and the standard deviation of the MTR values are calculated within each density interval to be plotted vs. the average

density in each interval. The shaded region in Figure 5.7(b) shows the mean value of MTR+/-the standard deviation vs. density in the single-lane road configuration. It is observed from the plot that the MTR values are higher than would be the case in homogeneous traffic at densities higher than the critical density. The discrepancy starts at density ($k_c \approx 1/(U_{max}+1) = 1/6$) when traffic is no longer in free-flow. As a result, a longer MTR is needed to maintain the network connectivity in traffic conditions that exhibit mixed state of free-flow and traffic jams.

As density increases, traffic jams increase in size and merge with other traffic jams until the entire road is composed of one wide traffic jam. Consequently, the MTR decreases until it reach its minimum value of $1/k_{jam}$ (the distance from front-bumper to front-bumper between two vehicles).

The plot of the average maximum MTR is compared with two relations. The maximum MTR, r_{max}, for a network of finite length, L, is obtained by assuming that all but one vehicle are packed at distance of $1/k_{jam}$ from each other at one side of the road while the remaining vehicle is located at the opposite side; thus the longest possible transmission range, r_{max}, is needed to preserve the network's connectivity. This range is:

$$r_{max} = L\left(1 - \frac{k}{k_{jam}}\right) + \frac{1}{k_{jam}} . \tag{5.24}$$

In addition, the graph in Figure 5.7(b) shows that the average upper bound MTR can be approximated by shifting the upper bound estimated in [124] higher by a factor, αL,

$$r \leq \sqrt{L\ln(L)/k} + \alpha L , \tag{5.25}$$

where $\alpha = 0.25$. The proximity of the MTR to the upper bound estimate of (5.25) declines as the densities increases beyond the intersection point between (5.24) and (5.25) where the MTR declines rapidly towards the minimum value of $1/k_{jam}$.

Traffic jams continue to affect traffic in multi-lane roads as discussed previously. Recall that the density is expressed by the number of vehicles that occupy a unit distance per lane. As a result, the number of vehicles in a unit distance of a 3-lane road is three times that of a 1-lane road. Since more vehicles are packed in the same distance, the MTR needed in a multi-lane is less that that of a single-lane of the same

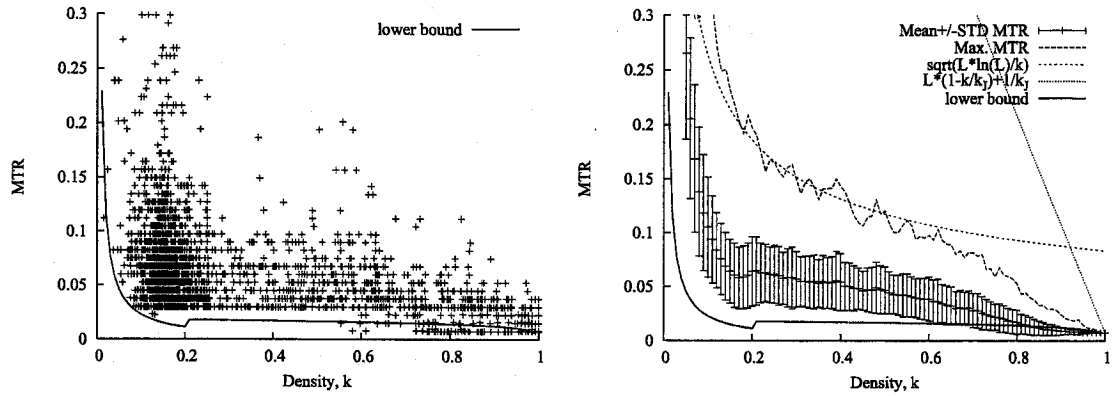

Figure 5.8: MTR in three-lane road.

density value. As a result, Figure 5.8(a) shows that the lower bound for the MTR is reduced by a factor of three (which is equal to the number of lanes). Figure 5.8(b) shows an increase in the mean MTR value near the critical density, which is located at $k \approx \frac{1}{5}$ due to the lower average free-flow speed. The average maximum MTR can be approximated by (5.24) with $\alpha = 0$.

Note that equation (5.20) is developed for 1-lane highway (1-dimentional VANET); as the number of lanes increases, the vertical distance between vehicles (at the same horizontal positions but between different lanes) become a factor in determining the MTR. In other words, the network becomes two-dimensional as the number of lanes increases. The study of this type of network is outside the scope of this thesis.

5.7 Summary and conclusions

This chapter provides the link between the phenomenon of traffic jams and the connectivity of a VANET. It is shown that traffic jams affect the homogeneous distribution of vehicles in congested (high density) traffic. The consequence to VANETs is manifested in the need for a higher transmission range than would be needed if the distribution were homogenous.

The main contribution of this chapter in this regard is summarized in equation (5.20) where an analytical lower-bound for the MTR is derived. The relationship

takes into account the non-homogenous distribution of vehicles at densities beyond the free-flow densities.

The change of vehicle distribution between homogenous and non-homogeneous is verified through simulations. The simulations show that regardless of the number of lanes or vehicle speed, vehicle distribution changes from homogenous in densities below a critical density to non-homogeneous in intermediate densities. Vehicle distribution returns gradually to a homogenous state as densities approach wide traffic jams. The latter condition is due to vehicles being stationary in long queues.

Simulation results show that the lower bound for MTR values can be estimated accurately for low and moderate densities. At high densities (near wide traffic jam conditions), vehicle distribution returns to the homogenous phase; thus the MTR values are lower than the estimates. The multi-lane scenario shows that MTR values are lower than those of a single-lane due to the additional number of vehicles for the same density values. This observation implies that the presence of multiple lanes improves connectivity by lowering the MTR requirements.

Chapter 6

Minimum Transmission Range Across Intersections

This chapter formulates two relationships between vehicle flow and the MTR required to maintain connectivity in VANETs that spans two sides of an intersection. A pdf for the MTR is derived for a signalized intersection. The resultant MTR estimates are compared with *RoadSim* simulations. An empirical relationship between traffic flows and the MTR is obtained from traffic simulations for an unsignalized intersection.

6.1 Introduction

Connectivity in a VANET is greatly effected by the distribution of vehicles in the transportation network. It is shown in the previous chapters that traffic jams result in disturbing the homogenous distribution of vehicles by concentrating the vehicles in some parts of the roads more than others. The consequence to VANETs is that a larger transmission range is needed to maintain connectivity. Intersections, access ramps, speed controls, road constructions, and accidents, can also cause disruption to the flow of traffic by creating traffic jams and large gaps between vehicles traveling along the same road.

This chapter analyzes the gaps (distances) forced between consecutive vehicles

by two types of intersections, signalized and unsignalized intersections. These gaps have a negative impact on the connectivity of VANETs, which is represented by the increase of the transmission range needed to connect the vehicles across and downstream of the intersection. The main cause of the gaps is the delay experienced by vehicles while waiting for the opportunity to enter the intersection safely. The delay at the intersection translates into longer headways between vehicles downstream of the intersection.

Analytical approaches that study intersections, such as the ones reviewed in [120, 138], aim at predicting the delays experienced by drivers and the effect on the road's capacity. These models are useful in the discussion of the connectivity among vehicles. However, they do not model the distance between vehicles. As a result, simple probabilistic analysis and simulations are derived in this chapter to estimate the MTR needed in either type of intersection. The simulations are based on the extensions described in Section 4.3.5, which add the support of intersections to the NaSch model.

Section 6.2 describes the effect of intersections on the MTR and defines the terms that are used throughout this chapter. In Section 6.3, the delay caused by several factors at a signalized intersection is estimated and used to derive a pdf for the MTR in this type of intersection. Simulations in Section 6.4 are employed to evaluate the results of the previous section. In Section 6.5 simulations are used to derive an empirical estimate of the MTR at an unsignalized intersection. The conclusions of this chapter are summarized in Section 6.6.

6.2 Connectivity across intersections

Intersections disturb the normal flow of traffic by forcing vehicles to slow down or stop for some time. If the waiting time at the intersection is relatively long, the VANET, composed of vehicles at both sides of the intersection, will be split into two regions, as depicted in Figure 6.1. A queue of vehicles will form behind the intersection creating a region of high vehicle density, a traffic jam. Downstream of the intersection, vehicle density will drop considerably as vehicles travel away from the intersection.

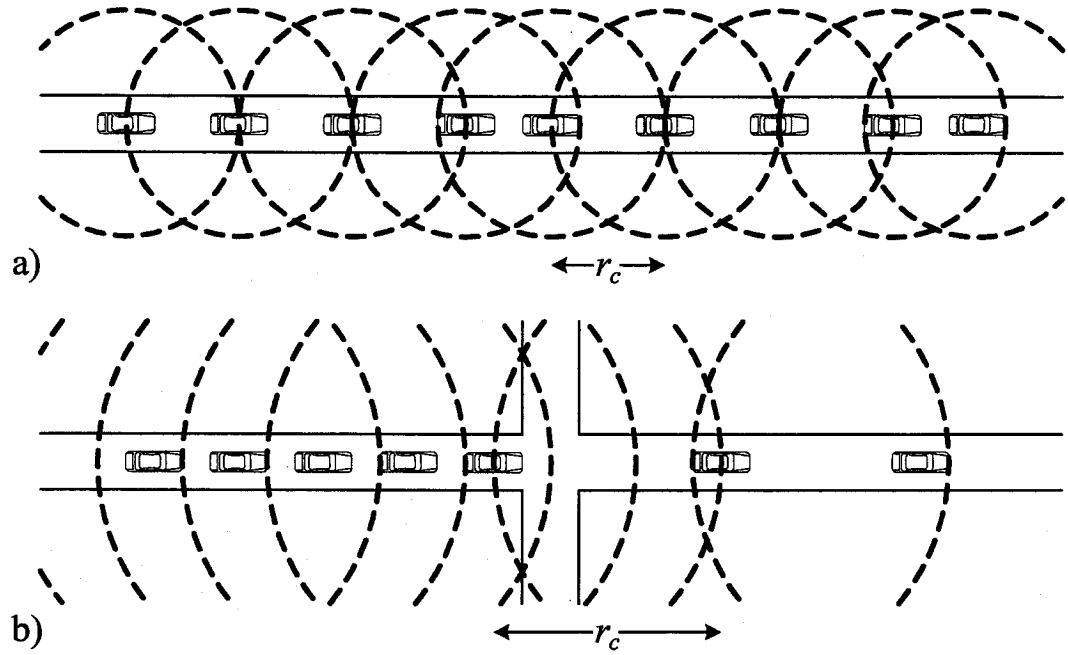

Figure 6.1: The MTR value, r_c in a) an uninterrupted road, and b) across an intersection.

In general, a longer MTR is needed to maintain connectivity across an intersection than what would be needed to maintain connectivity when vehicles are homogeneously distributed on the road. This is due to the increased distance between vehicles that are waiting to cross the intersection and those that just passed it.

Figure 6.2 illustrates the definitions of the terms used throughout this chapter:

Definition 6.1 *Intersection is an area where two highways join one another at, or approximately at, right angles and at the same elevation level.*

Definition 6.2 *Signalized intersection is an intersection that depends on (electrical) traffic signals to indicate which vehicle traffic can enter the intersection at any particular time.*

Definition 6.3 *Unsignalized intersection is an intersection that employs traffic signs (Stop or Yield) to indicate which vehicle has the priority to enter the intersection, but leave the driver to decide when it is safe to enter the intersection.*

Definition 6.4 *Main highway is a highway that carries frequent, high volume vehicle traffic.*

Definition 6.5 *Secondary highway is a highway that carries infrequent, low volume vehicle traffic.*

Definition 6.6 *Interfering lane is a lane whose traffic direction intersects with the direction of a vehicle attempting to enter the intersection, which raises the possibility of a collision.*

Definition 6.7 *Priority traffic is a vehicle traffic on the main highway that faces no traffic sign when approaching an unsignalized intersection.*

Definition 6.8 *Non-priority traffic is a vehicle traffic on the secondary highway that faces a Stop or Yield sign when approaching an unsignalized intersection.*

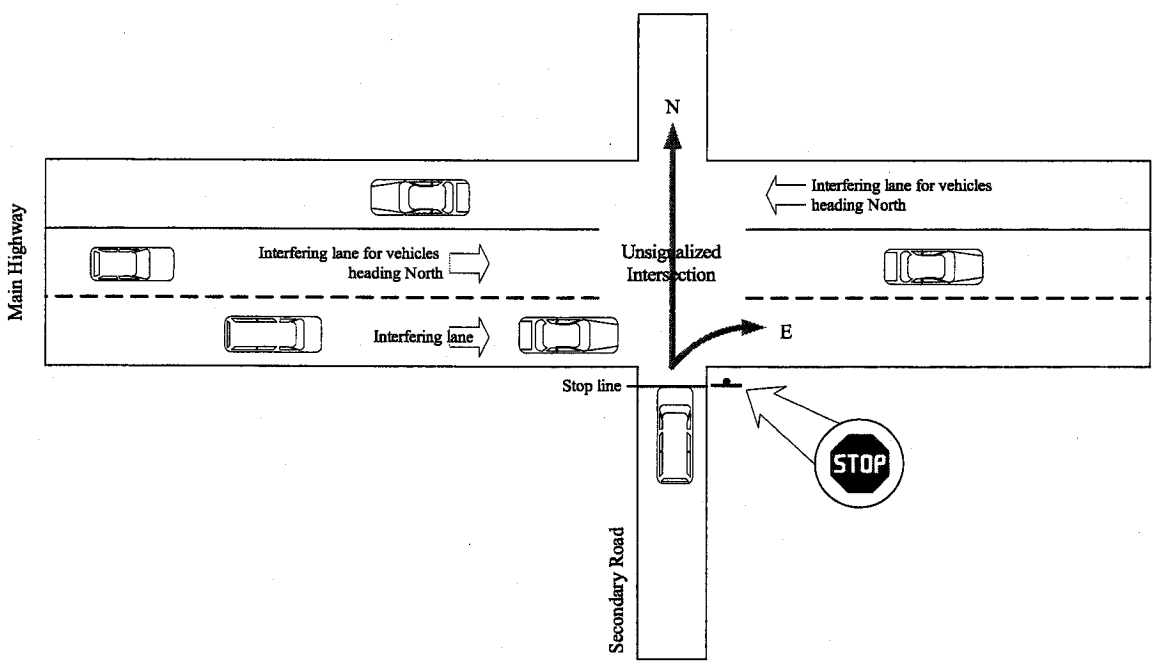

Figure 6.2: An example of intersection that illustrates some of the used terminology.

The discussions of this chapter are relevant to highway configurations where two single-lane highways meet at an intersection. In signalized intersections, a traffic light

controls which traffic stream is allowed to enter the intersection at any given time. In an unsignalized intersection, entry to the intersection is controlled by a stop or yield sign. The traffic stream on the secondary highway may face a traffic sign that directs vehicles to stop or slow down before entering the intersection in order to allow traffic on the main highway to proceed. The traffic on the main highway does not face any traffic sign and can proceed through the intersection without delay (4-way stop intersections are not included in the discussions).

Since not all traffic that passes through the intersection is delayed, the analysis of the MTR is limited to the traffic affected by the intersection. In the signalized intersection, both traffic streams are equally affected by the intersection if they have the same flow and same light cycle. In the unsignalized intersection, only traffic on the secondary highway is affected by the intersection.

In order to simplify the analysis of the MTR across the intersections, it is assumed that: 1) The traffic light consists of two phases only, red and green. 2) All traffic approaching the intersection will eventually continue to travel in the same direction (i.e. no turning). 3) The intersection's dimensions are negligible such that the time needed for a vehicle to cross the intersection can be ignored. 4) The traffic ahead of the intersection is low so that it does not block or slow down the vehicles crossing the intersection.

As shown in Chapter 5, the lower bound of the MTR, r_c, in a 1-D network of homogeneously distributed nodes is inversely proportional to the node density, k. From [124]:

$$r_c(k) \geq \frac{\ln(L)}{k}\,, \tag{6.1}$$

where L is the network length.

From the fundamental relationship (3.5), the vehicle density is related to traffic flow and average time headway,

$$k = \frac{q}{u} = \frac{1}{u\bar{h}}\,. \tag{6.2}$$

Therefore, substituting (6.2) in (6.1) results in a new relationship that relates the MTR and the average speed and flow (or headway) between vehicles in a 1-D VANET

in free-flow traffic.

$$r_c \geq \frac{u_f}{q} \ln(L) = u_f \bar{h} \ln(L) \, . \tag{6.3}$$

Equation (6.3) shows the significant effect of intersections in VANETs. The equation indicates that the MTR is directly related to the headway between vehicles. The delays experienced by vehicles at the intersection increase the headway between vehicles leaving the intersection, which results in an increase in the MTR value.

To illustrate the effect of intersections on the MTR, *RoadSim* was used to simulate both types of intersection. In these simulations, the MTR measurements were taken in two segments of equal length (1 km) located upstream and downstream of an intersection similar to the one shown in Figure 6.1b.

Figure 6.3 shows a scatter plot of the MTR values vs. the vehicle density as measured in the upstream (left column) and downstream (right column) segments in every simulated time step. Equation (6.1) is also plotted in each case. Figure 6.3(b,d,f) show that vehicle density is within the free-flow range in the traffic downstream of the intersection. The delay experienced by vehicles at the intersection, because of a red light or because of waiting for a safe gap in the interfering traffic, reduces the vehicle density significantly downstream of the intersection. Once a vehicle can move, it can travel at its free-flow speed unobstructed by any traffic ahead. As a result, a large MTR is generally needed to maintain connectivity in this area of the highway.

The intersection has the opposite effect on the region upstream of the intersection. Generally, the waiting time at the intersection generates queues of vehicles, i.e., traffic jams of high vehicle density. Consequently a small MTR is needed. The size of the jam depends on the flow of vehicles approaching the intersection and the delay encountered at the intersection. These factors correspond to the inter-arrival time and the service time in queuing theory. The size of the jam and the speed of the traffic waves propagating in both directions of the intersection can be calculated directly from the shock wave equation (3.8).

Figure 6.3a shows that the traffic light creates an area of large density traffic when traffic is stopped behind a red light. In a stop-sign intersection, the waiting time at the stop line depends on the flow of vehicles in the interfering lane(s) ($q_p = 900$ veh/hr in this case). Figure 6.3c shows a pattern similar to that of the signalized

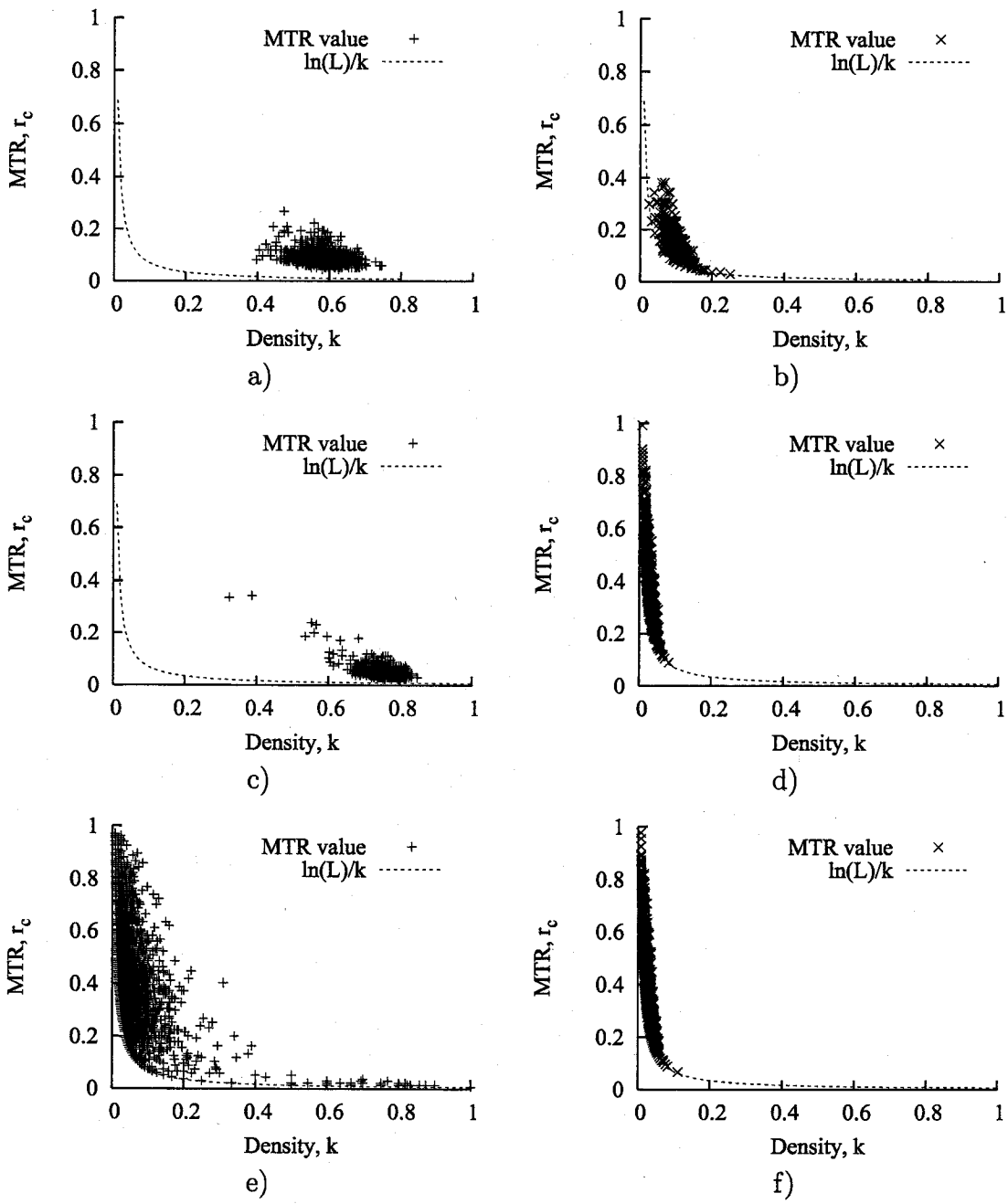

Figure 6.3: MTR values in VANETs across a,b) a signalized intersection with a approaching traffic flow of 1800 veh/hr, c,d) a stop-sign intersection with an approaching traffic flow of $q_n = 600$ veh/hr, and e,f) a stop sign intersection with an approaching flow of $q_n = 400$ veh/hr. The left and right columns represent the data collected in the upstream and downstream segments, respectively. More than 99% of points were removed to reduce the clutter.

intersection where most of the upstream traffic is in a traffic jam behind the stop line. This is due to the relatively small headway between vehicles (high flow rate) in the approaching traffic, relative to the waiting time at the intersection ($q_n = 600$ veh/hr). In Figure 6.3e, the flow rate is lower ($q_n = 400$ veh/hr). As a result, the upstream traffic remains mostly in free flow, i.e. queues behind the stop line dissipate quickly.

Note that in all cases of Figure 6.3, the density of vehicles changes abruptly from high to low. This situation is an ideal example of the challenges facing VANETs. In order to cope with this change in traffic conditions without losing connectivity, vehicles must be equipped with a transceiver of a high transmission range. However, such transmission range has an adverse effect on the capacity of the VANET during traffic jams.

An investigation of a possible trade-off that avoids an extremely high transmission range at the expense of some partitioning of the VANET is presented in [22] as a preliminary work leading to the discussion in this chapter. The paper illustrates the effect of intersections on the MTR using *RoadSim* simulations of 1-lane, 2-lane, and 2-directional highways. This chapter provides estimates of the lower bound of the MTR in the downstream segment of the intersection and employs simulations to verify the results in intersecting 1-lane highways.

6.3 Signalized intersection

A signalized intersection is characterized by traffic lights that control which traffic stream is allowed to enter the intersection at any given time. When a secondary highway intersects with a main highway, the traffic light provides an opportunity for traffic coming from the secondary highway to cross the main highway, which otherwise will be difficult or dangerous.

The traffic lights affect vehicle traffic in two ways; they create traffic jams behind the intersection, which result in reducing the distance between vehicles, and they create areas of low density traffic ahead of the intersection, which increases the distance between vehicles. A homogenous transmission range for all vehicles in a VANET must

be greater than or equal to the largest distance between any two vehicles in order to keep the entire network connected (compare Figure 6.1a with Figure 6.1b).

Main studies of signalized intersections focus on determining the level of service in a transportation network by providing estimates for performance measures such as traffic delays and queues length. Other studies focus on signal timing [120]. Unlike these studies, the focus of this section is to formulate a relationship for the MTR needed among vehicles to maintain the connectivity of the VANET across the intersection. Towards this goal, three models of increasing complexity are used to estimate the transmission range between the vehicle stopped at the intersection and the nearest vehicle in the downstream traffic.

The effect of a signalized intersection on the connectivity is illustrated by a simple example. Let a pair of vehicles approach a signalized intersection at speed, u_0, at the end of the green phase. The lead vehicle, v_0, enters the intersection just as the light turns to red (assuming there is no amber period) while the following vehicle v_1, stops at the traffic light for the period of the red phase, τ_0. During the red phase, the vehicle v_0 continues to travel away from the intersection, thus increasing its distance to vehicle v_1. At the end of the red phase, the distance between the vehicles is,

$$s = u_0 \times \tau_0 \,. \tag{6.4}$$

Figure 6.4 illustrates the space-time diagram of the scenario described above. The diagram on the left shows the locations of vehicles v_0 and v_1 just before v_1 starts to enter the intersection (when the green phase returns). The solid lines in the space-time diagram show the trajectories of the vehicles as time progresses where the slope of the lines represent the speed. After the light turns green, vehicle v_1, will be able to resume travel at free-flow speed, u_f, due to the wide gap ahead. Equation (6.4) shows that the maximum distance between the two vehicles depends on the initial speed u_0 and the red-phase period but not on the original distance between the two vehicles before they arrive at the intersection.

The dotted line in Figure 6.4 shows a case when the initial headway, h, between the two vehicles is greater than the red time, in which case the traffic light does not change the distance between the vehicles.

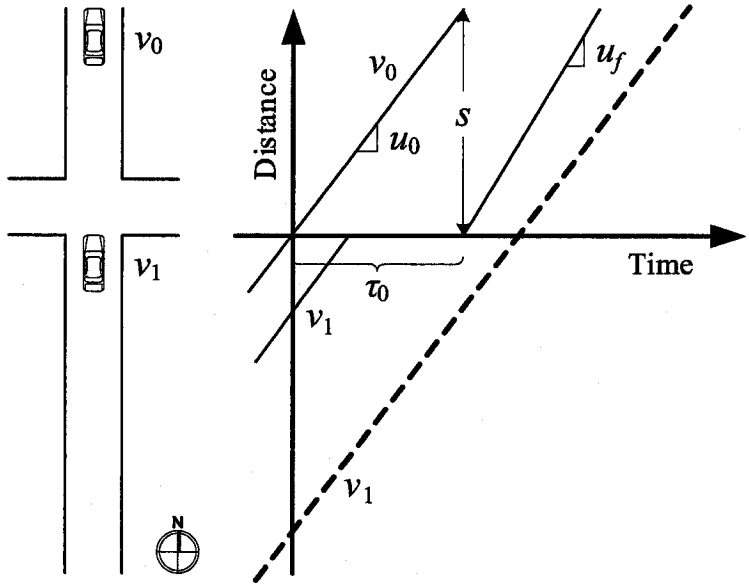

Figure 6.4: Traffic light increases the headway in traffic of moderate density.

This simple example shows that, in moderate or high traffic density (when $\tau_0 > \bar{h}$), the traffic light has the effect of increasing the headway between vehicles. As a result, the transmission range in a VANET that spans the two sides of a signalized intersection, r_L, must have a minimum value of,

$$r_L \geq s = u_0 \times \tau_0 \,, \tag{6.5}$$

in order to maintain the connectivity during the red-phase. Note that the green-phase has negligible influence on the connectivity since the maximum distance always occurs between the last vehicle that enters the intersection at the end of the green-phase and the first vehicle to enter the intersection at the beginning of the next green phase, notwithstanding the low traffic flow when the mean headway is greater than the red-phase period. Equation (6.5) provides a lower bound for the MTR, which is based on the average speed of vehicles and the red-phase period.

A second model can provide a more accurate estimate of the MTR by considering additional factors that contribute to increasing the headway between vehicles beyond the red time. Figure 6.5 illustrates three of these factors: The change of traffic light to red does not always coincide with a vehicle passing the intersection as assumed in the example of Figure 6.4. Instead, there is usually a time difference between the instant

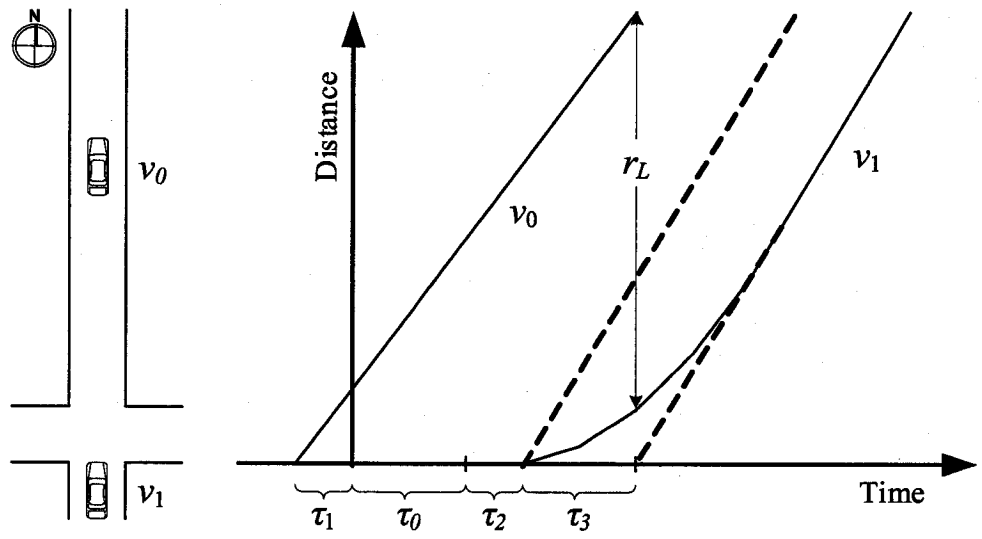

Figure 6.5: Headway between vehicles across intersection.

the last vehicle leaves the intersection and the start of the red-phase; the average of the time difference is denoted τ_1. In addition, due to variable driver reaction time, the stopped vehicles may require an additional time after the light turns green before they move; this time is denoted τ_2. Moreover, a stopped vehicle takes longer to get through the intersection while it accelerates to its maximum speed, which increases the time gap by τ_3 relative to a vehicle capable of instant acceleration.

The complete dotted line in Figure 6.5 represent the trajectory of vehicle v_1 assuming that the vehicle is capable of accelerating instantly to its free-flow speed, u_f. In this case, the longest distance between the vehicles occurs at time $\tau = \tau_0 + \tau_1 + \tau_2$. As time progresses, the distance will decrease gradually as v_1 catches up to the traffic ahead of the intersection (the distance remains the same if $u_0 = u_f$). Since a typical vehicle cannot accelerate to its desired speed instantaneously, the distance between the vehicles v_0 and v_1 will continue to increase as v_1 accelerates at a constant rate, a, until the speed of the following vehicle reaches the speed of the leading vehicle. During this time, the distance between the two vehicles at time t is given by

$$s(t) = \mid u_0 t - \frac{1}{2} a(t-\tau)^2 \mid , \tag{6.6}$$

where τ is the time when v_1 starts to accelerate. The maximum distance between

the two vehicles occurs at time τ_L,

$$\tau_L = \frac{u_0}{a} + \tau \ . \tag{6.7}$$

From (6.6) and (6.7), the maximum distance between the two vehicles is,

$$s_{max} = \frac{u_0^2}{2a} + u_0\tau \ . \tag{6.8}$$

It appears from Figure 6.5 that the distance of (6.8) is equivalent to the one that results from a vehicle capable of instant acceleration to speed u_0 (or higher) at time $\tau + \tau_3$ (compare the dotted line with the extension of the curved solid line). The distance between v_0 and v_1 after time $\tau + \tau_3$ (assuming instant acceleration):

$$s(t) = \mid u_0 t - u_0 \left(t - (\tau + \tau_3)\right) \mid \tag{6.9}$$

By substituting (6.8) in (6.9), the value of τ_3 at maximum distance s_{max}, is found to be,

$$\tau_3 = \frac{u_0}{2a} \ . \tag{6.10}$$

Therefore, the MTR between the vehicles of Figure 6.5, depends on the speed of the lead vehicle, u_0, and the sum, τ_L, of the four sources of delay that are described above,

$$\tau_L = \tau_0 + \tau_1 + \tau_2 + \tau_3 \ . \tag{6.11}$$

The delay terms of equation (6.11) represent deterministic averages. In the third model, the delay factor can be split into two components; a deterministic component, which is experienced by all vehicles, and a stochastic component that causes the time-gap to be different for each vehicle. In a single intersection, the red time, τ_0, remains constant for an extended period of time and it represents the major source of delay, which can be an order of magnitude longer than other sources. The delay caused by acceleration, τ_3, is also assumed to be deterministic. The values of the remaining delays are random. Therefore, the total delay can be represented by a Random Variable (RV), T_L.

$$T_L = T_r + \tau_d \ , \tag{6.12}$$

where T_r is a RV that represents the stochastic part of the time-gap, and $\tau_d = \tau_0 + \tau_3$.

The first component of T_r is the elapsed time since the last vehicle has passed the intersection when the light changes to red. Let T_1 be a RV that takes the value of this time difference. Also, assume that the inter-arrival time between vehicles approaching the intersection is based on Exponential distribution. Given the Poisson Arrivals See Time Averages (PASTA) property, T_1 has the same Exponential distribution as the vehicles inter-arrival time, with an arrival rate equal to the flow, q. The cumulative distribution function (cdf) of the Exponential distribution is,

$$F_{T_1}(t) = 1 - e^{qt} \quad t \geq 0\,. \tag{6.13}$$

The delay in a driver's reaction to the change of traffic light, known as Perception-Response Time (PRT), and the subsequent movement can be represented by another RV, T_2. The PRT depends on several factors, which include the type of stimulus and whether it was expected, and it is usually modeled by a Lognormal distribution [83].

$$F_{T_2} = \Phi\left(\frac{\ln(t) - \mu_{\ln(t)}}{\sigma_{\ln(t)}}\right)\,, \tag{6.14}$$

where $\Phi(\cdot)$ is the cdf of the Normal distribution of zero mean and unit variance. The $\mu_{\ln(t)}$ and $\sigma_{\ln(t)}$ are the mean and the standard deviation of Lognormal distribution, respectively.

Since the inter-arrival time of vehicles and the drivers' reaction time can be assumed independent, the joint pdf of T_r is obtained by convolving the pdfs of T_1 and T_2. The convolution is carried out numerically, as shown in the example in Figure 6.6 where the resultant pdf, $f_{T_r}(t) = f_{T_1}(t) * f_{T_2}(t)$, is plotted along with the Exponential and the Lognormal distributions.

The joint pdf has the following mean μ_{T_r}, and variance $\sigma^2_{T_r}$:

$$\mu_{T_r} = E[T_r] = E[T_1] + E[T_2]\,, \tag{6.15}$$

$$\sigma^2_{T_r} = \sigma^2_{T_1} + \sigma^2_{T_2}\,, \tag{6.16}$$

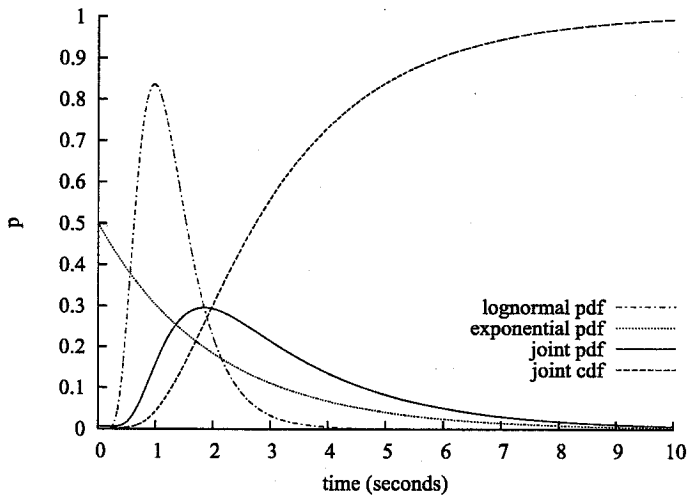

Figure 6.6: The pdf and cdf of the sum of Lognormal and Exponential distributions with parameters $\mu_{\ln(t)} = 1.31$, $\sigma_{\ln(t)} = 0.61$, and $q = 0.5$ (seconds).

where $E[\cdot]$ is the expected value of a RV. Consequently, the time-gap, T_L, has a pdf that is a displaced version of the pdf of T_r,

$$T_L = T_r + \tau_d \,, \tag{6.17}$$

with the following mean and variance:

$$\mu_{T_L} = \mu_{T_r} + \tau_d \,, \tag{6.18}$$

$$\sigma^2_{T_L} = \sigma^2_{T_r} \,. \tag{6.19}$$

Note that in light of (6.18), the value of τ_L in equation (6.11) can be viewed as the sum of the mean values of all delay sources (i.e., $\tau_1 = E[T_1]$, $\tau_2 = E[T_2]$, and $\tau_L = \mu_{T_L}$).

The distance that separates vehicles v_0 and v_1 is related to the speed of vehicle v_0 and the time-gap. Therefore, the transmission range across a signalized intersection R_L, is also a RV, which takes the value of:

$$R_L = u_0 \times T_L \,. \tag{6.20}$$

Therefore, from (6.17) and (6.20), the cdf can be obtained $P[R_L \leq r] = P[T_r \leq (r/u_0 - \tau_d))]$. The pdf is,

$$f_{R_L}(r) = f_{T_r}\left(\frac{r}{u_0} - \tau_d\right) . \tag{6.21}$$

The mean and variance of R_L are:

$$\mu_{R_L} = u_0\mu_{T_r} + u_0\tau_d , \tag{6.22}$$

$$\sigma^2_{R_L} = \mu_0^2\sigma^2_{T_r} . \tag{6.23}$$

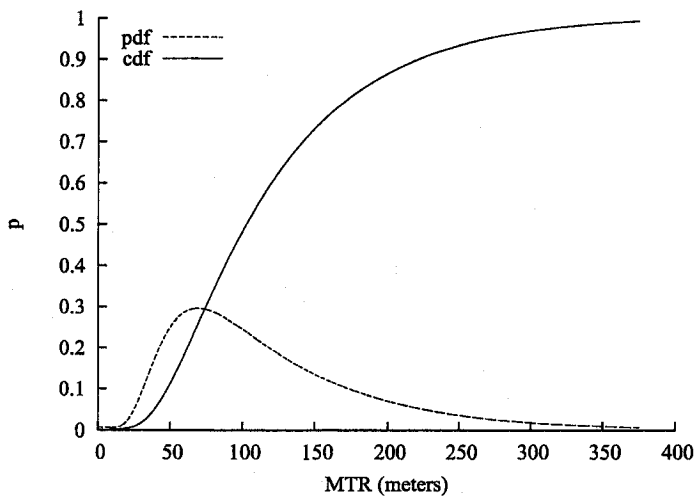

Figure 6.7: A plot of $f_{r_L}(r)$ and $F_{r_L}(r)$.

Figure 6.7 shows the pdf and cdf of R_L using the following parameters: The mean and variance of the PRT are 1.31s and 0.61s, respectively [83], vehicles flow is 0.5 veh/s (1800 veh/hr), and their speed is 37.5 m/s (135 km/hr). The sum of the red light period and acceleration delay is set to zero ($\tau_d = 0$) since its effect is limited to shifting the origin of the plot by the same amount.

Equation (6.21) is solved in Figure 6.7 by assuming some values for the PRT. The PRT is not defined explicitly in the NaSch-S2S model; instead, the slow-to-start probability, p_{s2s}, is used to model several phenomena including drivers' reaction time.

Due to the slow-to-start rule, the delay (measured in number of time steps, n_{s2s}) that a stopped vehicle may wait before it moves (once there is enough gap ahead), follows a geometric distribution,

$$P[N_{s2s} = n_{s2s}] = (1 - p_{s2s})^{n_{s2s}} p_{s2s} \, . \tag{6.24}$$

where N_{s2s} is a random variable that takes the value of number of time steps (with a mean of $(1 - p_{s2s})/p_{s2s}$ and a standard deviation of $(1 - p_{s2s})/p_{s2s}^2$).

An Exponential distribution with a rate $\gamma = 0.6931$ can be used to approximate the geometric distribution ($P[N_{s2s} = 1] = e^{-0.6931} \approx p_{s2s} = 0.5$) in representing the PRT. As a result, the pdf of the MTR, $f_{RL}(r)$ is reduced to a special case of a displaced gamma distribution with two parameters,

$$f_{R_L} = \begin{cases} q^2 \dfrac{r}{u_0 - \tau_d} \exp\left(\dfrac{-qr}{u_0 - \tau_d}\right) & q = \gamma, \, r > 0 \\ \dfrac{q\gamma}{q - \gamma}\left[\exp\left(\dfrac{-qr}{u_0 - \tau_d}\right) - \exp\left(\dfrac{-\gamma r}{u_0 - \tau_d}\right)\right] & q \neq \gamma, \, r > 0 \end{cases} \tag{6.25}$$

The derived equation of (6.25) provides the pdf for the MTR needed to maintain connectivity in the VANET across or downstream of a signalized intersection that connects two single-lane, one-way roads. The pdf of (6.25) is based on the NaSch-S2S model, but it can be generalized using an appropriate model for the PRT and vehicle arrival rate as described above.

6.4 Simulation of signalized intersections

All traffic simulations in this chapter are based on the road configuration shown in Figure 6.8. The road topology consists of two intersecting single-lane, one-way highways. The eastbound highway is 1000-cell (7.5km) long, and the northbound road is 1500-cell (11.25km) long. The intersection is located in the middle of eastbound road and one-third the length from the south end of the northbound road.

Vehicles of the eastbound stream enter the road from a parking facility near the west end of the road and leave through another parking facility located near the east end. Vehicles of the northbound traffic stream enter the road from a parking facility

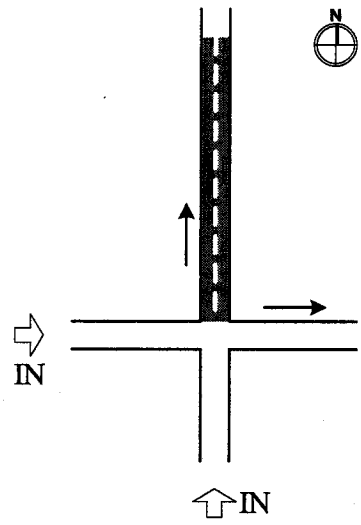

Figure 6.8: Simulated highway configuration.

near the south end of the road and leave through another parking facility located near the north end. Vehicles in both streams emerge from the parking facilities at time intervals drawn from a displaced Exponential distribution, which was described in Section 4.3.7.

Simulation data is collected in a single segment of 900-cell (6.75km) length that starts immediately downstream of the intersection on the northbound road (the shaded area in Figure 6.8). This segment is selected to measure the effect of the intersection on the northbound traffic. The data is collected in every simulation time-step (one second). Simulations are executed 20 times for each setup; the duration of each simulation run is 20,000s. The data within the initialization period is discarded from each run.

The flow of the northbound traffic is set to $\frac{1}{6}$ veh/s (600 veh/hr) at the speed of $u_f \approx 5$ cell/s ($\approx$ 135km/hr). These rates ensure that vehicles are in free-flow condition when they approach the intersection. Moreover, these rates ensure that the queues formed behind the intersection at the red light can dissipate quickly within the green phase (i.e. the service time of the traffic light is shorter than the arrival time of vehicles).

After passing the intersection, the vehicles will travel for 7.5 km before they exit

to another parking facility. The traffic light has a red-green sequence of 20 seconds each. The choice of the light cycle and the road length ensures that multiple platoons of vehicles are observed in the road segment downstream of the traffic lights. The platoons are formed due to consecutive discharges from the traffic light; thus, they are separated by the time-gap induced by the traffic light. Also, the red light period is chosen to be long enough to distinguish it from other sources of delay in (6.11).

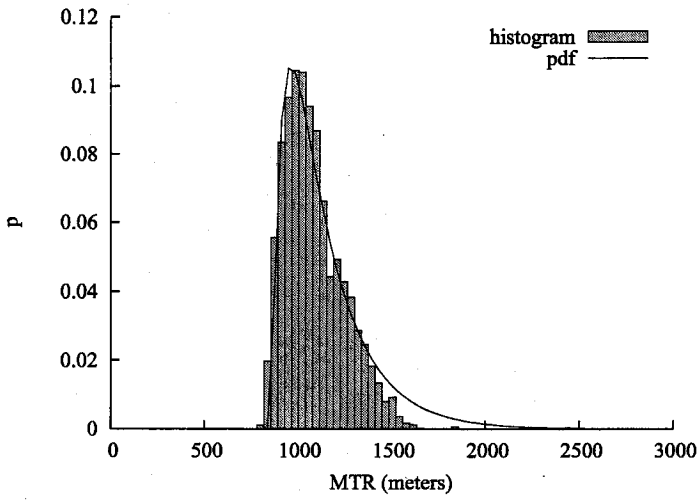

Figure 6.9: Histogram of MTR values collected in simulations of signalized intersection.

RoadSim simulations are employed to measure the MTR among the vehicles that pass through the signalized intersection described above. Since the traffic streams on the intersecting highways are affected equally by the traffic lights under the same conditions (red time and vehicle flow), only the northbound highway is used to collect the simulation data.

Figure 6.9 shows the histogram of the MTR values collected, after discarding an initialization period, from 9,440 traffic light cycles of 20 simulation runs. The plot of $f_{r_L}(r)$ of equation (6.25), with parameters $q = \frac{1}{6}$ and $\gamma = 0.6931$, is plotted over the histogram. The figure shows that the distribution of MTR closely matches the analytical distribution; however, the analytical pdf overestimates the percentage of high MTR values. Table 6.1 shows that the mean MTR obtained analytically and from simulations are virtually identical, but the standard deviation is much lower in the

simulation results. The discrepancy is due to the limit imposed on the measurement distance which does not permit the capture of the larger distances since the vehicles exit the road shortly after this distance.

Table 6.1: Descriptive statistics.

	Simulation	Analytical (6.25)
Mean	1087.72	1087.50
Std. deviation	165.53	237.17

6.5 Unsignalized intersection

Unsignalized intersections are the most common intersection type. They give no positive indication to the driver about when to enter the intersection. Instead, the driver must wait for a safe opportunity or "gap" in the interfering traffic before entering the intersection. This technique has been described as gap acceptance [138]. This gap is measured in time and is equivalent to headway.

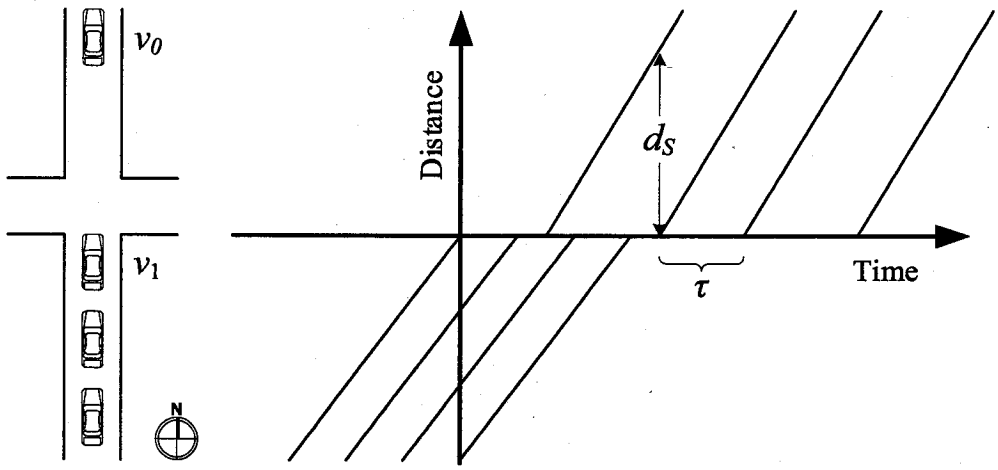

Figure 6.10: Vehicle trajectories upstream and downstream from a stop-sign intersection.

Figure 6.10 provides an example that illustrates the effect of the unsignalized intersection on connectivity. A stream of vehicles, traveling northbound on a secondary

highway, is approaching an intersection. Once the lead vehicle v_0, arrives at the intersection, it has to stop and wait for a safe gap in the interfering stream, the eastbound traffic on the main highway. Suppose that vehicle v_0 enters the intersection at $t = t_0$ and accelerates. The following vehicle v_1, moves near the stop-line and waits for the next opportunity to enter the intersection. Finally, vehicle v_1 can enter the intersection at $t = t_1$. This scenario changes the mean headway between the vehicles on the north-bound stream to τ_U. The resultant mean headway τ_U, depends not only on the flow of vehicles on the secondary highway, but also on the flow of the interfering stream. Consequently, the MTR value of equation (6.3) may also depend on the flow of the interfering traffic.

In the field of transportation engineering, unsignalized intersections are analyzed to determine their effect on the capacity of the transportation network. The gap acceptance theory [138] is commonly used to define the extent to which drivers are able to utilize a time gap of a particular duration. The theory is used to provide information such as whether a driver can leave the stop line at a secondary highway (see Figure 6.2) if the time between successive vehicles in the interfering traffic is ten seconds; or the number of drivers that can depart in this ten-second interval. The major challenges in this theory result from the difficulty in finding an appropriate vehicle distribution model so that time headways and gap distributions can be estimated. In addition, it is difficult to estimate the time gap the drivers consider safe to cross an intersection.

Traffic analysis for unsignalized intersections can be based on a simple queuing model in which the crossing of two traffic streams is considered [138]. A priority traffic stream (on the main highway) of flow q_p, and a non-priority traffic stream (traffic on the secondary road) of flow q_n, are involved in this queuing model. Vehicles in the priority stream can cross the intersection without any delay. Vehicles in the non-priority stream are only allowed to enter the intersection if the next vehicle from the priority stream is still t_c seconds away (t_c is the safety gap), otherwise they have to wait. Moreover, vehicles in the non-priority stream can only enter the intersection t_f seconds after the departure of the previous vehicle (t_f is the follow-up time). The following is an estimate of the flow q_p based on the assumption that the inter-vehicle

headway follows an Exponential distribution [138].

$$q_n = q_p \frac{\exp(-q_p t_c)}{1 - \exp(-q_p t_f)} \tag{6.26}$$

Similar models are also described in [138]; however, the discussion of these models are beyond the scope of this work. An estimate of q_n can be used directly to determine the value of the MTR by substituting (6.26) in equations (6.2) and (6.3) under free-flow conditions such that the average speed of vehicles crossing the intersection is assumed to be u_f.

Analytical methods are not always capable of providing a practical solution, given the complexity and the assumptions required to be made to analyze unsignalized intersections in a completely realistic manner. Stochastic simulations, however, are able to provide any desired degree of reality, within the capabilities of the available computers.

The remainder of this section describes simulations that are used to derive an empirical estimate of the MTR. The simulations are based on the highway configuration of Figure 6.8. In this configuration, vehicles traveling on the secondary highway (northbound) face a stop sign behind which the vehicles must stop and wait for a safe gap in the interfering traffic before they can proceed North. The traffic stream on the main highway (eastbound) does not face any traffic sign and can proceed without delays. See Section 4.3.5 for more details about the safety gap.

The MTR is determined in every simulated time-step in a 900-cell segment of the road immediately downstream of the intersection since the VANET among vehicles within this road segment is the most affected by the intersection (due to increase in MTR). The effect on the VANET at the other side of the intersection is manifested in a traffic jam.

The flow of the vehicles on the main road and the flow of the interfering vehicles are varied independently such that the priority flow takes the values $q_p = \{100, 200, 300, 400, 600, 720, 900, 1200, 1800\}$ (veh/hr), and the non-priority flow takes the values $q_n = \{300, 400, 600, 900\}$ (veh/hr). To create a flow, vehicles are loaded into the roads at intervals determined by the displaced Exponential distribution (4.7) with a flow rate taken from the above sets.

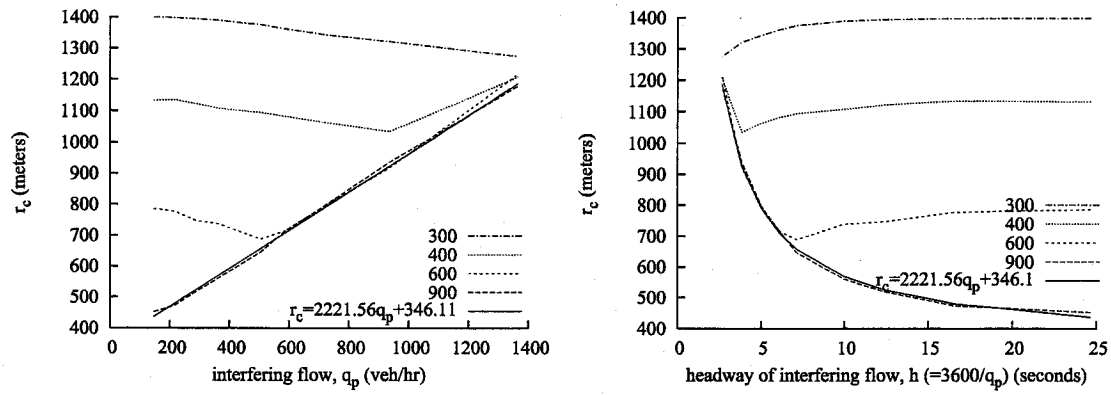

Figure 6.11: The MTR as a function of the interfering traffic flow.

The main simulation results are summarized in Figure 6.11 where the average MTR values in the non-priority traffic are plotted versus the interfering flow. The quantities in the figure represent the measured flows, which were found to be slightly lower than the input values due to the interaction between vehicles. Each curve in Figure 6.11 represents a single value of non-priority flow. The figure shows that the MTR in the network downstream from the intersection remains similar to that of uninterrupted highways when the flow of the interfering traffic is very low ($\leq$ 200 veh/hr). Table 6.2 compares the minimum and average values of MTR obtained from simulations with the lower bound obtained from (6.3) by assuming that the traffic downstream of the intersection is in free-flow state. The table shows that the measured value of the MTR remains close to the calculated value of the MTR using (6.3).

Table 6.2: MTR values (meters) downstream of a stop-sign intersection in low interfering flow.

Flow (veh/hr)	r_c (simulation)	r_{avg} (simulation)	$u_f \ln(L)/q_n$	Ratios
300	480.00	1399.65	529.04	0.91, 2.65
400	435.00	1133.04	396.79	1.10, 2.86
600	300.00	785.67	264.52	1.13, 2.97
900	232.50	451.64	176.35	1.32, 2.56

As the interfering flow increases, its affect on the delay encountered by the vehicles becomes more dominant. As Figure 6.11a shows, increasing the interfering flow does not increase the average MTR for the 300 veh/hr flow; to the contrary, the MTR is slightly reduced as a result of slowing and waiting at the intersection. This phenomenon also occurs in higher traffic flows up to a point where the delay at the intersection, because of the interfering traffic, becomes much higher than the average headway between vehicles in the non-priority flow.

From Figure 6.11a and the comparison with equation (6.3) in Table 6.2, the empirical lower bound of the MTR at a stop-sign intersection is given by,

$$r_c \geq \max\left(\frac{u_f}{q_n}\ln(L),\ 700.56q_p + 214.97\right)\ , \tag{6.27}$$

while the average MTR is,

$$r_{avg} \approx \max\left(2.5\frac{u_f}{q_n}\ln(L),\ 2221.56q_p + 346.11\right)\ . \tag{6.28}$$

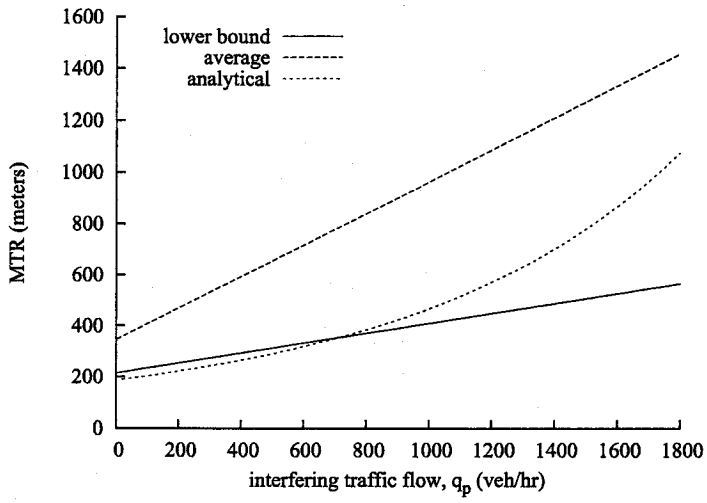

Figure 6.12: Analytical and empirical estimates of the lower bound and mean MTR across an unsignalized intersection.

The estimates of the lower bound and the average MTR obtained from the simulations (equations (6.27) and (6.28), respectively) are compared with those obtained from equation (6.26) under similar conditions (using $t_f = 5$ and $t_c = 5.5$ seconds).

Figure 6.12 indicates that the average MTR obtained from simulations is 200-500 metres higher than the analytical estimate of equation (6.26). The analytical estimate, however, may represent the lower bound MTR closely for low values of flow up to 1000 veh/hr.

6.6 Summary and conclusions

This chapter discusses two examples of traffic constraints that cause disturbance in traffic flow which results in an increase of the MTR. When compared to the discussion in the previous chapter, the departure from the homogenous distribution of vehicles along the road does not result from the increase in density and fluctuations in speed, but from a bottleneck that exists in the road. In the latter case, vehicle traffic is split into two regions of distinct traffic densities. In the case of the intersection, the two regions are clearly marked by the intersection boundaries.

The estimates of the MTR values are provided for VANETs downstream from an isolated intersection based on the characteristics of the incoming traffic and the type of intersection. In the signalized intersection, the lower bound of MTR is directly related to the duration of the red phase and the average speed of vehicles passing the intersection during the green phase. In Section 6.4, a pdf for the MTR is derived based on the NaSch-S2S model. The pdf can be generalized by determining the pdf of the drivers' PRT.

A stop-sign intersection is used as an example of an unsignalized intersection. The lower bound and the mean MTR values are estimated using simulations and found to be related to the interacting flows. It is also found that intersections do not have a significant effect on incoming traffic of low density (or flow) since the delay caused by the intersection is small relative to the mean headway among vehicles.

The results of this chapter are applicable to isolated intersections connecting single-lane, one-way highways. The MTR estimates are applicable to a VANET that spans both sides of the intersection and may continue to be valid for a long distance downstream of the intersection if traffic conditions remain unchanged. Alternative highway configurations may result in different MTR estimates. For instance,

a VANET over two-way road may require a lower MTR than the estimates provided above due to the presence of nearby vehicles on the other side of the unsignalized intersection. In addition, vehicles form the priority traffic that turn to the direction of the non-priority traffic at the intersection will contribute to increasing the vehicle density in that direction; thus, lowering the transmission range. On the other hand, vehicles that attempt to cross a two-way highway must wait for a safe gap in each direction, which means, intuitively, longer delays and higher MTR. Similar observation applies also to multi-lane highways.

These examples emphasize the challenge in estimating the MTR in complex systems such as the ones presented in this chapter. Similar systems are also encountered in traffic situations that include accidents, road constructions, or changing the number of lanes. These situations also affect the traffic by creating traffic jams and changing the vehicle density.

Chapter 7

Estimation of Local Vehicle Density

In this chapter, a relationship is derived to allow a vehicle to estimate the local traffic density. As a result, the vehicle will be able to estimate the density of the surrounding traffic and distinguish between free-flow and congested traffic conditions based on its own travel pattern and without any exchange of information with other vehicles or a fixed infrastructure.

7.1 Introduction

Node density has a great impact on the performance of ad hoc networks by influencing factors such as capacity, routing efficiency, delay, and robustness. Waves of traffic jams, whether caused by constraints in the transportation network, traffic controls, or driving fluctuations, cause the network's density to vary from one location to another; thus disturbing the homogenous distribution of nodes. Moreover, the abrupt and frequent change in density creates a highly dynamic topology. This topology change would cause severe degradation to the network's performance (increased collisions and interference, excessive broadcasts, too many routing paths, etc.) if protocols in VANETs were not designed to handle such conditions.

The main contribution of this chapter is the formulation of a local density estimate based on the relationships provided by the car-following model (Section 3.4.2), the two-fluid model (Section 3.4.3), and the NaSch-S2S model (Section 4.2). This contribution represents a novel approach to density estimation that depends only on the vehicles mobility pattern. Compared to elaborate systems such as [145], the density estimate derived here does not require any exchange of information among vehicles or with a central infrastructure.

Moreover, this chapter shows that a vehicle can distinguish between free-flow and congested traffic condition by monitoring its own fraction of stopped time. This time serves as an order parameter to detect the local traffic condition. This is a direct application of the two-fluid model that can be significant in identifying the density region where the local density estimate is valid.

The chapter is organized as follows. The derivation of the local density estimate is provided in Section 7.2. In Section 7.3 a unified framework of the car-following, two-fluid, and NaSch-S2S models is presented. This framework introduces a link between the models and provides an analytical estimate of the sensitivity factor in the car-following model that was estimated experimentally in Section 4.4.3. Section 7.4 provides simulation results that show the possibility of detecting the local traffic condition by individual vehicles. Section 7.5 describes the highway configurations used to evaluate the local density estimates. Some of the configurations described in this chapter are also used in Chapter 8. The results of the simulations are presented in Section 7.6. The chapter is concluded in Section 7.7.

7.2 Estimation of local density

This section provides the derivation of the vehicle's local estimate using the assumption and results from the car-following model, the two-fluid model and the NaSch-S2S model described in Section 3.4 and Section 4.2, respectively.

Car-following models (see Section 3.4.2) suggest a number of relationships between the average speed and density of vehicles such as the Pipes' equation. From such

relationships, the average vehicle speed can be expressed as a function of density,

$$u = u(k) \; . \tag{7.1}$$

In addition, the two-fluid theory (see Section 3.4.3) relates the fraction of vehicles stopped in traffic, f_s, to the average speed of all vehicles (including the stopped vehicles) in (3.14) [21, 70].

$$u = u_{max} \left(1 - f_s\right)^{\eta+1} \; . \tag{7.2}$$

Recall, that η is a parameter that indicates the quality of service in the transportation network. The value of f_s can be measured by an external observer counting the number of vehicles in the traffic.

Moreover, the two-fluid theory relates the stopping time, T_s, of a test vehicle circulating in a network during a trip of time, T_t, to the average fraction of stopped vehicles by equation (3.15) [21, 70],

$$f_s = \frac{T_s}{T_t} \tag{7.3}$$

Equation (7.3) represents an ergodic principle embedded in the model, i.e., the network conditions can be represented by a single vehicle appropriately sampling the network. Because of this property, a vehicle is able to estimate the density of the surrounding traffic.

To proceed with the derivation of the density estimate, assume that the speed-density relationship is given by Pipes' equation (3.10),

$$u = \lambda \left(\frac{1}{k} - \frac{1}{k_{jam}}\right) \; . \tag{7.4}$$

This is a reasonable assumption given that the equation is derived from a constant headway car-following model (in which drivers try to maintain a minimum safety headway), and it closely matches the speed-density relationship of the NaSch and NaSch-S2S models, as shown in the experiments of Section 4.4.1, Section 4.4.2, and Section 4.4.3.

From (7.4), the normalized vehicle density, k', is given by

$$k' = \left(\frac{u'}{\lambda'} + 1\right)^{-1} \; , \tag{7.5}$$

where, $k' = k/k_{jam}$, $u' = u/u_{max}$, and $\lambda' = \lambda/(u_{max}k_{jam})$, respectively.

From (7.2) and (7.3), the normalized average vehicles' speed is:

$$u' = \left(1 - \frac{T_s}{T_t}\right)^{\eta+1} . \tag{7.6}$$

Equation (7.6) can be substituted in (7.5) to provide the means for a vehicle to estimate the density of the surrounding traffic by monitoring its own stopping time. The resultant local density estimate is denoted K. Therefore,

$$K = \left[\frac{(1 - T_s/T_t)^{\eta+1}}{\lambda'} + 1\right]^{-1} . \tag{7.7}$$

The difference between the density obtained from (7.7) and the one obtained directly from (7.5) is that the latter provides the global traffic density in a highway segment. Measuring this density requires information about the average speed of vehicles located within the segment, which cannot be obtained without the assistance of an external observer or an elaborate information exchange among the vehicles, such as in [145]. The local density estimate, K, on the other hand, depends only on the traffic pattern of the vehicle performing the estimation, given by T_s, and reflects the local traffic conditions surrounding the vehicle.

Before estimating vehicle density using (7.7), the values of η, λ, and T_t must be determined. Both η and λ reflect the traffic service level of the road and can be determined statistically or by simulations as in Section 4.4.3 and Section 4.4.4. Both values were also determined analytically for the NaSch-S2S model in Section 7.3.

The trip time, T_t, can be a fixed period of time within which the stopping time of a vehicle is measured. The choice of this period, which is equivalent to the window size of a moving average filter, depends highly on the rate of change in traffic conditions. A small value of T_t results in a noisy estimate, while a large T_t increases the estimate lag beyond usefulness. Trial simulations show that a choice of $T_t = 10s$ results in a high correlation between the actual density and its estimate.

Equation (7.7) inherits the limitations of the car-following model, which means that it cannot provide an estimate of density in free-flow traffic where there is no interactions between vehicles. Therefore, a vehicle should be able to identify when the estimate is valid.

In free-flow traffic, all vehicles are moving; thus, $f_s = 0$. Once a traffic jam occurs, vehicles stop when they join the traffic jam at its end while other vehicles at the front accelerate away from the traffic jam. From an observer's perspective, there is always a fraction of vehicles that are stopped completely, $fs > 0$.

From a single vehicle perspective, only the presence of a local order (a local traffic jam) is detectable if T_s/T_t is used [113]. This provides useful information since a vehicle in a VANET is most affected by its local conditions (e.g. contention during access of a shared communication channel). Therefore, a vehicle may use the value of T_s/T_t directly to detect whether it is traveling in free-flow or congested traffic.

Note that the use of the ratio T_s/T_t to estimate density offers a couple of practical advantages over the use of the vehicle's speed directly in (7.5) (assuming that speed is ergodic): 1) the stopped time is easily measured and it is independent of the vehicle's speed; and 2) the speed capabilities are different among vehicles, which results in different density estimates within the same traffic condition.

7.3 Unified framework for traffic models

The two-fluid theory proposes a relationship between the fraction of stopped vehicles, f_s, and the average speed in a transportation network, u, in (3.14),

$$u = u_{max} \left(1 - f_s\right)^{\eta+1} . \tag{7.8}$$

In the NaSch-S2S model, the fraction of running vehicles is given by equation (5.13), which can be written in the form of a linear equation.

$$\frac{N_F}{N} = \frac{k_{jam}}{k_{jam}k_F^{-1} - 1} \cdot \frac{1}{k} - \frac{1}{k_{jam}k_F^{-1} - 1} . \tag{7.9}$$

Given that $1 - f_s = N_F/N$, equation (7.9) can be substituted into (7.8). The simulations in Section 4.4.4 show that there is a linear relationship between $(1 - f_s)$ and u in the NaSch-S2S model that justifies assuming $\eta = 0$ (the quality of service indicator) in (7.8). Therefore,

$$u = \frac{u_{max}k_{jam}}{k_{jam}k_F^{-1} - 1} \cdot \frac{1}{k} - \frac{u_{max}}{k_{jam}k_F^{-1} - 1} . \tag{7.10}$$

Also, from the car-following model of (3.10), the average speed is,

$$u = \frac{\lambda}{k} - \frac{\lambda}{k_{jam}} . \tag{7.11}$$

By comparing equation (7.10) with (7.11), the value of λ is,

$$\lambda = \frac{u_{max}}{k_F^{-1} - k_{jam}^{-1}} . \tag{7.12}$$

Note that the value of u_{max} represents the average maximum speed of vehicles in free-flow traffic, as discussed in Section 3.4. In the NaSch/NaSch-S2S model, the average maximum speed is denoted, u_f. Therefore, using (4.2),

$$u_{max} = u_f = (U_{max} - p_{\text{noise}}) \times 27 \quad \text{(km/hr)} . \tag{7.13}$$

By substituting (5.8) into (7.12),

$$\lambda = \frac{(U_{max} - p_{\text{noise}})(1 - p_{\text{s2s}})}{(U_{max} - p_{\text{noise}}) - (1 - p_{\text{s2s}})} . \tag{7.14}$$

At $U_{max} = 5$ cell/s, the value of $\lambda = 0.5557$ (second^{-1}) is close to the value obtained using simulations in Section 4.4.3, where $\lambda' = \lambda/(U_{max} k_{jam}) = 0.1111$.

It can be concluded from the above that using the ratio of stopped vehicles, ($f_s = 1 - N_F/N$), as provided by the NaSch-S2S model in equation (7.9), provides two ways to estimate the average speed of vehicles. The first is directly from the two-fluid model using equation (7.8). The second is from the equation (7.11) if vehicle density is provided.

7.4 Fraction of stopped vehicles as an order parameter

Section 3.5 suggests that the state of the vehicle traffic can be detected by the use of an order parameter. The order parameter has a non-zero value in congested (ordered) traffic state and a value of zero in the free-flow (disordered) state. The fraction of stopped vehicles, f_s can be used as an order parameter since it exhibits similar characteristics [140, 100].

In free-flow traffic, all vehicles are moving ($f_s = 0$). Once a traffic jam is created, vehicles stop when they join the traffic jam at its end while other vehicles at the front accelerate away from the traffic jam. From an external observer's perspective, there is always a fraction of vehicles which are completely stopped ($f_s > 0$).

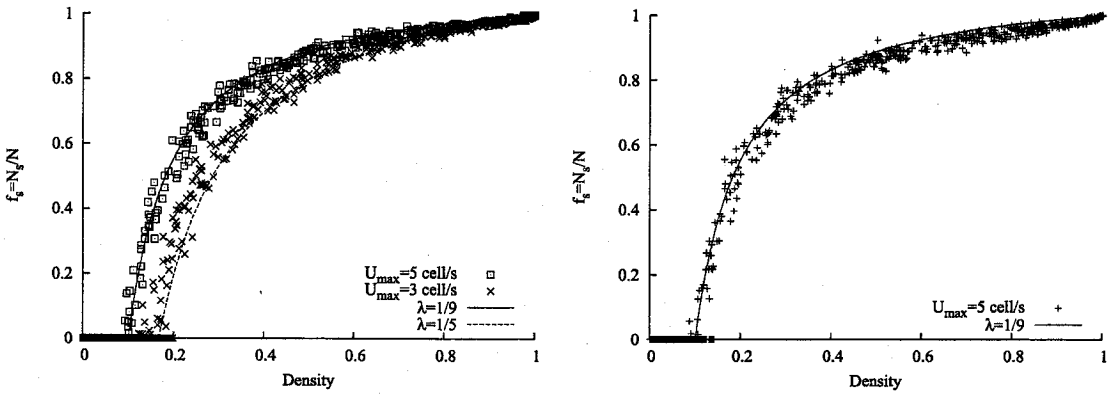

Figure 7.1: The order parameter ($f_s = N_s/N$) in a) 1-lane road, and b) 3-lane road.

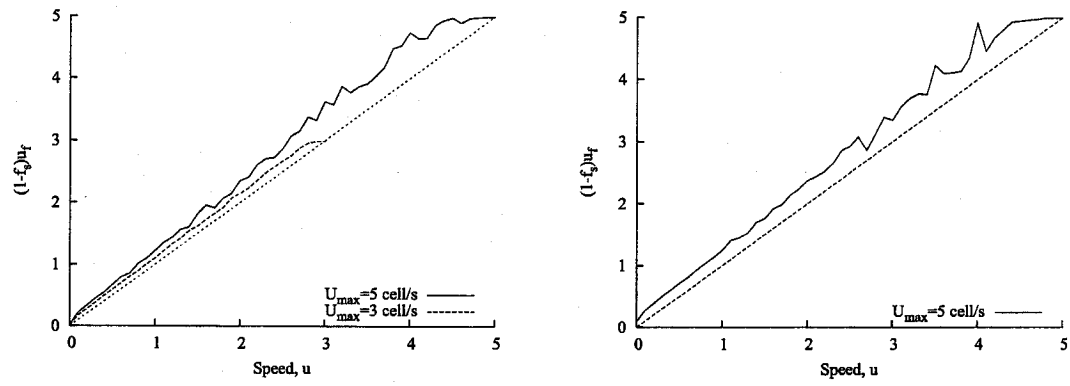

Figure 7.2: The average speed of vehicles is compared to the $(1 - f_s)$ as measured in a small section of the road in a) 1-lane road, and b) 3-lane road.

Using the road configuration of Section 5.6, the number of vehicles, N, and the number of stopped vehicles, N_s, are counted in one road section of length $l = 5$ cells every time step. Then block measurements of 120 time steps are used to obtain a single value of the fraction $f_s = N_s/N$. The values of f_s, is plotted versus the

density value k_l, which is obtained in the same location. Figure 7.1 summarizes the results for three road scenarios: a) 1-lane road where vehicles have a maximum speed of $U_{max} = 5$ cell/s; b) $U_{max} = 3$ cell/s; and c) 3-lane road where vehicles have a maximum speed of $U_{max} = 5$ cell/s.

Data points in all cases are compared with the function,

$$f_s = 1 - \lambda \left(\frac{1}{k} - 1 \right) , \tag{7.15}$$

which is obtained from the speed-density relationship (3.10) by replacing u with $1 - f_s$. Table 7.1 lists the values of λ used in each scenario. These values are calculated using equation (7.14). Note that the value of $1/\lambda$ is linked to the safety time headway between vehicles that results in a flow, $q(k_1)$ 2000 veh/hr/lane.

Table 7.1: Calculated values of λ, k_1 and k_c.

Road configurations	1-lane, $U_{max} = 5$	1-lane, $U_{max} = 3$	3-lane, $U_{max} = 5$
λ	0.5557	0.6004	0.5557
k_1	0.0911	0.1433	0.0911
k_c	0.1667	0.2500	0.1667

The data points in Figure 7.1 are shown without averaging to clearly illustrate the presence of the coexistence traffic state. In this figure, the value of f_s rises above zero starting from density k_1 (see Section 7.4); however, in some instances the free-flow traffic ($f_s = 0$) may exist in densities up to $k_c > k1$ beyond which the high density does not allow free-flow traffic.

The observations in Figure 7.1, Figure 7.2, and Table 7.1 support the discussion of Section 7.2. The value of $f_s = T_s/T_t$ can be used to distinguish between free-flow and congested traffic conditions.

7.5 Simulated highway configurations

The analytical relationship that was derived in Section 7.2 is verified through simulations of vehicle traffic. This section describes six highway configurations that are used in Section 7.6 to simulate vehicle traffic and evaluate a vehicle's ability to estimate

its local density. The same configurations are used also in Chapter 8 to evaluate the DTRA algorithm.

Configuration (A): In two configurations (represented by Figure 7.3(a)), traffic density is increased gradually in a closed-loop highway so that traffic conditions can change gradually from free-flow to congested traffic. In configuration (A), vehicles travel in a single-lane highway where overtaking is not allowed. The highway is in the form of a racetrack of 1000-cell (7.5 km) length as shown in Figure 7.3(a) Vehicles enter from a parking facility at a rate (flow) of $\frac{1}{60}$ veh/s (60 veh/hr) and continue to travel around the track indefinitely, which causes vehicle density to increase until the jam density is reached and no more vehicles can enter. All vehicles have the same maximum speed of 5 cell/s (135 km/hr).

Configuration (B): The racetrack in configuration (B) allows the vehicles to travel on three lanes and pass each other. Vehicles in this configuration are divided into three classes. Slow vehicles compose 15% of all vehicles and their maximum speed is set to 3 cell/s (81km/hr). Another 15% of vehicles can travel at maximum speed of 5 cell/s (135km/hr). The remaining vehicles have a maximum speed of 4 cell/s (108km/hr). This distribution reflects the 85^{th} percentile rule that is used as a guide to set the speed limit on highways so that 85% of vehicles will travel below the limit. Note that the maximum speeds are meaningful only as free-flow speeds. In higher densities, vehicles travel at lower speed, which is unrelated to their maximum speed. The flow rate of vehicles is set to $\frac{1}{12}$ veh/s (300veh/hr).

Configuration (C): In the other four configurations (represented by Figure 7.3(b)), free-flow traffic is interrupted by an intersection, which causes a rapid change in vehicle density across the intersection. Configuration (C) consists of a single-lane highway of 1000 cells with a signalized intersection in the middle. Vehicles enter from a parking facility at one end of the highway, at flow of 0.5 veh/s (1800 veh/hr), and exit from the other end. The traffic signal has a cycle of one minute divided equally between red and green phases. In this open-loop highway, a traffic jam occurs behind the red light. The combination of traffic

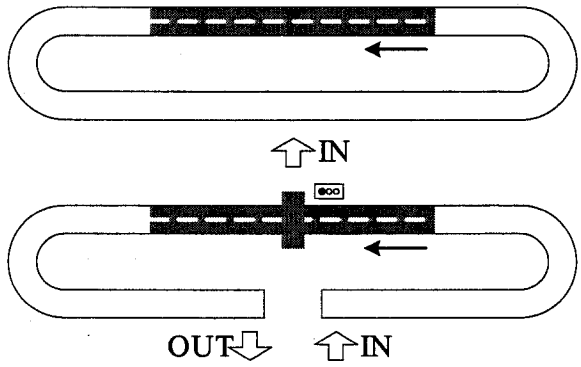

Figure 7.3: Highway configurations used to evaluate the local density estimate and DTRA algorithm: a) Racetrack configurations (A and B); b) Intersection configurations (C, D, E, and F). The data collection is limited to the shaded area.

inflow and the red time ensures that the traffic jam is created periodically throughout the simulation.

Configuration (D): This configuration is virtually identical to the previous configuration except that the flow is $\frac{1}{6}$ veh/s (600 veh/hr), and the signal time is 15 seconds for each phase.

Configuration (E): There are two traffic flows in the remaining configurations; non-priority traffic faces a stop-sign at an unsignalized intersection, while the priority traffic can proceed through the intersection uninterrupted. In configuration (E), the priority flow is set to $q_p = \frac{1}{4}$ veh/s (900veh/hr), while the non-priority flow is set to $q_n = \frac{1}{6}$ veh/s (600veh/hr).

Configuration (F): The configuration is similar to the previous configuration except that the non-priority flow is $q_n = \frac{1}{9}$ veh/s (400veh/hr).

In all experiments, data is collected from 20 simulation runs. Depending on the configuration, simulation time ranges from 25,000 to 60,000 seconds.

7.6 Simulation results

Simulation of the highway configurations of Section 7.5, are used to determine whether (7.7) can provide an accurate estimate of the local density. During simulations, vehicles calculate K in every time step. This information is compared with the actual local density from an observer's perspective. Since vehicle density changes over space and time, the measure of the density over the entire highway segment does not necessarily reflect the local traffic conditions experienced by vehicles at a given location. Therefore, to provide accurate measurement of local densities, the entire highway segment of 134 cells (1005 metres) is divided into short sections of 20 cells (150 metres) each. The density in each of these segments is determined independently in every time step.

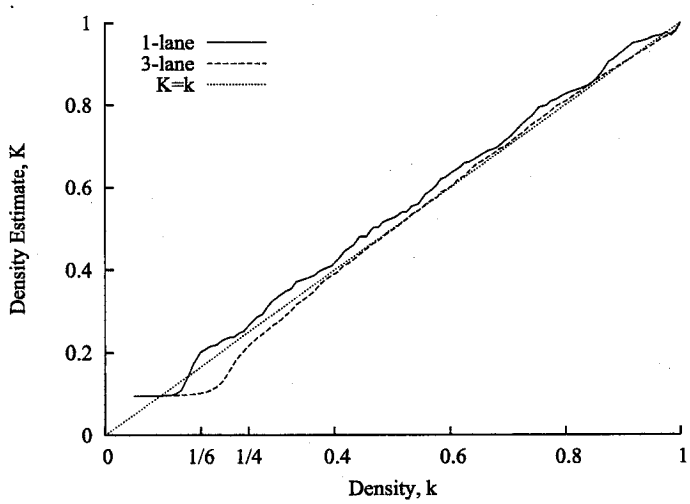

Figure 7.4: Estimation of local vehicle density.

Figure 7.4 shows the relationship between the average estimated local density, K, from vehicles on a highway segment and the actual density, k, in the same segment. Note that the K–k relation approaches a straight line at densities higher than the critical density. From Table 7.1, these densities are $k > k_c = \frac{1}{6}$ for 1-lane configuration and $k > k_c = \frac{1}{4}$ for 3-lane configuration. Within the free-flow range, equation (7.7) yields a constant value of $\lambda'/(\lambda'+1)$ when $T_s = 0$ (the vehicle is in continuous motion) These results indicates that vehicles are capable of accurately estimating their local

density using (7.7).

7.7 Summary and conclusions

The main contribution of this chapter is the formulation of a local density estimate based on the relationships provided by the car-following model, the two-fluid model, and the NaSch-S2S model. This estimate represents a novel approach to predicting vehicle density that depends only on the vehicles mobility pattern.

Simulations show that the fraction of stopped vehicles can be used as an order parameter to distinguish between the two phases of traffic flow. Earlier in the chapter, a link between the NaSch-S2S model and the two-fluid model was established by deriving a relationship between the fraction of stopped vehicles and the vehicle density. This connection is applied in Section 7.2 to estimate the local density.

The ability to estimate the local vehicle density can be useful for many applications in VANET. Many protocols in ad hoc networks are effected by the density of nodes (number of neighbours). For instance, protocols that depend on message broadcast can degrade the network performance due to excessive flooding. Information about local density allow these protocols to adapt their operation to mitigate the negative effects of flooding. Examples may include adjusting the interval between 'Hello' beacons according to the change in density, adjusting the routing update interval for proactive routing protocols, or determining the probability of a packet retransmission during message flooding. The local density information does not require any additional overhead and adapts to vehicles mobility. Chapter 8 applies the density estimate in an algorithm that adjusts the transmission range of a vehicle dynamically.

Chapter 8

Dynamic Transmission Range Assignment Algorithm

This chapter proposes a Dynamic Transmission Range Assignment (DTRA) algorithm. This algorithm employs the local density estimate derived in the previous chapter to set a vehicle's transmission range dynamically. The algorithm does not require any exchange of information with other vehicles or a fixed infrastructure. Therefore, there is no communication overhead involved since the algorithm uses only the vehicle's internal state to determine the transmission range. As a result, the algorithm produces a dynamic transmission range that is highly adaptable to the change in vehicle traffic conditions (density and speed). The algorithm is transparent to the data communications protocols. Therefore, it can be integrated with existing systems with little or no change to the latter.

8.1 Introduction

In the literature of ad hoc networks, power control techniques are considered for throughput enhancement, link quality protection, Topology Control (TC), power conservation and/or a combination of them. The power control at the MAC layer can effectively increase the throughput, by allowing more concurrent transmissions in the

network, if the designed protocol carefully restricts the packet losses on the channel due to the decreased transmission power of the nodes. Moreover, since the transmission power controls the Bit Error Rate (BER) at the receiver, it helps in maintaining the quality and reliability of the wireless link. Transmission Power Control (TPC) is an effective mechanism for obtaining the desired network topology. Therefore, TC at the network layer is considered for various goals like capacity/throughput enhancement, maintaining connectivity, and conserving energy. Finally, energy can be conserved in the network by employing TPC mechanisms.

Controlling the communication range by adjusting the transmission power can be used to mitigate the adverse effects of high density conditions. The choice of the communication range has a direct impact on a fundamental property of an ad hoc network, the connectivity. In a VANET, a static transmission range cannot maintain the network's connectivity due to the non-homogenous distribution of vehicles and rapid change of traffic conditions. It is shown in [62, 114] that a dynamic transmission range is needed to maintain connectivity in non-homogeneous networks to take advantage of power saving and increased capacity.

The DTRA algorithm proposed in Section 8.4 employs information about the local vehicle density estimate and local traffic condition (free-flow vs. congested traffic) to set a vehicle's transmission range dynamically. The proposed algorithm can be classified as a TPC mechanism. In the DTRA algorithm, no information about neighbouring nodes is collected and no central authority is required. A vehicle can determine its transmission range based on its own mobility pattern, which provides hints about the local traffic density. In this regard, the algorithm is related to a class of algorithms that require no message exchange for their operation. However, unlike these protocols that depend on overhearing of data and control traffic [92, 114, 25] to determine the transmitting power level, the DTRA depends on estimation of vehicle density. As a result, the protocol is transparent to data communication protocols and can be used in conjunction with existing protocols.

The remainder of this chapter is organized as follows: Section 8.2 summarizes the work related to non-homogenous range assignment in the literature. The communication model assumed for the VANET discussed in this chapter is described in

Section 8.3. The DTRA algorithm is introduced in Section 8.4. The simulation evaluation of the algorithm is in Section 8.5. Section 8.6 presents the results of applying the DTRA algorithm to the IEEE 802.11 protocol. Section 8.7 discusses some matters related to the practical implementation of the DTRA algorithm. The conclusions of this chapter are in Section 8.8.

8.2 Non-homogenous range assignment

The topology of an ad hoc wireless network is the set of communication links between node pairs used to exchange information packets. Unlike wired networks, the topology of a wireless network may change form due to some uncontrollable factors such as node mobility, weather, interference, or noise. The topology can also be shaped by controlling some parameters such as transmission power and antenna direction [114].

Approaches to TC are concerned with determining the appropriate topology for an ad hoc network. TC mechanisms are used to remove redundant and unnecessary topology information in order to achieve higher network performance. What distinguishes the TC problem in the mobile ad hoc setting from traditional network design is that the topology needs to be determined in a completely distributed environment.

There are two approaches to TC in ad hoc networks: TPC and hierarchical topology organization. Power control mechanisms adjust the power on a per-node basis, so that one-hop neighbour connectivity is balanced and overall network connectivity is ensured. Power control can be employed also as a power saving mechanism in order to extend the lifetime of the power-limited nodes. In the hierarchical TC, a subset of the network nodes is selected to serve as the network backbone over which essential network control functions are supported [29]. A comprehensive survey of TC mechanisms can be found in [126].

There are several approaches to the distributed TC that result in non-homogenous transmission range assignments. In the location-based approaches [114, 90], the nodes are assumed to be able to obtain exact node locations. This information can be exchanged between nodes and used to build an optimum topology in a fully distributed manner. The drawback to this approach is that it requires location information that

can be provided only by an additional hardware (e.g. GPS) and/or message overhead.

In the direction-based approaches a receiver is assumed to be able to determine the direction of the sender when receiving a message. In [141, 89], it is shown that the network connectivity can be guaranteed if there exist at least one neighbour in each cone of a certain angle centred at the node. The neighbour-based approach is based on maintaining the number of neighbours reached by a node within certain thresholds by adjusting the transmission power [92]. This approach is simple but does not guarantee connectivity.

The effect of mobility on these schemes is the message overhead generated to update the nodes transmitting range in response to the change of topology. The amount of this overhead depends on the frequency of topology change. Therefore, it is intuitive that a mobility resilient topology control protocol should be based on a topology that can be computed locally and requires little maintenance in the presence of mobility. Many of the topology control protocols presented in the literature meet this requirement. However, only some of them have been defined to explicitly deal with node mobility [126]. The protocols [92, 114] are explicitly designed to deal with node mobility. They are zero-overhead protocols since the estimation of the number of neighbours is based on the overhearing of data and control traffic.

8.3 Communication model

In the discussion of connectivity, the VANET is modeled by a graph. The graph $G = (V, E)$ consists of a set of nodes $V \subset \mathbb{R}$ in the Euclidean plane and a set of edges $E \subseteq V^2$. Nodes represent vehicles, whereas edges represent communication links between vehicles.

It is assumed in this communication model that all vehicles are equipped with wireless transceivers. Vehicles can adjust their transmission power to any value between zero and the maximum power level. The maximum power level is assumed to be equal for all vehicles. An edge (v_i, v_j) may exist if and only if the Euclidean distance between vehicles v_i and v_j is less than or equal to the shortest transmission

range between them, i.e.,

$$E = \{(v_i, v_j) \in V^2 \mid |x_i - x_j| \leq \min(r_i, r_j)\} , \tag{8.1}$$

where x_i, r_i are the position and transmission range of the node v_i, respectively. Equation (8.1) results in an undirected graph. The choice of distance as the primary factor in connectivity is appropriate since the focus of the thesis is on vehicle distribution and density, which both affect the distance among vehicles.

The propagation model assumed in the network simulations of Section 8.6 is a combination of free space and two-ray reflection models. The simplified Friis free space model applies to unobstructed line-of-sight communication where the antenna gain and the system loss are assumed to have unit values [115]:

$$P_r = P_t \frac{\lambda_w^2}{(4\pi)^2 d^2} , \tag{8.2}$$

where P_r is the received signal power as a function of the nodes separation distance, d, P_t is the transmitted signal power, and λ_w is the wavelength.

The two-ray ground reflection model considers a ground reflected propagation path between communicating nodes.

$$P_r = P_t \frac{h_t^2 h_r^2}{d^4} , \tag{8.3}$$

where h_t and h_r are the heights of the transmitting and receiving antennas, respectively. This model has been found reasonably accurate in predicting the signal power for long distance separation ($d \gg \sqrt{h_t h_r}$) between nodes [115].

In the network simulations of Section 8.6, a cutoff distance, d_c is used to determine which model is used to calculate the transmission power. At $d < d_c$ equation (8.2) is used. At $d \geq d_c$ equation (8.3) is used. The cutoff distance is

$$d_c = \frac{4\pi h_t h_r}{\lambda_w} . \tag{8.4}$$

8.4 Dynamic transmission range assignment

It can be concluded from the results of Chapter 6 that if all vehicles had to use a homogenous transmission range for communication, the range should keep the vehicular network connected in all traffic conditions. This can be achieved only if the

transmission range is wide enough to accommodate conditions such as free-flow traffic and traffic across intersections.

Alternatively, estimation of traffic density provides the necessary means to develop a power control algorithm to set a vehicle's transmission range dynamically as traffic conditions change. In its basic form, the algorithm maps the time-varying values of T_s/T_t into a transmission range, r, at regular time intervals,

$$r = D(T_s/T_t) \; . \tag{8.5}$$

Algorithm 1 Calculate the dynamic transmission range.

Require: α, λ' {constants}

Require: MR {the maximum transmission range allowed}

Require: T_s/T_t {fraction of stopping time}

1: $f_s \leftarrow T_s/T_t$

2: **if** $f_s = 0$ **then**

3: $\quad$ TR $\leftarrow$ MR

4: **else**

5: $\quad K \leftarrow 1/\left[(1-f_s)/\lambda' + 1\right]$

6: $\quad \text{TR} \leftarrow \min\left[\text{MR} \times (1-K),\ \sqrt{\text{MR} \times \log(\text{MR})/K} + \alpha \times \text{MR}\right]$

7: **end if**

8: **return** TR {the dynamic transmission range}

Algorithm 1 provides one implementation of the mapping function (8.5). The transmission range is set to its maximum level in free-flow traffic. In dense traffic, r is determined by the minimum of equations (5.24) and (5.25). In general, $D(\cdot)$ may depend on other factors such as the desired level of path redundancy or the percentage of equipped vehicles. The choice of the maximum transmission range in free-flow is due to two reasons: 1) estimation of density within the free flow traffic range is difficult, but it is easy to detect the free-flow phase; 2) it is expected that the distance between vehicles in free-flow is long; therefore a longer than optimal transmission range does not have the same adverse affects as in a dense network and it can extend the lifetime of communication links as the network topology changes.

Note that a practical algorithm would determine a power level instead of a transmission range. The power level may take any value in a set of possible power levels available to the wireless interface. Here, the algorithm sets the transmission range directly for an easy comparison with the network's length and the distance between vehicles.

8.5 Performance evaluation

The DTRA algorithm described in Algorithm 1 is evaluated using simulations of the six highway configurations described in Section 7.5. During the simulations, each vehicle estimates the local density and applies the algorithm to determine its own transmission range. The following metrics are used in the evaluation:

1. Number of network partitions: this is used to measure the network connectivity; a connected network consists of one partition.

2. Average transmission range: a smaller value of the transmission range implies less power level and better network spatial reuse.

To count the number of partitions in the network: 1) A MST is constructed within the measurement section(s) (see below) of the highway in the same way that was used to determine the MTR in previous chapters. The edges of the MST represent the minimum distance between any two vehicles in the network. 2) Each edge in the MST is checked to determine if it satisfies equation (8.1). Otherwise, the network is partitioned at that point and the number of partitions is increased by one. Note that the procedure results in a network in which all communication links are bidirectional.

In the racetrack configurations (A) and (B) (of Section 7.5), data collection is restricted to a segment of length $L \approx$ 1km located at the furthest distance from of the entry point so that measurements are not effected by vehicle interactions at that point. In the intersection configurations (C) through (F), data is collected in two 1 km segments immediately upstream and downstream from the intersection. The segment is chosen to be of length comparable to the maximum transmission range of recent proposed standards such as DSRC [27, 151].

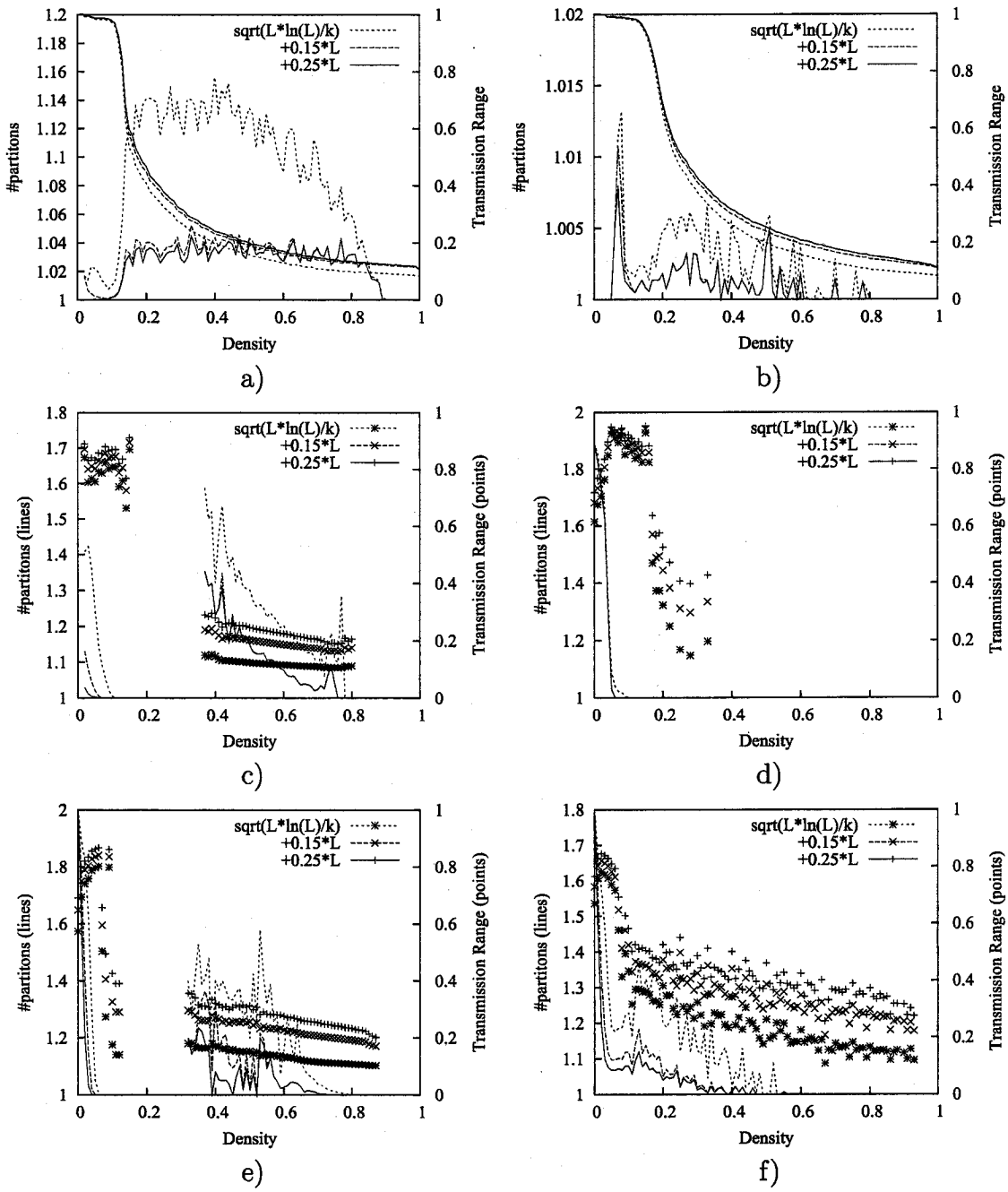

Figure 8.1: Vehicle density vs. the average transmission range and the resultant number of partitions in a) 1-lane racetrack, b) 3-lane racetrack, c) signalized intersection (q = 1800, red–time = 30 seconds), d) signalized intersection (q = 600 veh/hr, red–time = 15 seconds), e) unsignalized intersection with q_n = 600 veh/hr, and f) unsignalized intersection with q_n = 400 veh/hr.

Figure 8.1 shows the average number of partitions and the average transmission range along the density range in different highway configurations. The different line types correspond to different choices for the parameter α in equation (5.25), which sets the transmission range in the dense traffic. Figure 8.1(a,b) show that the average number of partitions remains very close to one in racetrack scenarios (A) and (B). The transmission range drops quickly near the critical density while maintaining (or improving) the level of connectivity in racetrack configurations.

The figures also show the effect of changing the upper bound of the transmission range by shifting it up by a factor of αL. While there is little difference between the choice of $0.25L$ and $0.15L$, the number of partitions increases noticeably at $0L$. The latter sets the upper bound below the mean MTR of the single-lane highway and at roughly the mean MTR in the multi-lane highway (see Figure 5.7 and Figure 5.8 in Section 5.6.2). This indicates that the vehicles are able to set their transmission range very close to the optimal value in dense traffic.

The intersection scenarios are challenging for the dynamic transmission range algorithm since the network's condition changes rapidly at both sides of the intersection, which requires fast switching of the transmission range from low (while vehicles are slowing or stopped) to high (after passing the intersection).

Figure 8.1(c,e,f) show higher number of partitions across the density range, which can be attributed to the slower reaction to the change in the traffic condition. Figure 8.1(c,e), which correspond to a signalized intersection, and a stop-sign intersection of high flow (configurations (C) and (E)), respectively, show similar results in the high density region. In both cases, the mean headway (inter-arrival time) between vehicles is smaller that the delay encountered at the intersection, which results in a traffic jam upstream of the intersection. The average transmission range in the high density region [0.4, 0.8] is slightly higher than the corresponding region in the racetrack scenarios, especially at the lower end. The reason for this difference is the influence of incoming vehicles that approach the intersection with a maximum transmission range (due to free-flow traffic upstream of the intersection) then decelerate rapidly to join the queue behind the intersection.

On the other hand, Figure 8.1(f), represents the scenario (F) where the vehicles approaching the intersection have a mean headway higher than the delay encountered at the intersection (while waiting for the next safe gap). As a result, there are no distinct regions of low and high densities in the figure. Since the stop at the intersection is too short for vehicles to adapt, the transmission range needed for the high density region (upstream of the intersection) remains higher than optimal.

Despite the relatively slower reaction to the change in traffic condition, which is expected due to the use of the time window, T_t, the DTRA algorithm is quite successful in maintaining the connectivity by keeping the average number of partitions low. Table 8.1 offers a detailed description of the network connectivity in each of the above configurations by listing the fraction of time in which the network is connected (one partition) or divided into two, three, or four partitions.

Table 8.1: Percentage of partitions during simulation time.

Road Configuration	α	partitions downstream				partitions upstream			
		1	2	3	4	1	2	3	4
(A) Racetrack	0.00	95.93	3.98	0.08	0.00				
(1 lane)	0.15	98.75	1.25	0.00	0.00				
	0.25	98.87	1.13	0.00	0.00				
(B) Racetrack	0.00	99.74	0.25	0.00	0.00				
(3 lanes)	0.15	99.89	0.11	0.00	0.00				
	0.25	99.90	0.10	0.00	0.00				
(C) Signalized	0.00	95.69	4.30	0.01	0.00	79.91	18.56	1.49	0.05
Intersection	0.15	99.77	0.23	0.00	0.00	90.94	8.80	0.26	0.01
	0.25	99.97	0.03	0.00	0.00	90.94	8.79	0.26	0.01
(E) Stop sign	0.00	39.01	55.89	5.10	0.00	98.24	1.75	0.01	0.00
Intersection	0.15	68.86	31.14	0.00	0.00	99.76	0.24	0.00	0.00
(q_n=600 veh/hr)	0.25	82.19	17.81	0.00	0.00	99.77	0.23	0.00	0.00
(F) Stop sign	0.00	41.86	54.35	3.79	0.00	63.66	36.34	0.00	0.00
Intersection	0.15	66.74	33.26	0.00	0.00	77.11	22.89	0.00	0.00
(q_n=400 veh/hr)	0.25	78.96	21.04	0.00	0.00	82.96	17.04	0.00	0.00

The main conclusions that can be drawn from Table 8.1 are:

- In the racetrack scenario, the upper bound of transmission range given by equation (5.25) ($\alpha = 0$) is sufficient to maintain the network connectivity 95.93% of the time, or higher.

- In the signalized intersection, the increase in the upper bound of transmission range has a significant impact on the connectivity since it increases the time

the network is connected by more than 11% upstream of the intersection (the congested side) and about 4% downstream (the free-flow side). It is also noted that the signalized intersection is the only highway configuration where the number of partitions may increase to four. This occurs in the congested area upstream of the intersection. This area is the most dynamic where some vehicles are discharging from the queue in the green-phase while others are joining the queue of stopped vehicles.

- In the stop-sign intersection of high flow rate (configuration (E)), the congested area upstream of the intersection remains connected most of the time. In the free-flow region downstream, the partitioning of the network is not due to the level of transmission range but due the slow reaction to the change in traffic conditions.

8.6 Modification of IEEE 802.11 using the DTRA algorithm

This section illustrates the benefits of using the DTRA algorithm directly to adjust vehicle transmission range in VANETs. The widely used IEEE 802.11 protocol works under the assumption that all nodes use a common transmission power. In the evaluation experiments described here, this restriction is relaxed by allowing each node to determine its own transmission range using the DTRA algorithm and adjust its transmission power accordingly. No optimization is made on the IEEE 802.11 protocol to enhance its performance under this modification. The performance of the modified protocol is compared with the original IEEE 802.11 protocol using ns-2 simulations [18]. The implementations of the physical layer and the mobile nodes in the Network Simulator v2.29 were modified to accommodate variable transmission powers.

As was described in Section 4.3.1, the simulator *RoadSim* is capable of generating movement scripts and connection scenarios that can be executed by ns-2. Network simulations are performed in two stages, in the first stage, *RoadSim* is used to simulate vehicle traffic in highway configurations (A), (C), and (E) of Section 7.5 and

generate the command scripts for the ns-2 simulations. In the second stage, ns-2 executes these command scripts and performs the simulation of communication protocols. Three script files are generated for each of the highway configurations. The movement script describes the movement of each vehicle during simulation time. The power assignment script updates the transmission power for each vehicle as determined by Algorithm 1 ($\alpha = 0.25$) during traffic simulations. The transmission power is determined using equations (8.2) and (8.3). The connections script generates data communication scenarios among the vehicles. In these scenarios, 10% of all vehicles within the simulated highway segment initiate a communication session with another vehicle within the same segment. The communication flows are composed of Constant-Bit-Rate (CBR) traffic over User Datagram Protocol (UDP) protocol. The data packets are routed using the AODV protocol. Examples of the three scripts are provided in Appendix C.

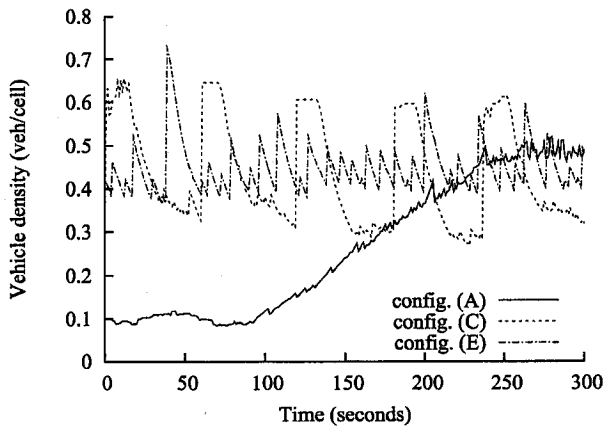

Figure 8.2: Change in vehicle density during network simulations of modified IEEE 802.11.

Highway configurations (A), (C), and (E) are selected because they represent traffic conditions that change abruptly within a few seconds, which allow the DTRA algorithm to be tested in highly dynamic topologies. Due to the high processing and memory requirements of ns-2 simulations, it is not possible to simulate VANETs of lifetimes longer than a few hundreds of seconds (in contrast to *RoadSim* that can simulate traffic for hours of simulated time). To accommodate these requirements,

only small sections of *RoadSim*-generated traffic are used for network simulations. In general, all simulations use small highway segment of 200-cell (1.5 km) long and cover a time of 300 seconds. Figure 8.2 shows the change in vehicle density within the highway segment during the simulation time. Note that, in configuration (A), the vehicle density during the selected time period changes from free-flow to congested traffic. In configurations (C) and (E), vehicle density appear to be within the congested region. However, the traffic downstream of the intersection is always in free-flow condition. It is important to point out that vehicles do not remain within the simulation area during the entire simulation time. Moreover, vehicles participate in the communication network only when they are within the simulation area.

In all simulations, the transmission range for the IEEE 802.11 is set to 250 metres. The transmission range for the modified protocol ranges from 110 to 1000 metres. Three performance metrics are used to compare the original IEEE 802.11 with the modified version, which will be called DTRA protocol for the reminder of this section:

1. The throughput: this is the actual received data rate (bit/s) by each vehicle participating in a communication link.

2. Packet delay: the average delay experienced by delivered packets reflects the overhead caused by congestion or waiting time in the buffer during the AODV route request phase.

3. Number of hops: the average length of the path traveled by the packets.

Figures 8.3 and 8.4 show plots of these metrics versus the offered load generated by each vehicle (bit/s). Each data point in these plots represents the average of 10 simulation runs of ns-2. Figure 8.3 summarizes the simulation results for configuration (A). In this case, the DTRA protocol delivers a data rate similar to that of the IEEE 802.11 when the offered load is 100Kbps or less. The DTRA protocol delivers a higher data rate as the offered load increases beyond 100Kbps. The reason for this performance is attributed to higher transmission range during free flow traffic, which results in the reduction of the number of hops as Figure 8.3(c) shows. The average latency for packets is reduced by about 50% as the offered load increases. This indicates the improved capacity of the network during congested traffic.

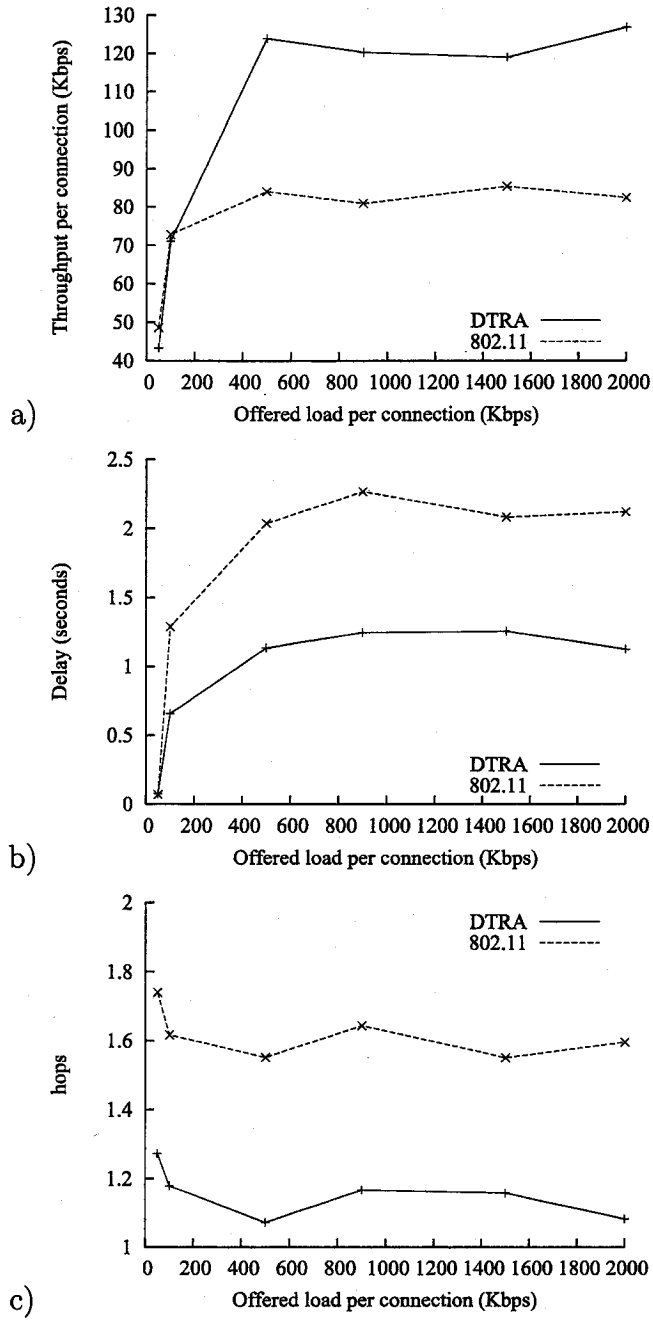

Figure 8.3: Performance comparison between IEEE 802.11 and DTRA protocols in the single-lane racetrack configuration: a) throughput, b) delay, and c) number of hops.

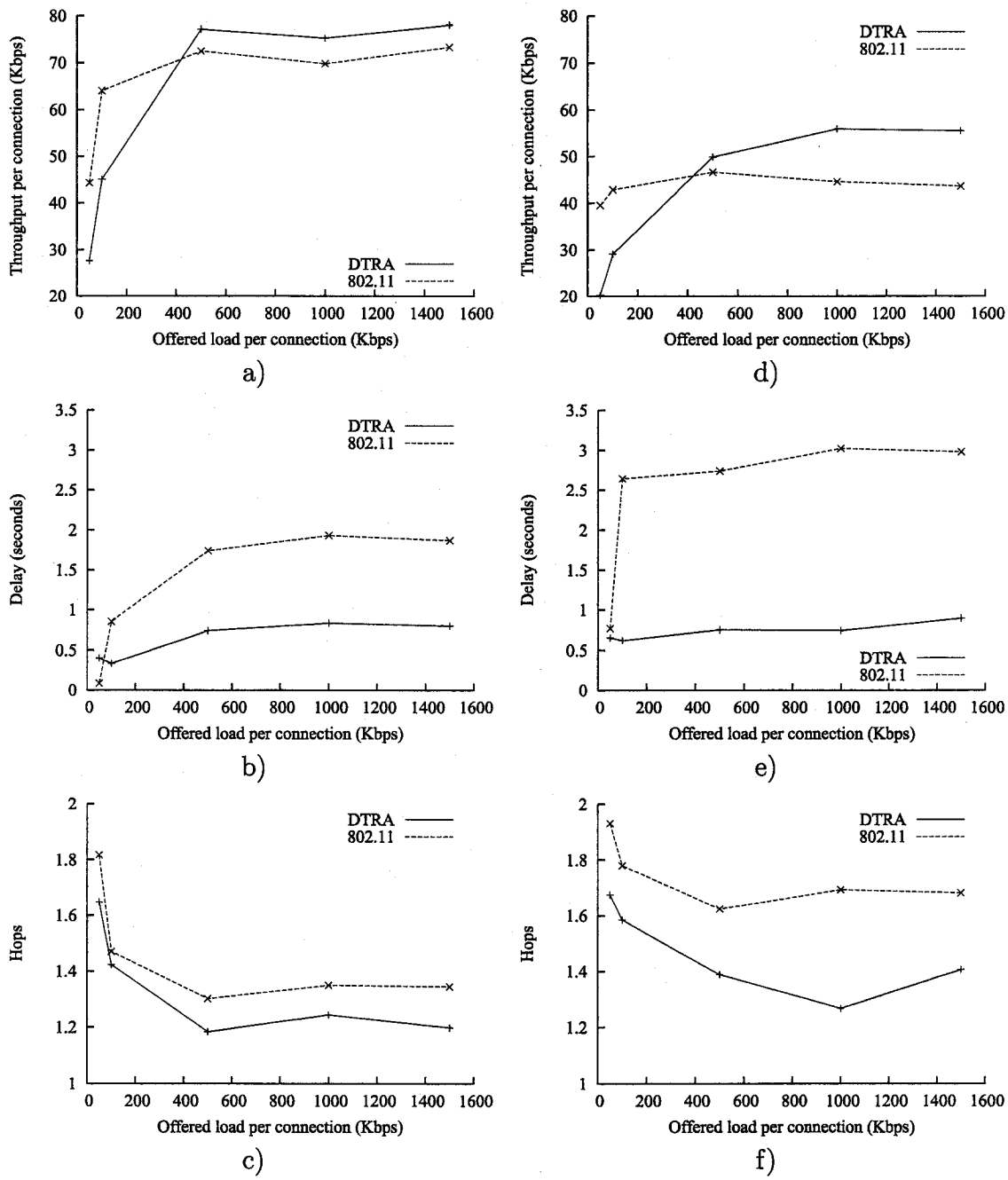

Figure 8.4: Performance comparison between IEEE 802.11 and DTRA protocols in the signalized (left column) and stop-sign (right column) intersection configurations: a,d) throughput, b,e) delay, and c,f) number of hops.

Highway configurations (C) and (E) represent highly dynamic topology in which a vehicle must adjust its transmission from low when it is stopped behind the intersection to maximum when it start to move. Yet, Figure 8.4 shows that the DTRA protocol shows throughput improvement when the offered load is 500Kbps or higher. The improvements include also smaller latencies and shorter routes.

8.7 Practical considerations

It was assumed in Section 8.4 that the DTRA algorithm produces its result in form of a real number that represents a distance. This was intentional in order to compare the results with the MTR under the same conditions. A practical algorithm will likely produce a power level index that corresponds to one of the power levels settings available for the transmitter. This scheme allows the algorithm to be more flexible for several practical considerations. For instance, in the early stages of VANETs implementation and marketing, only a small percentage of vehicles will be equipped with wireless transceivers. This will make the perceived vehicle density on the highway much less than the actual density because only the equipped vehicles will participate in the ad hoc network. As a result, a certain power index, may correspond to a higher power setting when the fraction of equipped vehicles is, say, 10% than what it would be if the fraction of equipped vehicles is 90%. Since the algorithm is based on the actual vehicle density, which is not affected by the marketing of VANET, the algorithm remains valid and need not to be changed as more vehicles become equipped. The same reasoning also applies to geographic, demographic, or regulatory situations that require the power levels in one region to be different than others.

Moreover, the association between the power index and the actual power level can be determined statically or dynamically:

- The range may be determined statically by, say, standards. These standards may choose different power levels for different geographic or regulatory regions.

- The range can be estimated directly from traffic models. In this case, the indexes must be set so that at least one corresponds to the free-flow traffic region while

the rest divides the remaining range equally. Algorithm 1 is a special case of this scheme.

- An additional protocol may be used to determine the power range for each index. The protocol does not need to be used as frequently as some of the proposed protocols in the literature (see Chapter 2) since the power level does not change frequently.

- The power level for each index may be determined dynamically by a central authority that broadcasts control messages to vehicles entering a specific region (e.g. highway or city centre). This suggests developing a protocol that optimizes power consumption for other factors, such as QoS, at the region level then transmits the power level for each index to the vehicles within the region.

8.8 Summary and conclusions

One application of the density estimate is the DTRA algorithm. The algorithm sets a vehicle's transmission range dynamically according to its local density. The result of using this algorithm is a VANET whose nodes have a MTR that is dynamic and non-homogenous. Simulations show that the DTRA algorithm is effective in maintaining a high degree of connectivity in highway configurations where the network topology changes rapidly.

The proposed scheme has several advantages. The algorithm does not require any global information such as vehicle locations, nor does it require any exchange of information among vehicles. Moreover, the algorithm inherently adapts to vehicle mobility. The algorithm is also transparent to communication protocols, which allows it to be used in combination with other TPC protocols to enhance their performance with respect to responsiveness to mobility, or to provide an initial estimate of transmission range before further refinement.

The DTRA algorithm was used to modify the IEEE 802.11 protocol to work in a highly dynamic VANET environment. The evaluation of the modified protocol shows an improved throughput at high offered load, reduced packet latency, and

shorter routes in all simulated scenarios when compared to the original IEEE 802.11 protocol.

Chapter 9

Conclusions and Future Research

This chapter provides a summary of the contributions of this thesis in Section 9.1. Future research directions and remaining challenges are listed in Section 9.2.

9.1 Summary

The main tool for the analysis and simulation of highway traffic in this work is the Nagle and Schreckenberg with Slow-to-Start rule (NaSch-S2S) model that was shown to be important to create a phase transition between free-flow traffic and congested traffic conditions. The NaSch-S2S model is used in this thesis to study congested traffic conditions. These conditions deserve special consideration in the design and analysis of Inter-Vehicle Communication (IVC) and Vehicular Ad Hoc Network (VANET). Some of the answers sought are the effect a traffic jam has on the connectivity of the network. Intersections also affect the normal flow of traffic and disturb vehicle distribution, even when vehicle density is low.

The first contribution of this thesis is a traffic microsimulator, *RoadSim*. *RoadSim* implements the NaSch-S2S model and provides many improvements that include handling of additional components such as multi-lane traffic and intersections, and adding several capabilities toward supporting VANET research such as building network graphs, and generating ns-2 scripts to port vehicle movement traces into

simulations of communication networks.

The thesis emphasizes a link between the phenomenon of traffic jams and the connectivity of VANETs. It is shown that traffic jams affect the homogeneous distribution of vehicles in congested traffic. The consequence to VANETs is manifested in the need for higher transmission range than would be needed if the distribution were homogenous.

The thesis contribution in this regard is a new analytical relationship that provides a lower-bound for the Minimum Transmission Range (MTR) in uninterrupted highways. The derived relationship takes into account the non-homogenous distribution of vehicles at densities beyond a critical density that separates the free-flow and congested traffic. The change of vehicle distribution between homogenous and non-homogeneous is verified through simulations. The simulations show that regardless of the number of lanes or vehicle speed, vehicle distribution changes from homogenous in densities below the critical density to non-homogeneous in higher densities. Vehicle distribution returns gradually to homogenous state as densities approach wide traffic jams.

The thesis also provides estimates of the MTR values for VANETs downstream from an isolated intersection based on the characteristics of the incoming traffic and the type of intersection. When compared to uninterrupted highways, the departure from the homogenous distribution of vehicles is not caused by the increase in density or fluctuations in speed, but from the delay encountered by vehicles at the intersection. In the signalized intersection, a probability density function for the MTR is derived based on the NaSch-S2S model. In this intersection type, the lower bound of MTR is directly related to the duration of the red phase and the average speed of vehicles passing the intersection during the green phase. In a stop-sign intersection, the lower bound and the mean MTR values are estimated using simulations and found to be related to the interacting vehicle flows. It is also found that intersections do not have a significant effect on incoming traffic of very low density (or flow) since the delay encountered at the intersection is small relative to the mean headway between consecutive vehicles.

These MTR estimates are applicable to a VANET that spans both sides of an

intersection and can continue to be valid for a long region downstream of the intersection if traffic conditions remain unchanged. Therefore, to maintain connectivity across the intersection, vehicles must employ a high transmission range or relay stations are to be installed near the intersections.

Another contribution of this thesis is the formulation of a local density estimate based on the relationships provided by the Pipes' car-following model, the two-fluid model, and the NaSch-S2S model. This estimate represents a novel approach to predicting vehicle density that depends only on the vehicle mobility pattern. Simulations show that the fraction of stopped vehicles can be used as an order parameter to distinguish between the two phases of traffic flow.

One application of the vehicle density estimate is the Dynamic Transmission Range Assignment (DTRA) algorithm. The algorithm adjusts a vehicle's transmission range dynamically according to its local density. The result of using this algorithm is a VANET whose nodes have a MTR that is dynamic and non-homogenous. Simulations show that the DTRA algorithm is effective in maintaining a high degree of connectivity in highway configurations where the network topology changes rapidly.

The proposed scheme has several advantages. The algorithm does not require any global information such as vehicle locations, nor does it require any exchange of information among vehicles. Moreover, the algorithm inherently adapts to vehicle mobility. The algorithm is also transparent to communication protocols, which allows it to be used in combination with other Transmission Power Control (TPC) protocols to enhance their performance with respect to responsiveness to mobility, or to provide an initial estimate of transmission range before further refinement.

To illustrate some of its advantages, the DTRA algorithm is used to modify the IEEE 802.11 WLAN protocol to work in a highly dynamic VANET environment. The evaluation of the modified protocol shows an improved throughput at high offered load, reduced packet latency, and shorter routes when compared to the original IEEE 802.11 protocol.

9.2 Future research

The following list contains a summary of several research topics that will be pursued in the near future as a continuation of this thesis:

- The Cellular Automata (CA) models have a promising potential in modelling node movements in general MANETs. Unlike the common mobility models such Random WayPoint (RWP), CA models will be able to generate more complex behaviour at the cost of little overhead in network simulations. The use of CA models can add several capabilities that are not easily achievable using the RWP model, including: 1) Correlating the node mobility with density to obtain more realistic movement patterns. 2) Changing the mobility pattern according to a node's function or location. 3) Simulating interactions between nodes or reaction to communication messages. 4) Simulating networks of different types of mobile nodes, such as in a city environment where people, cars, and transient buses interact.

- The Nagle and Schreckenberg (NaSch) model and its variations update vehicles positions at one-second intervals, which results in realistic data in terms of vehicle speed and flow. It is not known what effect, if any, this update interval has on the results obtained from simulating communication protocols. Motion and speed resolution can be increased by reducing both the cell size and the simulation time step. However, these modifications will result in more complex implementation of the CA grid that must account for vehicles that occupy multiple cells, and a higher computation overhead that results from updating the CA grid more often. The evaluation of these approaches and possible trade-offs will be the subject of further investigation.

- The simulator *RoadSim* can be used to advance the research in VANETs in several directions: 1) A VANET in an urban environment can be simulated using a grid of roads and intersections of various types. 2) Simulation of urban networks is not only useful in VANET research but also in infrastructure-based wireless networks such as cellular networks. 3) The rules of the CA models

can be amended to simulate vehicles reaction to communication messages when these messages affect manoeuvres such as acceleration, changing lanes, or route selection. These extensions can be used to evaluate the performance of VANET applications such as cruise-control, lane-merge, and navigation assistance.

- The ability to estimate the local vehicle density can be useful for many applications in VANETs. Often the performance of an ad hoc network protocol is affected by the density of nodes (number of neighbours). For instance, protocols that rely on periodic message broadcast can degrade the network's performance due to excessive flooding. Information about local density allows these protocols to adapt their operation to mitigate the negative effects of flooding. Examples may include adjusting the interval between 'Hello' beacons according to the change in density, adjusting the routing update interval for proactive routing protocols, or determining the probability of a packet retransmission during message flooding. The local density information does not require any additional overhead. Since mobility is highly correlated with density, this scheme allows the message exchange to be more frequent in a dynamic network, and less frequent in stationery network (i.e. in a traffic jam).

- Moreover, the vehicle density estimation can be used to turn a VANET into a sensor network to monitor traffic conditions. In such a network, each vehicle estimates its local density and transmits this data to one or more central nodes where the data collected from many vehicles is processed to obtain real-time information about the status of the transportation network. This scheme would help the traffic authorities to monitor and control traffic flows and avoid traffic jams.

- A future study will involve a performance comparison between the DTRA algorithm and other TPC algorithms that are based on message-exchange schemes. Several of the latter schemes can guarantee connectivity while achieving the optimum transmission range. However, they have not been evaluated in a highly dynamic VANET environment. Moreover, future work will discuss integrating the DTRA algorithm with other TPC protocols to achieve higher performance.

References

[1] Adachi, M., Morita, Y., Fujimura, K., Takatori, Y., and Hasegawa, T., "On an autonomous cruising traffic flow simulator including inter-vehicle and road-to-vehicle communication networks," in *Proc. The IEEE 5th International Conference on Intelligent Transportation Systems (ITSC'02)*, 2002, pp. 645–650.

[2] Agarwal, P. K., Guibas, L. J., Edelsbrunner, H., Erickson, J., Isard, M., Har-Peled, S., Hershberger, J., Jensen, C., Kavraki, L., Koehl, P., Lin, M., Manocha, D., Metaxas, D., Mirtich, B., Mount, D., Muthukrishnan, S., Pai, D., Sacks, E., Snoeyink, J., Suri, S., and Wolefson, O., "Algorithmic issues in modeling motion," *ACM Computing Surveys*, vol. 34, no. 4, pp. 550–572, 2002.

[3] Anonymous. (2002) COMCAR. [Online]. Available: http://www.comcar.de[2005,Nov.30]

[4] Anonymous. (2003) Chauffeur2. [Online]. Available: http://www.chauffeur2.net[2005,Nov.30]

[5] Anonymous. (2003) DRiVE homepage. [Online]. Available: http://www.ist-drive.org[2005,Nov.30]

[6] Anonymous. (2003) FleetNet. [Online]. Available: http://www.et2.tu-harburg.de/fleetnet[2005,Oct.29]

[7] Anonymous. (2003) OverDRiVE project homepage. [Online]. Available: http://www.ist-overdrive.org[2005,Nov.30]

[8] Anonymous. (2004, Oct.) CarTALK website. [Online]. Available: http://www.cartalk2000.net[2005,Nov.29]

[9] Anonymous. (2004, Mar.) Vehicle safety communications consortium. [Online]. Available: http://www-nrd.nhtsa.dot.gov/pdf/nrd-12/CAMP3/pages/VSCC.htm[2005,Nov.29]

[10] Anonymous. (2005, May 12) ADASE advanced driver assistance systems in europe. [Online]. Available: http://www.adase2.net[2006,Feb.1]

[11] Anonymous. (2005, Feb. 9) Advanced crusie-assist highway system research association. [Online]. Available: http://www.ahsra.or.jp/index_e.html[2005, Nov.30]

[12] Anonymous. (2005) invent-online. [Online]. Available: http://www.invent-online.de[2005,Nov.30]

[13] Anonymous. (2005, Nov.) NOW: Network on wheels. [Online]. Available: http://www.network-on-wheels.de[2005,Nov.30]

[14] Anonymous. (2005, Feb. 9) TRANSIMS. [Online]. Available: http://transims.tsasa.lanl.gov[2005,Nov.29]

[15] Anonymous. (2006, Jan.) California PATH - California partners for advanced transit and highways. [Online]. Available: http://www.path.berkeley.edu[2006, Feb.1]

[16] Anonymous. (2006, Jan.) Car 2 car communication consortium. [Online]. Available: http://www.car-2-car.org[2006,Feb.1]

[17] Anonymous. (2006, Feb. 15) Intelligent vehicle initiative. [Online]. Available: http://www.its.dot.gov/ivi/ivi.htm[2006,Feb.15]

[18] Anonymous. (2006, Feb.) The network simulator - ns-2. [Online]. Available: http://www.isi.edu/nsnam/ns[2006,Feb.1]

[19] Anonymous. (2006, Feb. 22) PReVENT. [Online]. Available: http://www.prevent-ip.org[2006,Feb.25]

[20] Anonymous. (2006, Feb. 15) Vehicle infrastructure integration (VII). [Online]. Available: http://www.its.dot.gov/vii/index.htm[2006,Feb.15]

[21] Ardekani, S. and Herman, R., "Urban network-wide traffic variables and their relations," *Transportation Science*, vol. 21, no. 1, pp. 1–16, Feb. 1987.

[22] Artimy, M. M., Phillips, W. J., and Robertson, W., "Connectivity with static transmission range in vehicular ad hoc networks," in *Proc. the 3rd Annual Communication Networks and Services Research Conference, (CNSR'05)*, Halifax, Canada, May 2005, pp. 237–242.

[23] Artimy, M. M., Robertson, W., and Phillips, W. J., "Connectivity in inter-vehicle ad hoc networks," in *Proc. IEEE Canadian Conference on Electrical and Computer Engineering (CCECE'04)*, vol. 1, Niagara Falls, Canada, May 2004, pp. 293–298.

[24] Artimy, M. M., Robertson, W., and Phillips, W. J., "Vehicle traffic microsimulator for ad hoc networks research," in *Proc. International Workshop on Wireless Ad-hoc Networks (IWWAN'04)*, Oulu, Finland, May 2004, pp. 105–109.

[25] Arvelo, E. C., "Open-loop power control based on estimations of packet error rate in a Bluetooth radio," in *Proc. IEEE Wireless Communications and Networking (WCNC'03)*, vol. 3, 2003, pp. 1465–1469.

[26] Ashton, W. D., *The theory of road traffic flow.* London, New York: Methuen, Wiley, 1966.

[27] ASTM E2213-03, *Standard Specification for Telecommunications and Information Exchange Between Roadside and Vehicle Systems – 5 GHz Band Dedicated Short Range Communications (DSRC) Medium Access Control (MAC) and Physical Layer (PHY) Specifications*, ASTM Std., Sept. 2003.

[28] Bai, F., Sadagopan, N., and Helmy, A., "IMPORTANT: a framework to systematically analyze the impact of mobility on performance of routing protocols for ad hoc networks," in *Proc. Twenty-Second Annual Joint Conference of the IEEE Computer and Communications Societies (INFOCOM'03)*, vol. 2, 2003, pp. 825–835.

[29] Bao, L. and Garcia-Luna-Aceves, J. J., "Topology management in ad hoc networks," in *Proc. The 4th ACM International Symposium on Mobile Ad Hoc Networking & Computing (MobiHoc'03).* Annapolis, Maryland, USA: ACM Press, 2003, pp. 129–140.

[30] Barlovic, R., Santen, L., Schadschneider, A., and Schreckenberg, M., "Metastable states in cellular automata for traffic flow," *The European Physical Journal B - Condensed Matter*, vol. 5, no. 3, pp. 793–800, Oct. 1998.

[31] Bettstetter, C., "On the connectivity of wireless multihop networks with homogeneous and inhomogeneous range assignment," in *Proc. The 56th IEEE Semiannual Vehicular Technology Conference (VTC'02-Fall)*, vol. 3, 2002, pp. 1706–1710 vol.3.

[32] Bettstetter, C., Resta, G., and Santi, P., "The node distribution of the random waypoint mobility model for wireless ad hoc networks," *IEEE Transactions on Mobile Computing*, vol. 2, no. 3, pp. 257–269, 2003.

[33] Bettstetter, C., "Mobility modeling in wireless networks: categorization, smooth movement, and border effects," *ACM Mobile Computing and Communications Review*, vol. 5, no. 3, pp. 55–66, 2001.

[34] Bettstetter, C. and Hartmann, C., "Connectivity of wireless multihop networks in a shadow fading environment," in *Proc. The 6th ACM International Workshop on Modeling Analysis and Simulation of Wireless and Mobile Systems (MSWiM'03).* San Diego, CA, USA: ACM Press, 2003, pp. 28–32.

[35] Blough, D. M., Resta, G., and Santi, P., "A statistical analysis of the long-run node spatial distribution in mobile ad hoc networks," *Wireless Networks*, vol. 10, no. 5, pp. 543–554, 2004.

[36] Blum, J. J., Eskandarian, A., and Hoffman, L. J., "Challenges of intervehicle ad hoc networks," *IEEE Transactions on Intelligent Transportation Systems*, vol. 5, no. 4, pp. 347–351, 2004.

[37] Boxill, S. A. and Yu, L., "An evaluation of traffic simulation models for supporting ITS development," Center for Transportation Training and Research, Texas Southern University, Tech. Rep. SWUTC/00/167602-1, Oct. 2000.

[38] Briesemeister, L. and Hommel, G., "Role-based multicast in highly mobile but sparsely connected ad hoc networks," in *Proc. First Annual Workshop on Mobile and Ad Hoc Networking and Computing*, Aug. 2000, pp. 45–50.

[39] Briesemeister, L., Schäfers, L., and Hommel, G., "Disseminating messages among highly mobile hosts based on inter-vehicle communication," in *Proc. IEEE Intelligent Vehicles Symposium (IV'00)*, Oct. 2000, pp. 522–527.

[40] Brusaglino, G., "Safe and effective mobility in Europe – the contribution of the PROMETHEUS programme," in *IEE Colloquium on Prometheus and Drive*, 1992, pp. 1/1–1/10.

[41] Camp, T., Boleng, J., and Davis, V., "A survey of mobility models for ad hoc network research," *Wireless Communications and Mobile Computing*, vol. 2, no. 5, pp. 483–502, 2002.

[42] Cassidy, M. J., "Traffic flow and capacity," in *Handbook of Transportation Science*, 2nd ed., Hall, R. W., Ed. USA: Kluwer Academic Publishers, 2003, ch. 6, pp. 155–191.

[43] Chen, Z. D., Kung, H. T., and Vlah, D., "Ad hoc relay wireless networks over moving vehicles on highways," in *Proc. The 2nd ACM International Symposium on Mobile Ad Hoc Networking & Computing (MobiHoc'01)*. Long Beach, CA, USA: ACM Press, 2001, pp. 247–250.

[44] Cheng, Y. C. and Robertazzi, T. G., "Critical connectivity phenomena in multihop radio models," *IEEE Transactions on Communications*, vol. 37, no. 7, pp. 770–777, 1989.

[45] Choffnes, D. R. and Bustamante, F. E., "An integrated mobility and traffic model for vehicular wireless networks," in *Proc. The 2nd ACM International Workshop on Vehicular Ad Hoc Networks (VANET'05)*. Cologne, Germany: ACM Press, 2005, pp. 69–78.

[46] Chowdhury, D., Santen, L., Schadschneider, A., Sinha, S., and Pasupathy, A., "Spatio-temporal organization of vehicles in a cellular automata model of traffic with 'slow-to-start' rule," *Journal of Physics A: Mathematical and General*, vol. 32, no. 18, pp. 3229–3252, 1999.

[47] Clementi, A. E. F., Penna, P., and Silvestri, R., "Hardness results for the power range assignmet problem in packet radio networks," in *Proc. Third International Workshop on Approximation Algorithms for Combinatorial Optimization Problems (RANDOM-APPROX'99)*. Springer-Verlag, 1999, pp. 197–208.

[48] Clementi, A. E. F., Penna, P., and Silvestri, R., "On the power assignment problem in radio networks," *Mobile Networks and Applications*, vol. 9, no. 2, pp. 125–140, 2004.

[49] Cowan, R. J., "Adams' formula revised," *Traffic Engineering & Control*, vol. 25, no. 5, pp. 272–274, 1984 1984.

[50] Díaz, J., Penrose, M. D., Petit, J., and Serna, M., "Convergence theorems for some layout measures on random lattice and random geometric graphs," *Combinatorics, Probability and Computing*, vol. 9, no. 6, pp. 489–511, 2000.

[51] Dousse, O., Thiran, P., and Hasler, M., "Connectivity in ad-hoc and hybrid networks," in *Proc. Twenty-First Annual Joint Conference of the IEEE Computer and Communications Societies (INFOCOM'02)*, vol. 2, 2002, pp. 1079–1088.

[52] Ebner, A. and Rohling, H., "A self-organized radio network for automotive applications," in *Proc. 8th World Congress on Intelligent Transportation Systems (ITS'01)*, Sydney, Australia, Oct. 2001.

[53] Eisenblätter, B., Santen, L., Schadschneider, A., and Schreckenberg, M., "Jamming transition in a cellular automaton model for traffic flow," *Physical Review E*, vol. 37, no. 2, pp. 1309–1314, Feb. 1998.

[54] Enkelmann, W., "FleetNet - applications for inter-vehicle communication," in *Proc. IEEE Intelligent Vehicles Symposium (IV'03)*, 2003, pp. 162–167.

[55] Evans, D. H., Herman, R., and Weiss, G. H., "The highway merging and queuing problem," *Operations research*, vol. 12, no. 6, Special Transportation Science Issue, pp. 832–857, Nov./Dec. 1964.

[56] Franz, W., Eberhardt, R., and Luckenbach, T., "FleetNet – internet on the road," in *Proc. 8th World Congress on Intelligent Transport Systems (ITS'01)*, Sept./Oct. 2001.

[57] Franz, W., Hartenstein, H., and Bochow, B., "Internet on the road via inter-vehicle communications," in *GI Workshop, Communication over Wireless LANs*, Vienna, Austria, Sept. 2001.

[58] Fukui, M. and Ishibashi, Y., "Traffic flow in 1D cellular automaton model including cars moving with high speed," *Journal of the Physical Society of Japan*, vol. 65, no. 6, pp. 1868–1870, June 1996.

[59] Füßler, H., Mauve, M., Hartenstein, H., Vollmer, D., and Käsemann, M., "A comparison of routing strategies in vehicular ad-hoc networks," in *Reihe Informatik*, Mar. 2002.

[60] Gartner, N. H., Messer, C., and Rathi, A. K., *Traffic Flow Theory: A State of the Art Report - Revised Monograph on Traffic Flow Theory*, Gartner, N. H., Messer, C., and Rathi, A. K., Eds. Oak Ridge, Tennessee: Oak Ridge National Laboratory, 1997. [Online]. Available: http://www.tfhrc.gov/its/tft/tft.htm

[61] Ghandeharizade, S., Kapadia, S., and Krishnamachari, B., "Pavan: a policy framework for content availabilty in vehicular ad-hoc networks," in *Proc. The 1st ACM International Workshop on Vehicular Ad Hoc Networks (VANET'04)*. Philadelphia, PA, USA: ACM Press, 2004, pp. 57–65.

[62] Gomez, J. and Campbell, A. T., "A case for variable-range transmission power control in wireless multihop networks," in *Proc. Twenty-third Annual Joint Conference of the IEEE Computer and Communications Societies (INFOCOM'04)*, vol. 2, 2004, pp. 1425–1436.

[63] Greenshields, B. D., "A study of traffic capacity," in *Proceedings of the Highway Research Board*, vol. 14, 1935, p. 468.

[64] Gupta, P. and Kumar, P. R., "Critical power for asymptotic connectivity in wireless networks," in *Stochastic Analysis, Control, Optimization and Applications: A Volume in Honor of W.H. Fleming*, McEneany, W. M., Yin, G., and Zhan, Q., Eds. Birkhauser, Boston: Springer, 1998, pp. 547–566.

[65] Haberman, R., *Mathematical models : mechanical vibrations, population dynamics, and traffic flow : an introduction to applied mathematics.* Englewood Cliffs, N.J.: Prentice-Hall, 1977.

[66] Hafstein, S. F., Chrobok, R., Pottmeier, A., Schreckenberg, M., and Mazur, F. C., "A high-resolution cellular automata traffic simulation model with application in a freeway traffic information system," *Computer-Aided Civil and Infrastructure Engineering*, vol. 19, no. 5, pp. 338–350, 2004. [Online]. Available: http://www.blackwell-synergy.com/

[67] Hall, F. L., "Traffic stream characteristics," in *Traffic Flow Theory: A State of the Art Report - Revised Monograph on Traffic Flow Theory*, Gartner, N. H., Messer, C., and Rathi, A. K., Eds. Oak Ridge, Tennessee: Oak Ridge National Laboratory, 1997, ch. 2. [Online]. Available: http://www.tfhrc.gov/its/tft/tft.htm

[68] Hartenstein, H., Bochow, B., Ebner, A., Lott, M., Radimirsch, M., and Vollmer, D., "Position-aware ad hoc wireless networks for inter-vehicle communications: the FleetNet project," in *Proc. The 2nd ACM International Symposium on Mobile Ad Hoc Networking & Computing (MobiHoc'01)*, Long Beach, CA, USA, Oct. 2001.

[69] Hedrick, J. K., Tomizuka, M., and Varaiya, P., "Control issues in automated highway systems," *IEEE Control Systems Magazine*, vol. 14, no. 6, pp. 21–32, 1994.

[70] Herman, R. and Prigogine, I., "A two-fluid approach to town traffic," *Science*, vol. 204, no. 4389, pp. 148–151, Apr. 13 1979.

[71] Herman, R. and Weiss, G., "Comments on the highway-crossing problem," *Operations research*, vol. 9, no. 6, pp. 828–840, Nov./Dec. 1961.

[72] Hong, X., Gerla, M., Pei, G., and Chiang, C.-C., "A group mobility model for ad hoc wireless networks," in *Proc. The ACM International Workshop on Modeling and Simulation of Wireless and Mobile Systems (MSWiM'99)*. ACM Press, Aug. 1999, pp. 53–60.

[73] Horowitz, R. and Varaiya, P., "Control design of an automated highway system," *Proceedings of the IEEE*, vol. 88, no. 7, pp. 913–925, 2000.

[74] *IEEE Std 802.11-1997 Information Technology- telecommunications And Information exchange Between Systems-Local And Metropolitan Area Networks-specific Requirements-part 11: Wireless LAN Medium Access Control (MAC) And Physical Layer (PHY) Specifications*, IEEE Std., 1997.

[75] *Supplement to IEEE standard for information technology telecommunications and information exchange between systems - local and metropolitan area networks - specific requirements. Part 11: Wireless LAN Medium Access Control (MAC) and Physical Layer (PHY) specifications: high-speed physical layer in the 5 GHz band*, IEEE Std., 1999.

[76] Issariyakul, T., Hossain, E., and Kim, D. I., "Medium access control protocols for wireless mobile ad hoc networks: issues and approaches," *Wireless Communications and Mobile Computing*, vol. 3, no. 8, pp. 935–958, 2003.

[77] Jost, D. and Nagel, K., "Probabilistic traffic flow breakdown in stochastic car following models," in *Proc. Traffic and Granular Flow*, Hoogendoorn, S. P., Luding, S., Bovy, P. H. L., Schreckenberg, M., and Wolf, D. E., Eds., The Netherlands, Oct. 2003, pp. 87–103.

[78] Jost, D. and Nagel, K., "Probabilistic traffic flow breakdown in stochastic car following models," *Transportation Research Record*, vol. 1852, pp. 152–158, 2003.

[79] Kato, S., Tsugawa, S., Tokuda, K., Matsui, T., and Fujii, H., "Vehicle control algorithms for cooperative driving with automated vehicles and intervehicle communications," *IEEE Transactions on Intelligent Transportation Systems*, vol. 3, no. 3, pp. 155–161, 2002.

[80] Kerner, B. S., Klenov, S. L., and Wolf, D. E., "Cellular automata approach to three-phase traffic theory," *Journal of Physics A: Mathematical and General*, vol. 35, no. 47, pp. 9971–10 013, 2002.

[81] Knospe, W., Santen, L., Schadschneider, A., and Schreckenberg, M., "Towards a realistic microscopic description of highway traffic," *Journal of Physics A: Mathematical and General*, vol. 33, no. 48, pp. 477–485, 2000.

[82] Knospe, W., Santen, L., Schadschneider, A., and Schreckenberg, M., "A realistic two-lane traffic model for highway traffic," *Journal of Physics A: Mathematical and General*, vol. 35, no. 15, pp. 3369–3388, 2002.

[83] Koppa, R. J., "Human factors," in *Traffic Flow Theory: A State of the Art Report – Revised Monograph on Traffic Flow Theory*, Gartner, N. H., Messer, C., and Rathi, A. K., Eds. Oak Ridge, Tennessee: Oak Ridge National Laboratory, 1997, ch. 3. [Online]. Available: http://www.tfhrc.gov/its/tft/tft.htm

[84] Korkmaz, G., Ekici, E., Özgüner, F., and Özgüner, U., "Urban multi-hop broadcast protocol for inter-vehicle communication systems," in *Proc. The First ACM Workshop on Vehicular Ad Hoc Networks (VANET'04)*. Philadelphia, PA, USA: ACM Press, 2004, pp. 76–85.

[85] Kosch, T., Schwingenschlogl, C., and Ai, L., "Information dissemination in multihop inter-vehicle networks," in *Proc. The IEEE 5th International Conference on Intelligent Transportation Systems (ITSC'02)*, 2002, pp. 685–690.

[86] Kreith, F., Meyer, M. D., Leonard, J., Shuldiner, P. W., Black, K. B., Schonfeld, P., Norton, P., Reed, J. B., and Goehring, J. B., "Transportation," in *Mechanical Engineering Handbook*, Kreith, F., Ed. CRC Press LLC, 1999, ch. 10.

[87] Kuhne, R. and Michalopoulos, P., "Continuum flow models," in *Traffic Flow Theory: A State of the Art Report – Revised Monograph on Traffic Flow Theory*, Gartner, N. H., Messer, C., and Rathi, A. K., Eds. Oak Ridge, Tennessee: Oak Ridge National Laboratory, 1997, ch. 5. [Online]. Available: http://www.tfhrc.gov/its/tft/tft.htm

[88] Lárraga, M. E., del Río, J. A., and Schadschneider, A., "New kind of phase separation in a CA traffic model with anticipation," *Journal of Physics A: Mathematical and General*, vol. 37, no. 12, pp. 3769–3781, 2004.

[89] Li, L., Halpern, J. Y., Bahl, P., Wang, Y.-M., and Wattenhofer, R., "A cone-based distributed topology-control algorithm for wireless multi-hop networks," *IEEE/ACM Transactions on Networking*, vol. 13, no. 1, pp. 147–159, 2005.

[90] Li, N., Hou, J. C., and Sha, L., "Design and analysis of an MST-based topology control algorithm," in *Proc. Twenty-Second Annual Joint Conference of the IEEE Computer and Communications Societies (INFOCOM'03)*, vol. 3, 2003, pp. 1702–1712.

[91] Lieberman, E. and Rathi, A. K., "Traffic simulation," in *Traffic Flow Theory: A State of the Art Report - Revised Monograph on Traffic Flow Theory*, Gartner, N. H., Messer, C., and Rathi, A. K., Eds. Oak Ridge, Tennessee: Oak Ridge National Laboratory, 1997, ch. 10. [Online]. Available: http://www.tfhrc.gov/its/tft/tft.htm

[92] Liu, J. and Li, B., "MobileGrid: capacity-aware topology control in mobile ad hoc networks," in *Proc. Eleventh International Conference on Computer Communications and Networks*, 2002, pp. 570–574.

[93] Lizee, G. and Fapojuwo, A. O., "Highway traffic models for wireless networks," in *Proc. The 53rd IEEE Semiannual Vehicular Technology Conference (VTC'01-Spring)*, vol. 4, 2001, pp. 2766–2770.

[94] Lochert, C., Hartenstein, H., Tian, J., Füßler, H., Hermann, D., and Mauve, M., "A routing strategy for vehicular ad hoc networks in city environments," in *Proc. IEEE Intelligent Vehicles Symposium (IV'03)*, 2003, pp. 156–161.

[95] Lott, M., Halfmann, R., Schultz, E., and Radimirsch, M., "Medium access and radio resource management for ad hoc networks based on UTRA TDD," in *Proc. The 2nd ACM International Symposium on Mobile Ad Hoc Networking & Computing (MobiHoc'01)*. Long Beach, CA, USA: ACM Press, 2001, pp. 76–86.

[96] Lubashevsky, I. A. and Mahnke, R., "Order-parameter model for unstable multilane traffic flow," *Physical Review E*, vol. 62, no. 5, pp. 6082–6093, 2000.

[97] Mangharam, R., Weller, D. S., Stancil, D. D., Rajkumar, R., and Parikh, J. S., "GrooveSim: a topography-accurate simulator for geographic routing in vehicular networks," in *Proc. The 2nd ACM International Workshop on Vehicular Ad Hoc Networks (VANET'05)*. Cologne, Germany: ACM Press, 2005, pp. 59–68.

[98] Nagatani, T., "Bunching of cars in asymmetric exclusion models for freeway traffic," *Physical Review E*, vol. 51, no. 2, pp. 922–928, 1995.

[99] Nagatani, T., "Traffic jams induced by fluctuation of leading car," *Physical Review E*, vol. 61, no. 4, pp. 3534–3540, Apr. 2000.

[100] Nagatani, T., "The physics of traffic jams," *Reports on Progress in Physics*, vol. 65, no. 9, pp. 1331–1386, 2002.

[101] Nagel, K., "High-speed microsimulations of traffic flow," Ph.D. dissertation, University of Cologne, Cologne, Germany, 1995.

[102] Nagel, K., "Traffic neworks," in *Handbook of graphs and networks : from the genome to the internet*, 1st ed., Bornholdt, S. and Schuster, H. G., Eds. Weinheim: Wiley-VCH, 2003, ch. 11, pp. 248–272.

[103] Nagel, K. and Paczuski, M., "Emergent traffic jams," *Physical Review E*, vol. 51, pp. 2909–2918, 1995.

[104] Nagel, K. and Schreckenberg, M., "A cellular automaton model for freeway traffic," *Journal de Physique I France*, vol. 2, pp. 2221–2229, Dec. 1992.

[105] Nagel, K., Stretz, P., Pieck, M., Leckey, S., Donnelly, R., and Barrett, C. L., "TRANSIMS traffic flow characteristics," Los Alamos National Laboratory, Tech. Rep. LA-UR-97-3531, PREPRINT March 19 1999.

[106] Nagel, K., Wagner, P., and Woesler, R., "Still flowing: Approaches to traffic flow and traffic jam modeling," *Operations Research*, vol. 51, no. 5, pp. 681–710, Sept./Oct. 2003.

[107] Nagel, K., Wolf, D. E., Wagner, P., and Simon, P., "Two-lane traffic rules for cellular automata: A systematic approach," *Physical Review E*, vol. 58, no. 2, pp. 1425–1437, Aug. 1998.

[108] Penrose, M. D., "The longest edge of the random minimal spanning tree," *The Annals of Applied Probability*, vol. 7, no. 2, pp. 340–361, May 1997.

[109] Peterson, I., "Waves of gongestion," *Science News Online*, vol. 160, no. 10, Sept. 2001. [Online]. Available: http://www.sciencenews.org/articles/20010908/mathtrek.asp

[110] Philips, T. K., Panwar, S. S., and Tantawi, A. N., "Connectivity properties of a packet radio network model," *IEEE Transactions on Information Theory*, vol. 35, no. 5, pp. 1044–1047, 1989.

[111] Pipes, L. A., "An operational analysis of traffic dynamics," *Journal of Applied Physics*, vol. 24, no. 3, pp. 274–281, 1953.

[112] Piret, P., "On the connectivity of radio networks," *IEEE Transactions on Information Theory*, vol. 37, no. 5, pp. 1490–1492, Sept. 1991.

[113] Pivovarov, E. (2003, July 28) Traffic jams. [Online]. Available: http://physics.ucsd.edu/~epivovar/traffic.htm[2005,Nov.30]

[114] Ramanathan, R. and Rosales-Hain, R., "Topology control of multihop wireless networks using transmit power adjustment," in *Proc. Nineteenth Annual Joint Conference of the IEEE Computer and Communications Societies (INFOCOM'00)*, vol. 2, 2000, pp. 404–413.

[115] Rappaport, T. S., *Wireless communications : principles and practice.* Upper Saddle River, N.J.: Prentice Hall PTR, 1996.

[116] Reichardt, D., Miglietta, M., Moretti, L., Morsink, P., and Schulz, W., "CarTALK 2000 - safe and comfortable driving based upon inter-vehicle-communication," in *Proc. IEEE Intelligent Vehicle Symposium*, Versailles, June 2002.

[117] Rickert, M., Nagel, K., Schreckenberg, M., and Latour, A., "Two lane traffic simulations using cellular automata," *Physica A: Statistical and Theoretical Physics*, vol. 231, no. 4, pp. 534–550, Oct. 1996.

[118] Roters, L., Lubeck, S., and Usadel, K. D., "Critical behavior of a traffic flow model," *Physical Review E*, vol. 59, no. 3, pp. 2672–2676, 1999.

[119] Rothery, R. W., "Car-following models," in *Traffic Flow Theory: A State of the Art Report – Revised Monograph on Traffic Flow Theory*, Gartner, N. H., Messer, C., and Rathi, A. K., Eds. Oak Ridge, Tennessee: Oak Ridge National Laboratory, 1997, ch. 4. [Online]. Available: http://www.tfhrc.gov/its/tft/tft.htm

[120] Rouphail, N., Tarko, A., and Li, J., "Traffic flow at signalized intersections," in *Traffic Flow Theory: A State of the Art Report – Revised Monograph on Traffic Flow Theory*, Gartner, N. H., Messer, C., and Rathi, A. K., Eds. Oak Ridge, Tennessee: Oak Ridge National Laboratory, 1997, ch. 9. [Online]. Available: http://www.tfhrc.gov/its/tft/tft.htm

[121] Rudack, M., Meincke, M., Jobmann, K., and Lott, M., "On traffic dynamical aspects of inter vehicle communications (IVC)," in *Proc. The 58th IEEE Semiannual Vehicular Technology Conference (VTC'03-Fall)*, vol. 5, 2003, pp. 3368–3372.

[122] Rudack, M., Meincke, M., and Lott, M., "On the dynamics of ad hoc networks for inter vehicles communicaitons (IVC)," in *Proc. The 2002 International Conference on Wireless Networks*, Las Vegas, USA, June 2002.

[123] Sánchez, M., Manzoni, P., and Haas, Z. J., "Determination of critical transmission range in ad-hoc networks," in *Proc. Multiaccess, Mobility and Teletraffic for Wireless Communications Conference*, Venice, Italy, Oct. 1999.

[124] Santi, P. and Blough, D. M., "An evaluation of connectivity in mobile wireless ad hoc networks," in *Proc. International Conference on Dependable Systems and Networks*, June 2002, pp. 89–98.

[125] Santi, P. and Blough, D. M., "The critical transmitting range for connectivity in sparse wireless ad hoc networks," *IEEE Transactions on Mobile Computing,*, vol. 2, no. 1, pp. 25–39, 2003.

[126] Santi, P., "Topology control in wireless ad hoc and sensor networks," *ACM Computing Surveys*, vol. 37, no. 2, pp. 164–194, 2005.

[127] Santi, P., Blough, D. M., and Vainstein, F., "A probabilistic analysis for the range assignment problem in ad hoc networks," in *Proc. The 2nd ACM International Symposium on Mobile Ad Hoc Networking & Computing (MobiHoc'01)*. Long Beach, CA, USA: ACM Press, 2001, pp. 212–220.

[128] Sarkar, P., "A brief history of cellular automata," *ACM Computing Surveys*, vol. 32, no. 1, pp. 80–107, 2000.

[129] Sasaki, H., Iwasaki, H., and Suda, T., "Simulation of information propagation for vehicles in physical communication network models," in *Proc. 2004 Symposium on Applications and the Internet (SAINT'04)*, Jan. 2004, pp. 408–414.

[130] Schadschneider, A. (2000, Apr. 10) Modelling of traffic flow. [Online]. Available: http://www.thp.uni-koeln.de/~as/Mypage/traffic.html[2005,Oct.26]

[131] SENSE. (1998, Sept. 29) How should speed limits be set? at the 85th percentile, of course! [Online]. Available: http://www.sense.bc.ca/disc/disc-08.htm[2005,Oct.22]

[132] Stojmenovic, I., "Position-based routing in ad hoc networks," *IEEE Communications Magazine*, vol. 40, no. 7, pp. 128–134, 2002.

[133] Tarko, A. P., "Highway traffic operations," in *The Civil Engineering Handbook*, 2nd ed., Chen, W.-F. and Liew, J. Y. R., Eds. CRC Press LLC, Aug. 2002, ch. 64.

[134] Thomas, M., Peytchev, E., and Al-Dabass, D., "Auto-sensing and distribution of traffic information in vehicular ad hoc networks," in *Proc. United Kingdom Simulation Society Conference*, St Catherine's College, Oxford, Mar. 2004, pp. 124–128.

[135] Tian, J., Hahner, J., Becker, C., Stepanov, I., and Rothermel, K., "Graph-based mobility model for mobile ad hoc network simulation," in *Proc. 35th Annual Simulation Symposium*, 2002, pp. 337–344.

[136] Tian, J., Han, L., and Rothermel, K., "Spatially aware packet routing for mobile ad hoc inter-vehicle radio networks," in *Proc. IEEE Intelligent Transportation Systems*, vol. 2, Oct. 2003, pp. 1546–1551.

[137] Transport Canada, "An intelligent transportation systems (ITS) plan for Canada: En route to intelligent mobility," Transport Canada, Tech. Rep. TP 13501 E, Nov. 1999. [Online]. Available: http://www.its-sti.gc.ca/en/its_plan_for_canada.htm

[138] Troutbeck, R. J. and Brilon, W., "Unsignalized intersection theory," in *Traffic Flow Theory: A State of the Art Report – Revised Monograph on Traffic Flow Theory*, Gartner, N. H., Messer, C., and Rathi, A. K., Eds. Oak Ridge, Tennessee: Oak Ridge National Laboratory, 1997, ch. 8. [Online]. Available: http://www.tfhrc.gov/its/tft/tft.htm

[139] Varaiya, P., "Smart cars on smart roads: problems of control," *IEEE Transactions on Automatic Control*, vol. 38, no. 2, pp. 195–207, 1993.

[140] Vilar, L. C. Q. and de Souza, A. M. C., "Cellular automata models for general traffic conditions on a line," *Physica A: Statistical and Theoretical Physics*, vol. 211, no. 1, pp. 84–92, Oct. 1994.

[141] Wattenhofer, R., Li, L., Bahl, P., and Wang, Y. M., "Distributed topology control for power efficient operation in multihop wireless ad hoc networks," in *Proc. Twentieth Annual Joint Conference of the IEEE Computer and Communications Societies (INFOCOM'01)*, vol. 3, 2001, pp. 1388–1397.

[142] Weiss, G. H. and Maradudin, A. A., "Some problems in traffic delay," *Operations research*, vol. 10, no. 1, pp. 74–104, Jan./Feb. 1962.

[143] Williams, J. C., "Macroscopic flow models," in *Traffic Flow Theory: A State of the Art Report – Revised Monograph on Traffic Flow Theory*, Gartner, N. H., Messer, C., and Rathi, A. K., Eds. Oak Ridge, Tennessee: Oak Ridge National Laboratory, 1997, ch. 6. [Online]. Available: http://www.tfhrc.gov/its/tft/tft.htm

[144] Wischhof, L., Ebner, A., and Rohling, H., "Information dissemination in self-organizing intervehicle networks," *IEEE Transactions on Intelligent Transportation Systems*, vol. 6, no. 1, pp. 90–101, 2005.

[145] Wischhof, L., Ebner, A., Rohling, H., Lott, M., and Halfmann, R., "SOTIS - a self-organizing traffic information system," in *Proc. The 57th IEEE Semiannual Vehicular Technology Conference (VTC'03-Spring)*, vol. 4, 2003, pp. 2442–2446.

[146] Wolfram, S., *Theory and applications of cellular automata : including selected papers, 1983-1986.* Singapore: World Scientific, 1986, vol. 1.

[147] Wu, H., Fujimoto, R., Guensler, R., and Hunter, M., "MDDV: a mobility-centric data dissemination algorithm for vehicular networks," in *Proc. The 1st ACM International Workshop on Vehicular Ad Hoc Networks (VANET'04)*. Philadelphia, PA, USA: ACM Press, 2004, pp. 47–56.

[148] Xu, Q., Mak, T., Ko, J., and Sengupta, R., "Vehicle-to-vehicle safety messaging in DSRC," in *Proc. The 1st ACM International Workshop on Vehicular Ad Hoc Networks (VANET'04)*. Philadelphia, PA, USA: ACM Press, 2004, pp. 19–28.

[149] Xue, F. and Kumar, P. R., "The number of neighbors needed for connectivity of wireless networks," *Wireless Networks*, vol. 10, no. 2, pp. 169–181, 2004.

[150] Xue, Y., Dong, L., Li, L., and qiang Dai, S., "Effects of changing orders in the update rules on traffic flow," *Physical Review E*, vol. 71, no. 2, p. 026123, 2005.

[151] Yuan, R., "North American dedicated short range communications (DSRC) standards," in *Proc. IEEE Conference on Intelligent Transportation System*, Nov. 1997, pp. 537–542.

[152] Zhao, Y., "Telematics: Safe and fun driving," *Intelligent Systems*, vol. 17, no. 1, pp. 10–14, Jan./Feb. 2002.

Appendix A

ITS Related Projects

The following is a list of the main projects related to Intelligent Transportation Systems (ITS) around the world.

A.1 Projects in Germany

NOW (2004–present): The main objectives of the Network on Wheels (NOW) project are to answer key technical questions related to communication protocols and data security for Car-to-Car Communication (C2CC) and to submit the results to the standardization activities of the Car-to-Car Communication Consortium (C2CCC), which is an initiative of major European car manufacturers and suppliers. NOW will support active safety applications and infotainment applications and will provide an open communication platform for a broad spectrum of applications. Furthermore, NOW will provide a test bed for functional tests and demonstrations for C2CC Consortium specifications [13].

INVENT, (2000–2003): This project branches into the "driver assistance, active safety" project, which focuses on the development of the familiar cruise control and adaptive cruise control systems in order to assist the driver in stop–go traffic. The "traffic management" project attempts to control the problem of traffic jams in urban areas using driver assistant systems, which calculate the

optimum speeds, distances and lane changes so that traffic flows more smoothly, and navigation systems, which will be able to suggest alternative routes to avoid traffic jams. The latter approach depends on V2V communication. The "traffic management in transport and logistics" project develops driver assistants systems for commercial vehicles [12].

FleetNet, (2000–2003): FleetNet is a collaboration among six companies and three universities. Key objectives for FleetNet are the capability to distribute locally relevant data where generated and needed and to satisfy the vehicle drivers' and passengers' needs for location-dependent information and services [56, 6].

COMCAR, (1999–2002): The COMCAR project aims at using cellular communication networks to deliver asymmetric IP-based multimedia and telematics services in cars and railways [3].

A.2 Projects in Europe (including Germany)

PReVENT, (2004–2008): focuses on preventive safety applications that employs advanced sensors and communication and positioning technologies integrated into on-board systems for driver assistance [19].

C2CCC, (2002–present): This is a non-profit organization initiated by European vehicle manufacturers. The C2CCC objective to further increasing road traffic safety and efficiency by means of inter-vehicle communications. The C2CCC vision of inter-vehicle applications is similar to FleetNet [56]. These include advanced driver assistance, decentralized floating car data, user communications and information services [16].

CarTALK 2000, 2001–2004: The main objectives of the project are the development of co-operative driver assistance systems and the development of a self-organizing wireless ad-hoc network as a communication basis with the aim of preparing a future standard. CarTALK's consortium includes European car manufacturers, IT industry and suppliers, and research institutes [116, 8].

ADASE-II, (2001–2004): The Advanced Driver Assistance Systems in Europe - II (ADASE-II) is a cluster of European projects that include about 30 research projects for driver assistance systems and related activities. They represent a project value in excess of about 100M Euro [10].

DRiVE, (2000–2002): The objective of the Dynamic Radio for IP-Services in Vehicular Environments (DRiVE) project is to deliver in-vehicle multimedia services for education and entertainment applications using spectrum efficient high-quality wireless IP in a heterogeneous multi-radio environment [5].

OverDRiVE, (2002–2004): The research project OverDRiVE (Spectrum Efficient Uni- and Multicast Over Dynamic Radio Networks in Vehicular Environments) builds on the findings of the DRiVE project. The main objective of this project is to enable and demonstrate the delivery of spectrum efficient multi- and unicast services to vehicles [7].

CHAUFFEUR 2, (2000–2003): The aim of CHAUFFEUR 2 is to develop driver assistance systems (lane keeping systems and distance control systems) that enable a truck to follow any other truck or car at a safe following distance while being laterally guided. A further objective is the demonstration of automatic platoon formation of at least three trucks [4].

Prometheus, (1986–1994): The objectives of this projects were grouped in three categories: long range trip planning based on actual traffic situation, traffic flow harmonization based on cooperative driving through V2V and vehicle-to-infrastructure communication, and safe driving using intelligent driver's assisting electronics [40].

A.3 Projects in the United States

VSC, (2002–2004): The Vehicle Safety Communications (VSC) Project objectives is to identify vehicle safety applications enhanced or enabled by external communications, determine their respective communications requirements, evaluate emerging 5.9 GHz DSRC vehicle communications technology and influence

proposed DSRC communications protocols to meet the needs of vehicle safety applications [9].

PATH, (since 1986): California Partners for Advanced Transit and Highways (PATH) project joins the efforts of many universities, private industry, state and local agencies, and non-profit institutions in order to develop solutions to the problems of California's surface transportation systems through innovative research. PATH research is divided into four program areas: Policy and Behavioural Research, Transportation Safety Research, Traffic Operations Research, and Transit Operations Research [15].

IVI, (since 1998): Intelligent Vehicle Initiative (IVI) was initiated by the US Department of Transportation (USDOT) as part of an ITS program. IVI's mission is to reduce the number and severity of crashes through driver assistance systems. These safety systems, assume partial control of vehicles to avoid collisions [17].

VII, (2004–2010): The Vehicle-Infrastructure Integration Initiative (VII) is a collaboration between US federal and state organizations, and the automobile industry. The VII is aiming to use the communication between the vehicle and infrastructure for a range of applications that include real-time information and advanced safety applications such as intersection safety, road-departure applications, and emergency response [20].

A.4 Projects in Japan

AHS, (1989–2002): The Advanced Crusie-Assist Highway System (AHS) project was launched by the government and was supported by 13 private companies. AHS research is being carried out in three fields. The information field (AHS-i), focuses on providing information about traffic, closures, and hazards on the road ahead. The control field (AHS-c), provides vehicle control assistance, such as holding a vehicle within a lane or stopping of vehicles to coordinate

emergency response. The automated cruise field (AHS-a) supports automatic driving capabilities [11].

AHSRA, (since 1996): The Advanced Cruise-Assist Highway System Research Association (AHSRA) was established to oversee the R&D of the infrastructure side of the AHS. At present, it has 21 member companies from several industries and 360 supporting members that include organizations and private individuals [11].

ASV, (1991–2005): The Advanced Safety Vehicle (ASV) project represents the vehicle side of the AHS and focuses on accident prevention and avoidance with information, communication and electronics technologies, in contrast to conventional safety measures aimed at occupant protection after crash [11].

Appendix B

RoadSim Class Diagrams

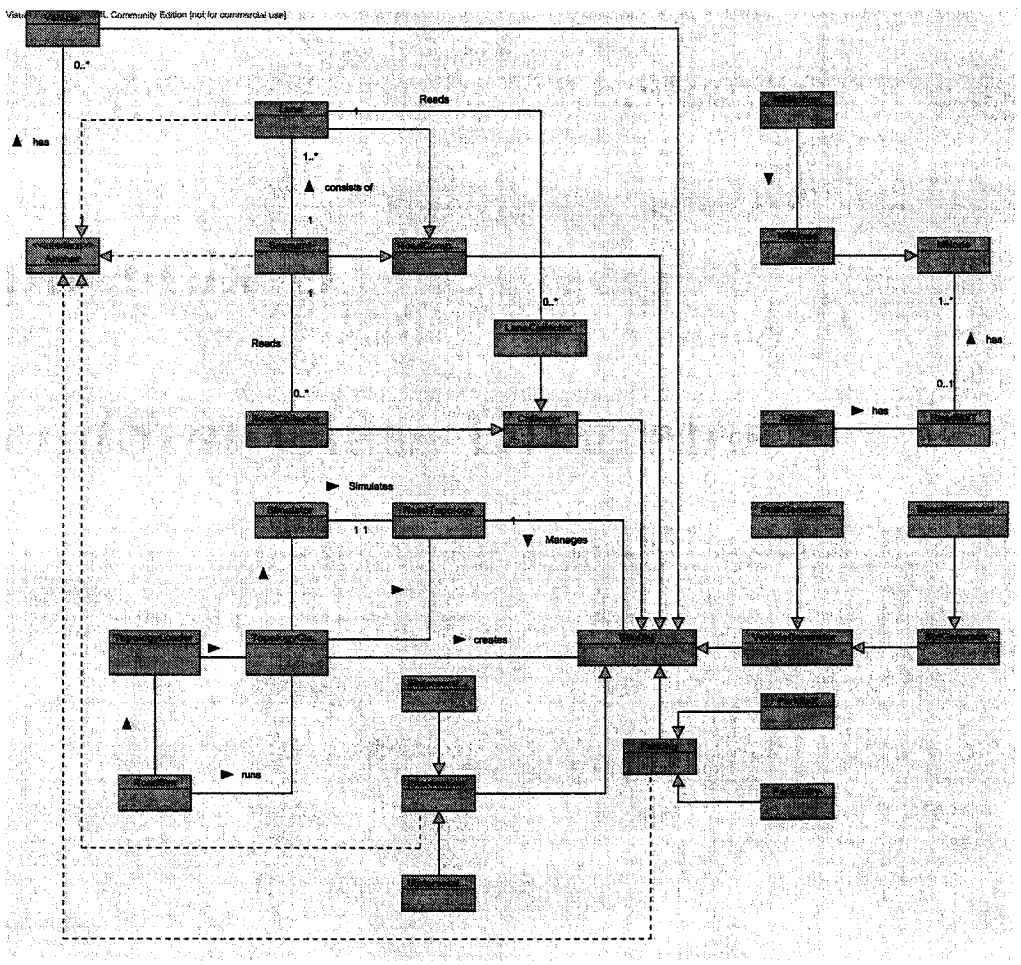

Appendix C

RoadSim Topologies and Generated ns-2 Scripts

RoadSim generates Network Simulator-2 (ns-2) script that can be used to run network simulations. The next section shows the *RoadSim* topology that generates traffic in a 1-lane closed-loop road. The following sections show the movement script, the power setting script, and connection scripts, respectively. The last section shows the main ns-2 script used in Section 8.6.

C.1 *RoadSim* racetrack topology

The following code generates vehicle movement in a closed-loop road.

```
import rs.util.*;
import rs.sim.*;
import rs.gui.*;
import rs.charting.*;
import java.util.*;

/**
 * This class creates a closed-loop road with 1 or more lanes.
 */
public class RacetrackTopology {
static int idx = 0;
static double p = 0.5;
static String fileName = "trace";
```

```
private static void processOptions(String[] args) {
int i=0;
while(i<args.length) {
if (args[i].charAt(0) == '-') {
if (args[i].startsWith("-r:")) { //random index
idx = Integer.parseInt(args[i].substring(3));
} else if (args[i].startsWith("-p:")) { //prob. value
p = Double.parseDouble(args[i].substring(3));
} else if (args[i].startsWith("-f:")) { //file suffix
fileName = args[i].substring(3);
}
} else {
}
i++;
}
}

public static void main(String[] args) {
processOptions(args);

// build the topology
Simulator sim = Simulator.getSimulator();

// set random variables
RNG rng = RNG.getRNG();
rng.setStream(idx);

// set global variables
int r_len = 1000;

// initialize a segment with one lane east-bound
Lane lane0 = new Lane("Lane_0");
Segment s = new Segment("Segment_1");
s.setLength(r_len);
s.addLane(0, lane0);
//Lane lane1 = new Lane("Lane_1"); // for multiple lanes
//s.addLane(1, lane1);
//Lane lane2 = new Lane("lane_2");
//s.addLane(2, lane2);
sim.add(s);

// initialize parking lots
ParkExit pkex = new ParkExit("ExitPark_L1");
pkex.setSegment(s, 20);
sim.add(pkex);

// initialize intersections
```

```
// East-bound traffic does not face any sign
UIntersection lnk = new UIntersection("XSect_1", null, null, s,
s, null, null, UIntersection.STOP, 0, 1, 0);
sim.add(lnk);

// initialize generators
//Generate vehicles at flow rate of 60 veh/hr
VehicleGenerator  vg =
VehicleFactory.getFactory().getGenerator("GNR_1", 60, 0, 0);
vg.setPark(pkex);
sim.add(vg);

// for NullAnalyzer
RoadCollector rc3 = new RoadCollector("RDCL_3", s, 450, null, 0, 200);
NullAnalyzer la3 = new NullAnalyzer("Null Analyzer");
rc3.addAnalyzer(la3);
sim.add(rc3);

Printer prn = Printer.getPrinter();
prn.addDataFile(la3.getDataSet(Analyzer.INFO), fileName);
sim.setSimTime(40000);
}
}
```

C.2 Motion script

The following script is used in the experiments described in Section 8.6 to generate vehicle movements in ns-2 simulations.

```
proc setVehicleMotion {} {
global ns_ node_

# Movement of Node: 117
$ns_ at    206.400 "$node_(117) set X_       3.75"
$ns_ at    206.400 "$node_(117) set Y_       1.60"
$ns_ at    206.400 "$node_(117) setdest     888.75       1.60      37.50"
$ns_ at    230.000 "$node_(117) setdest     918.75       1.60      30.00"
$ns_ at    231.000 "$node_(117) setdest     941.25       1.60      22.50"
$ns_ at    232.000 "$node_(117) setdest     941.25       1.60       0.00"

# Movement of Node: 111
$ns_ at    190.600 "$node_(111) set X_       3.75"
$ns_ at    190.600 "$node_(111) set Y_       1.60"
$ns_ at    190.600 "$node_(111) setdest     956.25       1.60      37.50"
$ns_ at    216.000 "$node_(111) setdest     986.25       1.60      30.00"
$ns_ at    217.000 "$node_(111) setdest     986.25       1.60       0.00"

# Movement of Node: 97
```

```
$ns_ at    163.600 "$node_(97) set X_       3.75"
$ns_ at    163.600 "$node_(97) set Y_       1.60"
$ns_ at    163.600 "$node_(97) setdest     168.75       1.60      37.50"
$ns_ at    168.000 "$node_(97) setdest     198.75       1.60      30.00"
$ns_ at    169.000 "$node_(97) setdest    1061.25       1.60      37.50"
$ns_ at    192.000 "$node_(97) setdest    1091.25       1.60      30.00"
$ns_ at    193.000 "$node_(97) setdest    1091.25       1.60       0.00"

# Movement of Node: 26
$ns_ at     16.800 "$node_(26) set X_       3.75"
$ns_ at     16.800 "$node_(26) set Y_       1.60"
$ns_ at     16.800 "$node_(26) setdest    1496.25       1.60      37.50"
$ns_ at     56.601 "$node_(26) setdest    1496.25       1.60       0.00"

# <some code is deleted>

# Movement of Node: 57
$ns_ at     80.400 "$node_(57) set X_       3.75"
$ns_ at     80.400 "$node_(57) set Y_       1.60"
$ns_ at     80.400 "$node_(57) setdest    1376.25       1.60      37.50"
$ns_ at    117.000 "$node_(57) setdest    1391.25       1.60      15.00"
$ns_ at    118.000 "$node_(57) setdest    1391.25       1.60       0.00"
$ns_ at    256.000 "$node_(57) setdest    1398.75       1.60       7.50"
$ns_ at    257.000 "$node_(57) setdest    1413.75       1.60      15.00"
$ns_ at    258.000 "$node_(57) setdest    1436.25       1.60      22.50"
$ns_ at    259.000 "$node_(57) setdest    1496.25       1.60      30.00"
$ns_ at    261.001 "$node_(57) setdest    1496.25       1.60       0.00"

# Movement of Node: 41
$ns_ at     43.800 "$node_(41) set X_       3.75"
$ns_ at     43.800 "$node_(41) set Y_       1.60"
$ns_ at     43.800 "$node_(41) setdest      11.25       1.60      37.50"
$ns_ at     44.000 "$node_(41) setdest      41.25       1.60      30.00"
$ns_ at     45.000 "$node_(41) setdest    1391.25       1.60      37.50"
$ns_ at     81.000 "$node_(41) setdest    1421.25       1.60      30.00"
$ns_ at     82.000 "$node_(41) setdest    1496.25       1.60      37.50"
$ns_ at     84.001 "$node_(41) setdest    1496.25       1.60       0.00"

# Movement of Node: 76
$ns_ at    126.400 "$node_(76) set X_       3.75"
$ns_ at    126.400 "$node_(76) set Y_       1.60"
$ns_ at    126.400 "$node_(76) setdest    1226.25       1.60      37.50"
$ns_ at    159.000 "$node_(76) setdest    1248.75       1.60      22.50"
$ns_ at    160.000 "$node_(76) setdest    1248.75       1.60       0.00"
$ns_ at    293.000 "$node_(76) setdest    1256.25       1.60       7.50"
$ns_ at    294.000 "$node_(76) setdest    1286.25       1.60      15.00"
$ns_ at    296.000 "$node_(76) setdest    1308.75       1.60      22.50"
$ns_ at    297.000 "$node_(76) setdest    1338.75       1.60      30.00"
$ns_ at    298.000 "$node_(76) setdest    1376.25       1.60      37.50"

# Movement of Node: 82
```

```
$ns_ at    135.600 "$node_(82) set X_       3.75"
$ns_ at    135.600 "$node_(82) set Y_       1.60"
$ns_ at    135.600 "$node_(82) setdest     693.75       1.60      37.50"
$ns_ at    154.000 "$node_(82) setdest     723.75       1.60      30.00"
$ns_ at    155.000 "$node_(82) setdest    1173.75       1.60      37.50"
$ns_ at    167.000 "$node_(82) setdest    1203.75       1.60      30.00"
$ns_ at    168.000 "$node_(82) setdest    1203.75       1.60       0.00"
}; # End of proc

proc setMotionParamters {} {

global num_nodes area_width area_height time_end
set num_nodes 166
set area_width    1500.00
set area_height       3.20
set time_end 300

}; # End of proc
```

C.3 Power assignment script

The following script is used in ns-2 simulations experiments described in Section 8.6 to adjust vehicles transmission range according to DTRA algorithm.

```
proc setVehicleRange {} {
global ns_ node_

# Range of Node: 117
$ns_ at  206.400 "$node_(117) set txPt_ 72.13827" ;# 1000m
$ns_ at  233.000 "$node_(117) set txPt_  5.27447" ;#  520m
$ns_ at  235.000 "$node_(117) set txPt_  4.88030" ;#  510m
$ns_ at  236.000 "$node_(117) set txPt_  3.82940" ;#  480m
$ns_ at  237.000 "$node_(117) set txPt_  2.95812" ;#  450m
$ns_ at  238.000 "$node_(117) set txPt_  2.24472" ;#  420m
$ns_ at  239.000 "$node_(117) set txPt_  1.50418" ;#  380m
$ns_ at  240.000 "$node_(117) set txPt_  1.21165" ;#  360m
$ns_ at  241.000 "$node_(117) set txPt_  0.28179" ;#  250m
$ns_ at  242.000 "$node_(117) set txPt_  0.01056" ;#  110m

# Range of Node: 111
$ns_ at  190.600 "$node_(111) set txPt_ 72.13827" ;# 1000m
$ns_ at  218.000 "$node_(111) set txPt_  5.27447" ;#  520m
$ns_ at  220.000 "$node_(111) set txPt_  4.88030" ;#  510m
$ns_ at  221.000 "$node_(111) set txPt_  3.82940" ;#  480m
$ns_ at  222.000 "$node_(111) set txPt_  2.95812" ;#  450m
$ns_ at  223.000 "$node_(111) set txPt_  2.24472" ;#  420m
$ns_ at  224.000 "$node_(111) set txPt_  1.50418" ;#  380m
$ns_ at  225.000 "$node_(111) set txPt_  1.21165" ;#  360m
```

```
$ns_ at  226.000 "$node_(111) set txPt_  0.28179" ;#  250m
$ns_ at  227.000 "$node_(111) set txPt_  0.01056" ;#  110m

# Range of Node: 97
$ns_ at  163.600 "$node_(97) set txPt_ 72.13827" ;# 1000m
$ns_ at  194.000 "$node_(97) set txPt_  5.27447" ;#  520m
$ns_ at  196.000 "$node_(97) set txPt_  4.88030" ;#  510m
$ns_ at  197.000 "$node_(97) set txPt_  3.82940" ;#  480m
$ns_ at  198.000 "$node_(97) set txPt_  2.95812" ;#  450m
$ns_ at  199.000 "$node_(97) set txPt_  2.24472" ;#  420m
$ns_ at  200.000 "$node_(97) set txPt_  1.50418" ;#  380m
$ns_ at  201.000 "$node_(97) set txPt_  1.21165" ;#  360m
$ns_ at  202.000 "$node_(97) set txPt_  0.28179" ;#  250m
$ns_ at  203.000 "$node_(97) set txPt_  0.01056" ;#  110m

# Range of Node: 26
$ns_ at   16.800 "$node_(26) set txPt_ 72.13827" ;# 1000m
$ns_ at   56.600 "$node_(26) set txPt_  0.00000" ;#    0m

# <some code is deleted>

# Range of Node: 57
$ns_ at   80.400 "$node_(57) set txPt_ 72.13827" ;# 1000m
$ns_ at  119.000 "$node_(57) set txPt_  5.27447" ;#  520m
$ns_ at  121.000 "$node_(57) set txPt_  4.88030" ;#  510m
$ns_ at  122.000 "$node_(57) set txPt_  3.82940" ;#  480m
$ns_ at  123.000 "$node_(57) set txPt_  2.95812" ;#  450m
$ns_ at  124.000 "$node_(57) set txPt_  2.24472" ;#  420m
$ns_ at  125.000 "$node_(57) set txPt_  1.50418" ;#  380m
$ns_ at  126.000 "$node_(57) set txPt_  1.21165" ;#  360m
$ns_ at  127.000 "$node_(57) set txPt_  0.28179" ;#  250m
$ns_ at  128.000 "$node_(57) set txPt_  0.01056" ;#  110m
$ns_ at  257.000 "$node_(57) set txPt_  0.28179" ;#  250m
$ns_ at  258.000 "$node_(57) set txPt_  1.21165" ;#  360m
$ns_ at  259.000 "$node_(57) set txPt_  1.50418" ;#  380m
$ns_ at  260.000 "$node_(57) set txPt_  2.24472" ;#  420m
$ns_ at  261.000 "$node_(57) set txPt_  0.00000" ;#    0m

# Range of Node: 41
$ns_ at   43.800 "$node_(41) set txPt_ 72.13827" ;# 1000m
$ns_ at   84.000 "$node_(41) set txPt_  0.00000" ;#    0m

# Range of Node: 76
$ns_ at  126.400 "$node_(76) set txPt_ 72.13827" ;# 1000m
$ns_ at  161.000 "$node_(76) set txPt_  5.27447" ;#  520m
$ns_ at  163.000 "$node_(76) set txPt_  4.88030" ;#  510m
$ns_ at  164.000 "$node_(76) set txPt_  3.82940" ;#  480m
$ns_ at  165.000 "$node_(76) set txPt_  2.95812" ;#  450m
$ns_ at  166.000 "$node_(76) set txPt_  2.24472" ;#  420m
$ns_ at  167.000 "$node_(76) set txPt_  1.50418" ;#  380m
$ns_ at  168.000 "$node_(76) set txPt_  1.21165" ;#  360m
```

```
$ns_ at  169.000 "$node_(76) set txPt_  0.28179" ;#  250m
$ns_ at  170.000 "$node_(76) set txPt_  0.01056" ;#  110m
$ns_ at  294.000 "$node_(76) set txPt_  0.28179" ;#  250m
$ns_ at  295.000 "$node_(76) set txPt_  1.21165" ;#  360m
$ns_ at  296.000 "$node_(76) set txPt_  1.50418" ;#  380m
$ns_ at  297.000 "$node_(76) set txPt_  2.24472" ;#  420m
$ns_ at  298.000 "$node_(76) set txPt_  2.95812" ;#  450m
$ns_ at  299.000 "$node_(76) set txPt_  3.82940" ;#  480m

# Range of Node: 82
$ns_ at  135.600 "$node_(82) set txPt_ 72.13827" ;# 1000m
$ns_ at  169.000 "$node_(82) set txPt_  5.27447" ;#  520m
$ns_ at  171.000 "$node_(82) set txPt_  4.88030" ;#  510m
$ns_ at  172.000 "$node_(82) set txPt_  3.82940" ;#  480m
$ns_ at  173.000 "$node_(82) set txPt_  2.95812" ;#  450m
$ns_ at  174.000 "$node_(82) set txPt_  2.24472" ;#  420m
$ns_ at  175.000 "$node_(82) set txPt_  1.50418" ;#  380m
$ns_ at  176.000 "$node_(82) set txPt_  1.21165" ;#  360m
$ns_ at  177.000 "$node_(82) set txPt_  0.28179" ;#  250m
$ns_ at  178.000 "$node_(82) set txPt_  0.01056" ;#  110m
}; # End of proc
```

C.4 Connection script

The following generates CBR connections between vehicles for the ns-2 simulations described in Section 8.6.

```
proc setConnections {} {
global ns_ node_ pktSize bitRate

# Connection: 0
set udp_(0) [new Agent/UDP]
$ns_ attach-agent $node_(4) $udp_(0)
set null_(0) [new Agent/Null]
$ns_ attach-agent $node_(13) $null_(0)
set cbr_(0) [new Application/Traffic/CBR]
$cbr_(0) set packetSize_ $pktSize
$cbr_(0) set rate_ $bitRate
$cbr_(0) set random_ 1
$cbr_(0) attach-agent $udp_(0)
$ns_ connect $udp_(0) $null_(0)
$ns_ at      0.000 "$cbr_(0) start"
$ns_ at     13.000 "$cbr_(0) stop"

# Connection: 1
set udp_(1) [new Agent/UDP]
$ns_ attach-agent $node_(17) $udp_(1)
```

```
set null_(1) [new Agent/Null]
$ns_ attach-agent $node_(9) $null_(1)
set cbr_(1) [new Application/Traffic/CBR]
$cbr_(1) set packetSize_ $pktSize
$cbr_(1) set rate_ $bitRate
$cbr_(1) set random_ 1
$cbr_(1) attach-agent $udp_(1)
$ns_ connect $udp_(1) $null_(1)
$ns_ at      0.000 "$cbr_(1) start"
$ns_ at      4.000 "$cbr_(1) stop"

# Connection: 2
set udp_(2) [new Agent/UDP]
$ns_ attach-agent $node_(11) $udp_(2)
set null_(2) [new Agent/Null]
$ns_ attach-agent $node_(15) $null_(2)
set cbr_(2) [new Application/Traffic/CBR]
$cbr_(2) set packetSize_ $pktSize
$cbr_(2) set rate_ $bitRate
$cbr_(2) set random_ 1
$cbr_(2) attach-agent $udp_(2)
$ns_ connect $udp_(2) $null_(2)
$ns_ at      4.000 "$cbr_(2) start"
$ns_ at      7.000 "$cbr_(2) stop"

# Connection: 3
set udp_(3) [new Agent/UDP]
$ns_ attach-agent $node_(20) $udp_(3)
set null_(3) [new Agent/Null]
$ns_ attach-agent $node_(2) $null_(3)
set cbr_(3) [new Application/Traffic/CBR]
$cbr_(3) set packetSize_ $pktSize
$cbr_(3) set rate_ $bitRate
$cbr_(3) set random_ 1
$cbr_(3) attach-agent $udp_(3)
$ns_ connect $udp_(3) $null_(3)
$ns_ at      7.000 "$cbr_(3) start"
$ns_ at     35.000 "$cbr_(3) stop"

# <some code is deleted>

# Connection: 26
set udp_(26) [new Agent/UDP]
$ns_ attach-agent $node_(109) $udp_(26)
set null_(26) [new Agent/Null]
$ns_ attach-agent $node_(99) $null_(26)
set cbr_(26) [new Application/Traffic/CBR]
$cbr_(26) set packetSize_ $pktSize
$cbr_(26) set rate_ $bitRate
$cbr_(26) set random_ 1
$cbr_(26) attach-agent $udp_(26)
```

```
$ns_ connect $udp_(26) $null_(26)
$ns_ at    252.000 "$cbr_(26) start"
$ns_ at    300.000 "$cbr_(26) stop"

# Connection: 27
set udp_(27) [new Agent/UDP]
$ns_ attach-agent $node_(109) $udp_(27)
set null_(27) [new Agent/Null]
$ns_ attach-agent $node_(112) $null_(27)
set cbr_(27) [new Application/Traffic/CBR]
$cbr_(27) set packetSize_ $pktSize
$cbr_(27) set rate_ $bitRate
$cbr_(27) set random_ 1
$cbr_(27) attach-agent $udp_(27)
$ns_ connect $udp_(27) $null_(27)
$ns_ at    254.000 "$cbr_(27) start"
$ns_ at    300.000 "$cbr_(27) stop"

# Connection: 28
set udp_(28) [new Agent/UDP]
$ns_ attach-agent $node_(133) $udp_(28)
set null_(28) [new Agent/Null]
$ns_ attach-agent $node_(93) $null_(28)
set cbr_(28) [new Application/Traffic/CBR]
$cbr_(28) set packetSize_ $pktSize
$cbr_(28) set rate_ $bitRate
$cbr_(28) set random_ 1
$cbr_(28) attach-agent $udp_(28)
$ns_ connect $udp_(28) $null_(28)
$ns_ at    270.000 "$cbr_(28) start"
$ns_ at    300.000 "$cbr_(28) stop"

# Connection: 29
set udp_(29) [new Agent/UDP]
$ns_ attach-agent $node_(75) $udp_(29)
set null_(29) [new Agent/Null]
$ns_ attach-agent $node_(112) $null_(29)
set cbr_(29) [new Application/Traffic/CBR]
$cbr_(29) set packetSize_ $pktSize
$cbr_(29) set rate_ $bitRate
$cbr_(29) set random_ 1
$cbr_(29) attach-agent $udp_(29)
$ns_ connect $udp_(29) $null_(29)
$ns_ at    282.000 "$cbr_(29) start"
$ns_ at    300.000 "$cbr_(29) stop"
}; # End of proc
```

C.5 Main ns-2 script

This is the main script files for the ns-2 simulations of Section 8.6.

```
# hw_motion.tcl
# By Maen Artimy

# ================================================
source support_lib.tcl

readInputArgs
set motionfl $scriptfl[set x "_motion.tcl"]
set rangefl $scriptfl[set x "_range.tcl"]
set connctfl $scriptfl[set x "_conn.tcl"]

# seed the default RNG, initiate ID RNG, and select substream

# ================================================
# Initialize ns-2 instance
set ns_ [new Simulator]
setRNGs $run

$ns_ use-newtrace
set trfd [open $outfl w]
$ns_ trace-all $trfd

set namfile [open vanet.nam w]
$ns_ namtrace-all-wireless  $namfile 1500 3.2

log-time

# ================================================
set pktSize 512
set bitRate $btr

# include vehicle RoadSim scripts
source $motionfl
#source $rangefl
source $connctfl

setMotionParamters
setGeneralOptions opt
defineNodes opt

setVehicleMotion
#setVehicleRange
setConnections

# un-comment the next statement if movement log is needed
#log-movement
```

```
$ns_ at $time_end "stop"
puts "Starting Simulation..."
$ns_ run
```

The following is a collection of supporting functions for ns-2 simulations.

```
# support_lib.tcl
# By Maen Artimy

# read input arguments
proc readInputArgs {} {
global argc argv scriptfl outfl run btr

if {$argc >= 2} {
set scriptfl [lindex $argv 0]
puts "input file prefix = $scriptfl"

set outfl [lindex $argv 1]
puts "output file = $outfl"

set btr [lindex $argv 2]
if {$btr < 0} { set btr 0.1Mb }
puts "bit rate = $btr"

set run [lindex $argv 3]
if {$run < 0} { set run 0 }
puts "run = $run"

} else {
puts "Usage: ns hw_motion.tcl <script file prefix> <out file>
\[bit rate\] \[replication number\]"
exit
}
}

proc setRNGs {run} {
# seeds the default RNG and ID RNG
# advances to the selected sub-stream

global defaultRNG id_

$defaultRNG seed 13405
set nodesRNG [new RNG]

for {set i 0} {$i < $run} {incr i} {
$defaultRNG next-substream
$nodesRNG next-substream
}

# setup the node id random variable
```

```
set id_ [new RandomVariable/Uniform]
$id_ use-rng $nodesRNG
}

proc stop {} {
    global ns_ trfd
    $ns_ flush-trace
    close $trfd
    puts "NS EXITING..."
    exit 0;
}

proc setGeneralOptions {opt} {
global num_nodes area_width area_height
upvar opt val

set val(chan)           Channel/WirelessChannel    ;# channel type
set val(prop)           Propagation/TwoRayGround   ;# radio-propagation model
set val(netif)          Phy/WirelessPhy            ;# network interface type
set val(mac)            Mac/802_11                 ;# MAC layer
set val(ifq)            Queue/DropTail/PriQueue    ;# interface queue type
set val(ll)             LL                         ;# link layer type
set val(ant)            Antenna/OmniAntenna        ;# antenna model
set val(ifqlen)         50                         ;# max packet in ifq
set val(nn)             $num_nodes                 ;# number of mobilenodes
set val(rp)             AODV    ;# routing protocol
set val(x) $area_width    ;# max x
set val(y) $area_height    ;# max y
set val(conn) 10    ;# number of connections
}

proc defineNodes {options} {
global ns_ node_
upvar $options val

# Set topology
set topo [new Topography]
$topo load_flatgrid $val(x) $val(y)
create-god $val(nn)

# set node configuration
set chan [new $val(chan)]
$ns_ node-config \
-adhocRouting $val(rp) \
-llType $val(ll) \
-macType $val(mac) \
-ifqType $val(ifq) \
-ifqLen $val(ifqlen) \
-antType $val(ant) \
-propType $val(prop) \
-phyType $val(netif) \
```

```
-topoInstance $topo \
-agentTrace ON \
-routerTrace OFF \
-macTrace OFF \
-movementTrace OFF \
-channel $chan

# set nodes
for {set i 0} {$i < $val(nn) } {incr i} {
set node_($i) [$ns_ node]
$node_($i) random-motion 0 ;# disable random motion
#$node_($i) log-movement

$ns_ initial_node_pos $node_($i) 1
}
}

proc log-movement {} {
    global logtimer ns_ ns

    set ns $ns_
    source /usr/ns-allinone-2.26/ns-2.26/tcl/mobility/timer.tcl
    Class LogTimer -superclass Timer
    LogTimer instproc timeout {} {
        global opt node_;
        for {set i 0} {$i < $opt(nn)} {incr i} {
            $node_($i) log-movement
        }
        $self sched 0.1
    }

    set logtimer [new LogTimer]
    $logtimer sched 0.1
}

proc log-time {} {
    global logtimer ns_ ns

    set ns $ns_
    source /usr/src/ns-allinone-2.29/ns-2.29/tcl/mobility/timer.tcl
    Class LogTimer -superclass Timer
    LogTimer instproc timeout {} {
        global opt node_ ns;
        puts "time past = [$ns now] "
        $self sched 10.0
    }

    set logtimer [new LogTimer]
    $logtimer sched 10.0
}
```